学位論文

Effects of thermal fluctuations on phase transitions in the early Universe

（初期宇宙の相転移における熱的揺動の影響とその意義）

平成 26 年 12 月博士（理学）申請

東京大学大学院理学系研究科
物理学専攻

宮本 裕平

Abstract

In this thesis, we study cosmological phase transitions with a hot thermal bath. We often use effective potentials in considering such phase transitions, which give a simple explanation of restoration of symmetry of the theory at high temperature. However, since the effective potential is a static and homogeneous limit of the effective action, the effective action plays an essential role in considering dynamical, inhomogeneous field configurations. It is known that the effective action based on the finite-temperature field theory generally contains an imaginary part, which can be rewritten by introducing stochastic noise terms. The equation of motion of the field of interest, derived from this effective action, becomes Langevin equation. Therefore, the thermal environment gives not only the correction to the effective potential but the thermal fluctuations as well. The thermal fluctuation term is one of the important information that the effective action includes. We review a method to extract thermal fluctuations for various interactions. Interestingly, all the interactions which have been considered so far leads to the same relation, known as fluctuation-dissipation relation. We verify this relation in scalar quantum electrodynamics, as a first step to fully understand the dynamics of scalar fields with general interactions including gauge theory.

We study the effects of thermal fluctuations on the phase transition at the end of thermal inflation late in this thesis. Thermal inflation is a short period of accelerated expansion after the primordial inflation, which can reconcile the theory of supersymmetry with cosmology by diluting dangerous particles predicted by the theory. The end of thermal inflation is just a phase transition in a hot environment created just after the primordial inflation. We study the scenario of thermal inflation taking thermal effects into account, and see that the scenario itself is not ruined but the phase transition at the end of thermal inflation proceeds through phase mixing, which is different from what has been expected. An observational consequences of this result is that even if thermal inflation has occurred in the early Universe, we cannot expect gravitational-wave production, which is a characteristic phenomenon with strong first-order phase transitions.

Contents

Chapter 1

Introduction

The modern cosmology, as the dynamics of spacetime, was born a hundred years ago when Albert Einstein constructed general relativity. This huge shift of paradigm in theoretical physics is now one of the basic common knowledge after astronomers found that the Universe is expanding[1)]. Further developments in observation technology enable us to conclude that the expansion of the Universe is now accelerated [2]. Not only the dynamics of background spacetime, but also the evolution of the density fluctuations of matter and the course of structure-formation has been gradually unveiled. On the other hand, looking at the beginning of the Universe, the paradigm of inflationary cosmology [3, 4] has been established but we have to say we do not know much about what were really happening during inflation and the following reheating.

The cosmology of the early Universe is trying to answer the two fundamental questions. The first is, of course, "How the Universe begins?" This may be the most fundamental question which humans have been asking since ancient times. Not only this historical question, it has potential to give suggestions of the second question: "What is the fundamental law of physics of this world?" Since energy scales of phenomena in the early Universe are much higher than that of artificial particle accelerators, we expect to get some suggestions from observing the sky and decoding signals which were produced about 14 billion years ago. Therefore the role of the cosmology of the early Universe, in the variety of fields of physics, comes to be more and more important.

We can divide the role into two parts. The first is to rule out or give constraints on the untested theories. Since the resources we can use to verify the high-energy theory are limited, there are so many hypotheses which predict unreachable scale phenomena. By considering physical processes and observational consequences which are predicted by these theories, we can evaluate their validity by comparing with the real sky. The second is the role as a window to utterly new physics. The modern physics is based on general relativity and the standard model of particle physics described with quantum field theory, but cosmology is requesting physics

[1)]The history of observations related to cosmic expansion is summarized in Ref. [1] by B. P. Schmidt, one of the winners of the Nobel Prize in Physics in 2011.

beyond these theories. That is, we probably need the inflaton field in addition to the known fields and also need an explanation of dark matter. Is the current accelerated expansion caused by cosmological constant? Or does the theory of gravity have to be updated and modified from general relativity? These questions have great possibilities to open the door to the new physics.

In this thesis, we focus on phase transitions in the early Universe. They have provided mechanisms of inflation, called "old inflation" [4] and "new inflation" [5]. In both of the models the vacuum energy before the end of the phase transition drives accelerated expansion. Not only the primordial inflation, but the so-called thermal inflation [6, 7], which is a relatively short accelerated period after the primordial inflation, is also caused by the potential energy of the flaton field. Though both thermal inflation and the primordial inflation describe accelerated expansion of the Universe and the name of thermal inflation make us feel it is one of the many models of the primordial inflation, its role in cosmology is different. Again, thermal inflation occurs after the primordial inflation, so that it can dilute dangerous particles such as gravitinos [8] and moduli [9, 10, 11]. Since they come to be problematic after the primordial inflation, thermal inflation provides a way to dilute them. Thermal inflation changes the expansion history of the Universe, not only are the moduli and gravitinos diluted but the primordial gravitational waves are damped as well [12]. On the other hand, collisions of bubbles generated during a phase transition are thought to produce gravitational waves [12, 13, 14]. These examples indicate that the phase transition is an important key to understand high-energy physics and the very early Universe, especially through observations of gravitational waves, by DECIGO [15] and BBO [16]. With this motivation we also study the description of thermal inflation, particularly on how it ends [17].

Before studying thermal inflation, we improve our tools of finite-temperature field theory to explore the hot early Universe, since precise descriptions of the dynamics of phase transitions are necessary to compare predictions of each theoretical model with observations. The finite-temperature field theory is a generalization of the quantum field theory treating fields in a thermal state. Since the Universe after inflation is so hot that we expect thermal effects. In many models of the early Universe, phase transitions are characterized by the expectation values of the scalar fields, which are deeply related to temperature change. While the effective potential is a useful quantity to derive properties of the phase transitions that happen quasi-statically, its use often comes short because of dynamical nature of the scalar fields. In such cases, we need to directly solve the evolution equations of the scalar fields derived from the effective action. It has been shown that the behavior of a scalar field in thermal bath can be described by the Langevin equation [18, 19, 20], which includes stochastic noise terms coming from interactions with other fields in thermal bath. These noise terms may change the types of phase transitions. For example, a previous study [19] indicates that the fermionic noise may lead to the phase mixing, which invalidates the description of a phase transition using the effective potential.

This thesis is organized as follows. In the next chapter we shortly review the basis of modern cosmology, that is, the theory of inflation and the physics in the hot Universe. As we briefly saw,

the role of thermal inflation is different from the primordial one. In Chapter 2 we review the fundamental role of primordial inflation, namely, generation of primordial fluctuations and realizing a hot Universe after accelerated expansion. In Chapter 3, we study the finite-temperature field theory as a fundamental tool to explore the hot Universe. We consider the phase transitions based on this formalism in Chapter 4. Chapter 5 is devoted to concluding remarks.

Chapter 2

Inflation and the subsequent Big-Bang Universe

2.1 Inflation

In this section we briefly have a look at the inflationary Universe, which is the standard paradigm of modern cosmology. To understand the inflationary Universe more comprehensively, one can study Ref. [22], with other reviews and textbooks on inflation.

2.1.1 Basic Idea

The standard model of cosmology, or the simplest description of our Universe, is called ΛCDM model, which assumes the cosmological constant Λ and the cold dark matter. Namely, we can describe the Universe as a dynamical spacetime satisfying the Einstein equation

$$R_{\mu\nu} - \frac{1}{2}Rg_{\mu\nu} + \Lambda g_{\mu\nu} = 8\pi G T_{\mu\nu}\,, \tag{2.1}$$

where $T_{\mu\nu}$ is the energy-momentum tensor of the matter in the Universe, including the dark matter in addition to "standard" particles like baryons. As for the spacetime metric $g_{\mu\nu}$, the homogeneous and isotropic Universe is described by Friedmann-Robertson-Walker (FRW) metric,

$$ds^2 = -dt^2 + a^2(t)\left[\frac{dr^2}{1-Kr^2} + r^2(d\theta^2 + \sin^2\theta d\phi^2)\right], \tag{2.2}$$

where $a(t)$ is the scale factor whose time dependence is determined by the energy contents of the Universe. The 00-component of the Einstein equation for FRW Universe, known as Friedmann equation, gives this relation as

$$\left(\frac{\dot{a}}{a}\right)^2 = H^2 = \frac{8\pi G}{3}\rho - \frac{K}{a^2}\,, \tag{2.3}$$

and the spatial components are reduced to

$$2\frac{\ddot{a}}{a} + \left(\frac{\dot{a}}{a}\right)^2 + \frac{K}{a^2} = -8\pi G p\,. \tag{2.4}$$

Therefore the energy density ρ and pressure p of the dominant component in the Universe determine how the Universe evolves. It is convenient to introduce a parameter w characterizing the equation of state as

$$w = \frac{p}{\rho}\,, \tag{2.5}$$

which takes the following value,

$$w = \begin{cases} 0 & \text{non} - \text{relativistic matter}, \\ \frac{1}{3} & \text{radiation}, \\ -1 & \text{cosmological constant}. \end{cases} \tag{2.6}$$

It is also convenient to introduce a constant called reduced Planck mass, as $M_{\rm Pl} = 1/\sqrt{8\pi G} = 2.4 \times 10^{18}$GeV. With these setups we can consider the expanding Universe and trace back its history. The current expansion suggests that the Universe was hotter and denser in earlier times. One of the observational evidence of the hot Universe, or the Big-Bang Universe is the Cosmic Microwave Background (CMB), a near-perfect blackbody background radiation of $T \sim 2.7$K, which is a snapshot of the Universe when the photons and electrons are decoupled and electrons combine with protons to become neutral hydrogen atoms (recombination).

The idea of the inflationary Universe was originally motivated by solving problems with the Big-Bang theory. First, the CMB is so homogeneous that we have to choose special initial conditions over the superhorizon regions at the beginning of the Universe. This is called horizon problem. Using the particle horizon, which means the largest causal distance after an initial time t_i,

$$d_p(t) = \int_{t_i}^{t} \frac{dt'}{a(t')}\,, \tag{2.7}$$

we can see this problem more quantitatively. The causal region at the decoupling corresponds to about 1degree^2 in the observed homogeneous CMB sky, that is, we see that the temperature of the Universe were almost homogeneous at least over 10^4 noncausal regions.

We also have to assume the smallness of the spatial curvature, which is known as flatness problem. In addition to these problems related to unnatural initial conditions, we have a more severe problem called monopole problem. Phase transitions of the Universe produces topological defects, like monopoles. Since the energy density of them decreases as $\propto a^{-3}$, the expansion history of the universe becomes different from our Universe. The exponential expansion of the Universe at its early stage solves all the problems above.

Here we briefly review a class of working models called slow-roll inflation. In these models we assume that inflation is driven by the homogeneous component of a scalar field, called

inflaton, whose value varies slowly as it slowly rolls down the potential. In this case the energy-momentum tensor becomes the form of a perfect fluid with

$$\begin{aligned} \rho =& \frac{1}{2}\dot{\phi}^2 + V[\phi]\,, \\ p =& \frac{1}{2}\dot{\phi}^2 - V[\phi]\,. \end{aligned} \tag{2.8}$$

Therefore we expect an accelerated expansion when the following condition is satisfied.

$$\frac{\ddot{a}}{a} = -\frac{1}{6M_{\rm Pl}^2}(\rho + 3p) = \frac{1}{3M_{\rm Pl}^2}(V[\phi] - \dot{\phi}^2) > 0\,. \tag{2.9}$$

In order to quantify the slowness of the roll of inflaton, it is convenient to introduce slow-roll parameters like

$$\begin{aligned} \epsilon_v =& \frac{M_{\rm Pl}^2}{2}\left(\frac{V'}{V}\right)^2, \\ \eta_v =& M_{\rm Pl}^2\frac{V''}{V}\,, \end{aligned} \tag{2.10}$$

which give the slow-roll conditions as $\epsilon_v < 1$ and $|\eta_v| < 1$. Actually the above parameters are slow-roll parameters defined by the shape of the inflaton potential hence we expect that we can use them to distinguish models of inflation. We can take other definition in which we can see the meaning of "slow-roll" more directly.

$$\begin{aligned} \epsilon_{\rm SR} =& \frac{1}{2M_{\rm Pl}^2}\frac{\dot{\phi}^2}{H^2}, \\ \eta_{\rm SR} =& -\frac{\ddot{\phi}}{H\dot{\phi}}\,. \end{aligned} \tag{2.11}$$

$\epsilon_{\rm SR}$ parametrizes the slowness of the time evolution of the inflaton compared with H and smallness of $\eta_{\rm SR}$ represents that the change of $\epsilon_{\rm SR}$ is small per Hubble time.

2.1.2 Generation of Primordial Fluctuations

The inflationary Universe becomes a key ingredient of the modern cosmology because it provides not only the solution of the problems with the Big-Bang model but also the generating mechanism of density fluctuations necessary for the structure formations. The basic picture of the generation of density perturbations in the inflationary Universe is that the perturbations of the inflaton field on its homogeneous, slowly rolling component classicalizes at its horizon exit. That is, quantum fluctuations consisting of modes with shorter wavelength than the horizon

length becomes classical when the subhorizon modes become superhorizon. Let us consider a test scalar field in de Sitter spacetime. The equation of motion is

$$\left(\frac{d^2}{dt^2} + 3H\frac{d}{dt} + \frac{|\vec{k}|^2}{a^2(t)} + m^2\right)\phi(t,\vec{k}) = 0\,. \tag{2.12}$$

Using the conformal time $\eta = -\frac{1}{aH}$, we obtain

$$\left(\frac{d^2}{d\eta^2} - \frac{2}{\eta}\frac{d}{d\eta} + |\vec{k}|^2 + \frac{m^2}{H^2\eta^2}\right)\phi(\eta,\vec{k}) = 0\,. \tag{2.13}$$

The general solution of this differential equation can be expressed as

$$C_1 \cdot (-k\eta)^{3/2}H_\nu^{(1)}(-k\eta) + C_2 \cdot (-k\eta)^{3/2}H_\nu^{(2)}(-k\eta)\,, \tag{2.14}$$

where $H_\nu^{(i)}$ is the Hankel function of the i-th kind and ν is equal to $\sqrt{\frac{9}{4} - \frac{m^2}{H^2}}$. We impose a boundary condition that in sub-horizon limit ($k\eta \gg 1$) the mode function becomes equal to positive-frequency mode in Minkowski spacetime. After normalization we obtain

$$\begin{aligned}\phi(\eta,\vec{k}) =& \sqrt{\frac{\pi}{4}}H(-\eta)^{3/2}H_\nu^{(1)}(-k\eta)\\ &\to \frac{1}{\sqrt{2k}}e^{-ik\eta} \times H\eta\left(1 + \frac{1}{ik\eta}\right),\end{aligned} \tag{2.15}$$

where we take $\nu \to 3/2$ and $-k\eta \to \infty$ in the second line. In the superhorizon limit $|k\eta| \ll 1$, it becomes a time-independent value, $\frac{iH}{\sqrt{2k^3}}$.

In considering realistic situations, we have to note that the inflaton or any matter in the Universe is not just a contents in the container of spacetime, but spacetime also have fluctuations. Therefore we should treat the fluctuations of spacetime and inflaton field together, since coordinate transformation enable us to reinterpret fluctuations of the metric as those of the energy-momentum tensor. This choice of coordinate to define fluctuating quantity is called "gauge" in cosmological perturbation theory. Though the fluctuations mix by coordinate transformation, we decompose them into scalar/vector/tensor-type perturbations according to their properties of coordinate transformation. The scalar-type perturbation represents the density fluctuation or the curvature fluctuation and tensor-type corresponds to gravitational waves. This decomposition is useful since they are decoupled at the linear order in the Fourier space. After the decomposition we define gauge-invariant perturbation variables.

Now we evaluate the amplitude of the primordial fluctuations. In order to see that the fluctuations of the spatial curvature are generated by inflation, we consider one example known as comoving gauge. In this gauge the inflaton has no inhomogeneity but there are spatial curvature as

$$ds^2 = -dt^2 + a(t)^2[(1 - 2\mathcal{R})\delta_{ij} + h_{ij}]\,, \tag{2.16}$$

where h_{ij} satisfies transverse-traceless condition, $\partial^i h_{ij} = h^i_i = 0$. We can expand the action up to the second order in $\mathcal{R}$ and obtain a dramatically simple form as

$$S_2 = \int d\eta d^3x \left[\frac{1}{2} v'^2 + \frac{1}{2} (\vec{\nabla} v)^2 + \frac{1}{2} \frac{z''}{z} v^2 \right], \tag{2.17}$$

where $z = \frac{a\dot{\phi}}{H}$ and $v = z\mathcal{R}$, which is known as Sasaki-Mukhanov variable [23]. This is an action of harmonic oscillators with time-dependent mass term. Note that the variable z can be expressed with slow-roll parameter ϵ as $z^2 = 2aM_{\rm Pl}^2 \epsilon_{\rm SR}$ hence the v becomes massless in the de Sitter limit. The autocorrelation of $\mathcal{R}$ for each mode is evaluated at its horizon-exit,

$$\langle \mathcal{R}(t, \vec{k}) \mathcal{R}(t, \vec{k}') \rangle = (2\pi)^3 \delta(\vec{k} + \vec{k}') \frac{H_*^4}{2k^3 \dot{\phi}_*^2} = (2\pi)^3 \delta(\vec{k} + \vec{k}') P_{\mathcal{R}}(k) \,, \tag{2.18}$$

where H_* and $\dot{\phi}_*$ represents values at the horizon exit. To consider the amplitude in the real space, it is convenient to define the dimensionless powerspectrum as

$$\Delta^2_{\mathcal{R}}(k) = \frac{4\pi k^3}{(2\pi)^3} P_{\mathcal{R}}(k) = \frac{H_*^4}{(2\pi)^2 \dot{\phi}_*^2} \,. \tag{2.19}$$

Namely, as the powerspectrum of scalar-type fluctuations we obtain

$$\Delta^2_{\rm s}(k) = \left. \frac{1}{24\pi^2 \epsilon_v} \frac{V}{M_{\rm Pl}^4} \right|_{k=aH} \,. \tag{2.20}$$

Next we consider the tensor-type perturbation, h_{ij}. We can decompose it as

$$h_{ij} = \int \frac{d^3k}{(2\pi)^3} \left[h_+(t, \vec{k}) e^+_{ij}(\vec{k}) + h_\times(t, \vec{k}) e^\times_{ij}(\vec{k}) \right] e^{i\vec{k}\cdot\vec{x}} \tag{2.21}$$

where e^P_{ij} are the polarization tensors satisfying $e^P_{ij}(\vec{k}) e^{P'}_{ij}(\vec{k}) = \delta^{PP'}$. By substituting eq. (2.21) into the action of gravity $S_{\rm G} = -\frac{M_{\rm Pl}^2}{2} \int \sqrt{-g} d^4x R$, we obtain

$$S_{\rm G} = M_{\rm Pl}^2 \int \frac{d^3k}{(2\pi)^3} a^3 \left[\frac{1}{2} |\dot{h}_+(t, \vec{k})|^2 + \frac{|\vec{k}|^2}{2a^2} |h_+(t, \vec{k})|^2 + \frac{1}{2} |\dot{h}_\times(t, \vec{k})|^2 + \frac{|\vec{k}|^2}{2a^2} |h_\times(t, \vec{k})|^2 \right]. \tag{2.22}$$

After redefining the two fields as

$$\varphi^P_{\rm h}(t, \vec{k}) = M_{\rm Pl} \cdot h_P(t, \vec{k}) \,, \quad (P = +, \times) \tag{2.23}$$

we can interpret the action of gravity as that of two canonical scalar fields since their equation of motion in de Sitter spacetime are

$$\left(\frac{d^2}{dt^2} + 3H \frac{d}{dt} + \frac{|\vec{k}|^2}{e^{2Ht}} \right) \varphi^P_{\rm h}(t, \vec{k}) = 0 \,, \tag{2.24}$$

which is equivalent to eq.(2.12). The powerspectrum of tensor-type fluctuations is

$$\Delta_{\rm t}^2(k) = \left.\frac{2}{3\pi^2}\frac{V}{M_{\rm Pl}^4}\right|_{k=aH} . \tag{2.25}$$

Since the amplitude of the scalar-type perturbations are well known through the CMB observations, the tensor-to-scalar ratio $r \equiv \Delta_{\rm t}^2/\Delta_{\rm s}^2$ is often used to express the magnitude of tensor-type perturbations. From eq. (2.19) and (2.25), we see

$$r = 16\epsilon . \tag{2.26}$$

In the slow-roll inflation, the Hubble parameter is slowly varying during inflation and the amplitude of perturbations at its horizon exit weakly depends on the wavenumber. To characterize the scale dependence of the powerspectrum, we often use the spectral index as

$$n_{\rm s} - 1 = \frac{d\ln\Delta_{\rm s}^2}{d\ln k} , \quad n_{\rm t} = \frac{d\ln\Delta_{\rm t}^2}{d\ln k} , \tag{2.27}$$

which are related to the slow-roll parameters as

$$n_{\rm s} - 1 = -4\epsilon_{\rm SR} + 2\eta_{\rm SR} , \quad n_{\rm t} = -2\epsilon_{\rm SR} . \tag{2.28}$$

Then using eq. (2.26) and (2.28) we obtain a consistency relation for slow-roll inflation driven by a single field,

$$r = -8n_{\rm t} . \tag{2.29}$$

These dependences on scales are important keys to distinguish many models of inflation.

2.1.3 Models

So far many theoretical models of inflation have been proposed and specification of the favored models is now ongoing. A comprehensive study of models is done by in Ref. [24]. Here we briefly consider several famous models of slow-roll inflation.

"old" and "new" inflation model: In the oldest inflation model, called old inflation [4], inflaton is trapped at the origin during inflation and its quantum tunneling, or a first-order phase transition, ends inflation. Though this model turned out to be useless, the idea of phase transitions was inherited to the new inflation [5]. In new inflation model, inflaton is also trapped at the origin of the potential but it slowly rolls down to the bottom of the potential, with non-zero potential energy. These models in which inflaton starts rolling down at the maximum of its potential are called hilltop inflation.

hybrid inflation model: Building inflation models has been deeply related to phase transitions. In the so-called hybrid inflation [25], inflaton spontaneously breaks symmetry due to the existence of waterfall field.

chaotic inflation model: A class of inflation model with simple potentials, called chaotic inflation was proposed by Linde [26]. One can construct inflation model by simply assuming the monomial inflaton potential like $V \propto \phi^n$ (n: even integer). The initial condition of chaotic inflation is $V \sim M_{\rm Pl}^4$, which corresponds to the name of this model of inflation. We expect this initial condition naturally by assuming the description of the Universe, or the classical evolution of spacetime, becomes possible below Planckian energy scale. Chaotic inflation ends when ϕ becomes as small as $M_{\rm Pl}$, and ϕ starts oscillation at the bottom of the potential.

inflation model related to theory of gravity: The idea of modified gravity is also applied to inflation model building. One of the simplest model of this kind of models is R^2-inflation proposed by Starobinsky [3]. In this model the action of gravity contains not only the Einstein-Hilbert term, R, but also $\frac{1}{M^2}R^2$ term. One can see that this modification of gravity can be interpreted as introducing an additional scalar field, called scalaron, to the Einstein gravity theory by performing an appropriate conformal transformation. Actually it drives inflation during it slowly rolls down the potential. One of the features of this model is the smallness of the tensor perturbation. When we obtain a stringent upper bound on the primordial tensor perturbations by observations in the near future, this model would become a strong candidate to explain the mechanism of inflation.

2.2 Hot Universe

We review basic thermodynamics in the expanding Universe in this section. Most of the considerations are based on Refs. [27, 28]. This section would help us to understand the gravitio problem and the cosmological moduli problem in Chapter 4, and the mechanism of reheating after inflation.

2.2.1 Boltzmann equation in FRW Universe

A set of many particles interacting with each other reaches a thermal equilibrium state. In this case the phase space distribution function $f(p^\mu, x^\mu)$ becomes a simple function of the energy E as

$$f(E) = \frac{1}{e^{\beta(E-\mu)} \mp 1}\,, \tag{2.30}$$

where μ is the chemical potential and minus (plus) sign corresponds to bosons (fermions). In order to consider the radiation bath in the early Universe, let us take $\mu = 0$ and consider the case of $T \gg m$ (or, $E \approx |\vec{p}|$). Then the number density n and energy density ρ are calculated as

$$n = \int \frac{d^3p}{(2\pi)^3} \frac{1}{e^{\beta|\vec{p}|} \mp 1} = \frac{T^3}{2\pi^2} \int dx\, x^2 \frac{1}{e^x \mp 1}\,, \tag{2.31}$$

$$\rho = \int \frac{d^3p}{(2\pi)^3} \frac{|\vec{p}|}{e^{\beta|\vec{p}|} \mp 1} = \frac{T^4}{2\pi^2} \int dx\, x^3 \frac{1}{e^x \mp 1}\,. \tag{2.32}$$

After evaluating the x-integrals we obtain

$$n = \frac{\zeta(3)}{\pi^2} T^3 \times \begin{cases} 1 & \text{boson,} \\ \frac{3}{4} & \text{fermion,} \end{cases} \tag{2.33}$$

$$\rho = \frac{\pi^2}{30} T^4 \times \begin{cases} 1 & \text{boson,} \\ \frac{7}{8} & \text{fermion.} \end{cases} \tag{2.34}$$

Since these results are applied to each single degree of freedom, it is convenient to express the energy density of a radiation bath as $\rho = \frac{\pi^2}{30} g_* T^4$, where g_* represents the effective number of particle species in the bath. It becomes 106.75 in the standard model for $T \gg 100$GeV. As the Universe expands and cools, g_* gradually decreases.

In the early Universe, however, interacting particles never reach the equilibrium if the interactions between them are too weak to take longer time to reach equilibrium than the expansion timescale of the Universe. To see this, let us start with the Boltzmann equation in the FRW Universe. In general it can be expressed formally as

$$\hat{L}[f] = C[f] \,. \tag{2.35}$$

C in the right hand side is the collision term, which represents interactions. In the left hand side, $\hat{L}$ is called Liouville operator and it is given by

$$\hat{L} = p^\mu \frac{\partial}{\partial x^\mu} - \Gamma^\mu_{\alpha\beta} p^\alpha p^\beta \frac{\partial}{\partial p^\mu} \,, \tag{2.36}$$

in the covariant form. In the FRW Universe, in which we are interested, it becomes

$$\hat{L}[f(E,t)] = \left(E \frac{\partial}{\partial t} - H(t) |\vec{p}|^2 \frac{\partial}{\partial E} \right) f(E,t) \,. \tag{2.37}$$

In considering "particles", it is convenient to use the number density $n(t)$, rather than $f(E,t)$. After performing a partial integral the Boltzmann equation becomes

$$\frac{d}{dt} n(t) + 3H(t) n(t) = \frac{g}{(2\pi)^3} \int d^3p \, \frac{1}{E} C[f] \,, \tag{2.38}$$

where g represents the inertial degrees of freedom.

Next let us consider the right hand side. Here we assume that the particles ϕ, a, b, $\cdots$ becomes A, B, $\cdots$ after the collision, where ϕ represents the particle of interest. The collision term appearing in the equation of ϕ-particle can be written as

$$\begin{aligned} &\frac{g}{(2\pi)^3} \int d^3p_\phi \frac{1}{E_\phi} C \\ &= - \int d\Pi_\phi d\Pi_a d\Pi_b \cdots d\Pi_A d\Pi_B \cdots (2\pi)^4 \delta^4(p_\phi + p_a + p_b + \cdots - p_A - p_B - \cdots) \\ &\quad \times \Big[\, |\mathcal{M}|^2_{\phi+a+b+\cdots \to A+B+\cdots} \times f_\phi f_a f_b \cdots (1 \pm f_A)(1 \pm f_B) \cdots \\ &\qquad - |\mathcal{M}|^2_{A+B+\cdots \to \phi+a+b\cdots} \times (1 \pm f_\phi)(1 \pm f_a)(1 \pm f_b) \cdots f_A f_B \cdots \Big] , \end{aligned} \tag{2.39}$$

where $d\Pi = \frac{g}{(2\pi)^3}\frac{d^3p}{2E}$ for each particle and "±" applies boson and fermion respectively. Here we consider two approximations. First is based on time-reversal symmetry, by which we can equate the two transition amplitudes,

$$|\mathcal{M}|^2_{\phi+a+b+\cdots\to A+B+\cdots} = |\mathcal{M}|^2_{A+B+\cdots\to\phi+a+b\cdots} \ (= |\mathcal{M}|^2)\,. \tag{2.40}$$

Second, if the difference between bosons and fermions is negligible, that is, the Bose-condensation and Fermi-Blocking effect are absent, we simply use the Maxwell-Boltzmann distribution. Since this is valid for $f \ll 1$, we further replace $(1 \pm f)$ with 1. Using the two approximations above, the Boltzmann equation for ϕ-particle becomes

$$\begin{aligned}&\frac{dn}{dt} + 3Hn\\ &= -\int d\Pi_\phi d\Pi_a d\Pi_b \cdots d\Pi_A d\Pi_B \cdots (2\pi)^4\delta^4(p_\phi + p_a + p_b + \cdots - p_A - p_B - \cdots)\\ &\quad\times |\mathcal{M}|^2[f_\phi f_a f_b \cdots - f_A f_B \cdots]\,.\end{aligned} \tag{2.41}$$

Due to the cosmic expansion, the number density decreases with time. Therefore it is convenient to consider the particle number per comoving volume. Using the fact that the entropy per comoving volume, s, is kept unchanged without production of entropy, it is often convenient to define a new quantity,

$$Y \equiv \frac{n}{s}\,. \tag{2.42}$$

We can see that using this variable the left hand side of the Boltzmann equation can be written as

$$\dot{n} + 3Hn = s\dot{Y}\,. \tag{2.43}$$

So far we consider the evolution of the number density based on the cosmic time t. However, in considering the interactions between particles, it is useful to use the temperature [1)] as time variable instead of the cosmic age. In the radiation-dominated Universe, the correspondence between the cosmic time and the temperature is

$$t = \frac{3\sqrt{10}}{2\pi} g_*^{-\frac{1}{2}} M_{\rm Pl}\, T^{-2} = 1.51 \times g_*^{-\frac{1}{2}} M_{\rm Pl}\, T^{-2}\,, \tag{2.44}$$

Since the temperature decreases with time, we define the dimensionless "time" variable x as $x = m/T$. Finally the Boltzmann equation can be expressed as

$$\begin{aligned}\frac{dY}{dx} = -\frac{x}{\tilde{H}(m)s}\int &d\Pi_\phi d\Pi_a d\Pi_b \cdots d\Pi_A d\Pi_B \cdots (2\pi)^4\delta^4(p_\phi + p_a + p_b + \cdots - p_A - p_B - \cdots)\\ &\times |\mathcal{M}|^2[f_\phi f_a f_b \cdots - f_A f_B \cdots]\,,\end{aligned} \tag{2.45}$$

where $\tilde{H}(m) = \frac{\pi}{\sqrt{90}} g_*^{1/2} \frac{m^2}{M_{\rm Pl}}$, which is equal to the Hubble parameter at $T = m$.

[1)] Here "temperature" means that of a thermal bath dominating the Universe. The particle species which have little interaction with bath particles may have different "temperature".

2.2.2 Decoupling

Here we consider the scenario that at some temperature ϕ-particle decouples from the thermal bath. As an example let us see the annihilation/pair-creation process like

$$\phi\ \bar{\phi} \longleftrightarrow \chi\ \bar{\chi}\,, \tag{2.46}$$

through which the number of ϕ-particles changes. Since χ-particles are in thermal equilibrium, we replace the distribution function of χ with its thermal-equilibrium value.

$$f_\chi f_{\bar{\chi}} = f_\chi^{\rm eq} f_{\bar{\chi}}^{\rm eq}\,. \tag{2.47}$$

One component of the delta function corresponding to the energy conservation enable us to rewrite it as

$$f_\chi^{\rm eq} f_{\bar{\chi}}^{\rm eq} = e^{-(E_\chi + E_{\bar{\chi}})/T} = e^{-(E_\phi + E_{\bar{\phi}})/T}\,. \tag{2.48}$$

As for f_ϕ, we also rewrite it as

$$f_\phi = e^{-(E_\phi - \mu)/T} = e^{-E_\phi/T} \times \frac{n_\phi}{n_\phi^{\rm eq}}\,, \tag{2.49}$$

which also applies to $f_{\bar{\phi}}$ and we neglect the difference between ϕ and $\bar{\phi}$. Using the thermally-averaged cross section,

$$\begin{aligned}\langle\sigma v\rangle = \frac{1}{(n_\phi^{\rm eq})^2} \int & d\Pi_\phi d\Pi_{\bar{\phi}} d\Pi_\chi d\Pi_{\bar{\chi}} \\ & (2\pi)^4 \delta^4(p_\phi + p_{\bar{\phi}} - p_\chi - p_{\bar{\chi}}) |\mathcal{M}|^2 e^{-E_\phi/T} e^{-E_{\bar{\phi}}/T}\,,\end{aligned} \tag{2.50}$$

we obtain a simple equation

$$\frac{dn_\phi}{dt} + 3Hn_\phi = -\langle\sigma v\rangle \left(n_\phi^2 - (n_\phi^{\rm eq})^2\right)\,, \tag{2.51}$$

or with Y and x,

$$\frac{dY}{dx} = -\frac{x \cdot s \cdot \langle\sigma v\rangle}{\tilde{H}(m)} \left(Y^2 - Y_{\rm eq}^2\right)\,. \tag{2.52}$$

Thermal-equilibrium values are given by

$$Y_{\rm eq} = \begin{cases} \frac{45}{2\pi^4} \cdot \left(\frac{\pi}{8}\right)^{\frac{1}{2}} \cdot \frac{g}{g_{*\rm s}} x^{\frac{3}{2}} e^{-x} = 0.145 \times \frac{g}{g_{*\rm s}} x^{\frac{3}{2}} e^{-x} & (x \gg 1,\ \text{non} - \text{relativistic})\,, \\ \frac{45}{2\pi^4} \cdot \zeta(3) \cdot \frac{g_{\rm eff}}{g_{*\rm s}} = 0.278 \times \frac{g_{\rm eff}}{g_{*\rm s}} & (x \ll 1,\ \text{relativistic})\,, \end{cases} \tag{2.53}$$

where in evaluating its relativistic limit we go back to the Bose-Einstein/Fermi-Dirac distribution. Therefore the factor $g_{\rm eff}$ depends on the particle species, $g_{\rm eff} = g\,(3g/4)$ for bosons (fermions).

Equation (2.52) tells us a simple but important criterion of decoupling. Remembering that $\tilde{H}(m) = \frac{\pi}{\sqrt{90}} g_*^{1/2} \frac{m^2}{M_{\rm Pl}}$ represents the Hubble parameter at $T = m$, or $x = 1$, the Hubble parameter at x is $H(x) = \tilde{H}(m) \times x^{-2}$. Using this relation we obtain

$$\frac{x}{Y_{\rm eq}} \frac{dY}{dx} = -\frac{\Gamma}{H(x)} \left[\left(\frac{Y}{Y_{\rm eq}} \right)^2 - 1 \right], \tag{2.54}$$

where $\Gamma = n_{\rm eq} \langle \sigma v \rangle$ is the annihilation rate. We can see that the ratio of Γ/H is important to consider decoupling. When the annihilation rate Γ becomes smaller than H, the change of Y stops and ϕ-particles decouple from the thermal bath.

2.2.3 Entropy Production by Decoupled Particle

In this subsection we consider a non-relativistic particle ψ, who decouples from the thermal bath, decays with the lifetime τ. This consideration is applicable to not only reheating of the Universe after the primordial inflation, but also the cosmological moduli problem we see late in this thesis. The time evolution of the number density is

$$\frac{d}{dt}(a^3 n_\psi) = -\tau^{-1}(a^3 n_\psi), \tag{2.55}$$

and the solution is

$$n_\psi(a(t)) = n_\psi(a(t_i)) \left(\frac{a(t)}{a(t_i)} \right)^3 e^{-\frac{t-t_i}{\tau}}, \quad \text{or} \quad \rho_\psi(a(t)) = \rho_\psi(a(t_i)) \left(\frac{a(t)}{a(t_i)} \right)^3 e^{-\frac{t-t_i}{\tau}}, \tag{2.56}$$

where t_i is some initial time and $\rho_\psi = m_\psi n_\psi$ is the energy density of ψ-particle.

Assuming that the energy released by the decay of ψ-particle instantly thermalizes, we obtain the equation for the energy density of radiations,

$$\frac{d}{dt}\rho_{\rm rad} + 4H\rho_{\rm rad} = -\tau^{-1}\rho_\psi \,. \tag{2.57}$$

This equation is valid if the effective degrees of freedom are unchanged. In general we have to consider the second law of thermodynamics in the comoving volume, which is given by

$$dS = \frac{dQ}{T} = -\frac{d(a^3\rho_\psi)}{T} = \frac{a^3\rho_\psi}{T}\frac{dt}{\tau}, \tag{2.58}$$

which becomes a differential equation for entropy S,

$$S^{\frac{1}{3}} \frac{dS}{dt} = \left(\frac{2\pi^2}{45} g_* \right)^{\frac{1}{3}} a^4 \rho_\psi \tau^{-1} \,. \tag{2.59}$$

The formal solution is

$$S^{\frac{4}{3}} = S^{\frac{4}{3}}(t_i) + \frac{4}{3}\rho_\psi(t_i) a_i^4 \tau^{-1} \int_{t_i}^{t} dt' \left(\frac{2\pi^2}{45} g_* \right)^{\frac{1}{3}} \frac{a(t')}{a(t_i)} e^{-\frac{t'}{\tau}} \,. \tag{2.60}$$

As a case of our interest, now we consider the Universe dominated by ψ until it decays. In such a matter-dominant Universe the scale factor evolves as $a \propto t^{2/3}$ and the radiation energy density decreases as

$$\rho_{\rm rad}(a) = \rho_{\rm rad} \cdot \left(\frac{a_i}{a}\right)^4 + \frac{5}{3}\rho_\psi(a_i)\frac{t_i^2}{t \cdot \tau} \,. \tag{2.61}$$

The first term represents the effect of cosmic expansion and the second one is the energy converted from ψ. We show the time evolution of the two energy densities in Fig.2.1. The dominant energy density of the Universe changes around $t \sim \tau$.

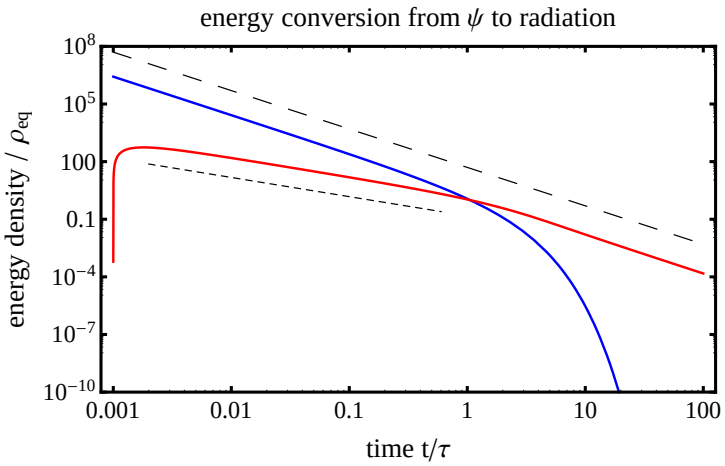

Figure 2.1: The evolution of ρ_ψ (blue line) and $\rho_{\rm rad}$ (red line) are shown. As an example we impose $\rho_{\rm rad} = 0$ at $t = 0.01\tau$. We normalize the energy density by $\rho_{\rm eq}$, which is the energy density of ψ and radiation when they are equal. The equality time is $t = 1.05\tau$. The long (short) dashed line is proportional to t^{-2} (t^{-1}), showing that the dominant energy component evolves as t^{-2} and $\rho_{\rm rad}$ before the decay of ψ evolves as t^{-1}.

Now we consider the entropy production from the decay of ψ. Using the solution (eq.(2.60)), the ratio of entropy per comoving volume before and after the decay becomes

$$\frac{S_{\rm after}}{S_{\rm before}} = \left[1 + \frac{4}{3}\left(\frac{2\pi^2}{45}g_{*\rm before}\right)^{-\frac{1}{3}}\frac{mY_{\rm before}}{T_{\rm before}} \times I\right]^{\frac{3}{4}} , \tag{2.62}$$

where I is given by

$$I = \tau^{-1}\int_{t_{\rm before}}^{\infty} dt' \left(\frac{2\pi^2}{45}g_*\right)^{\frac{1}{3}}\frac{a(t')}{a_{\rm before}}e^{-\frac{(t'-t_{\rm before})}{\tau}} \,. \tag{2.63}$$

If ψ is the dominant component in the Universe before its decay, we obtain [2)]

$$I = 1.09 \times \left(\frac{2\pi}{45}\right)^{\frac{1}{3}} \langle g_*^{\frac{1}{3}} \rangle \left(\frac{\rho_\psi(t_{\rm before})}{3M_{\rm Pl}^2}\right)^{\frac{1}{3}} \tau^{\frac{2}{3}} , \tag{2.64}$$

where $\langle g_*^{\frac{1}{3}} \rangle$ represents a kind of averaged value over the integration time. The entropy ratio becomes

$$\frac{S_{\rm after}}{S_{\rm before}} \approx 0.817 \times \langle g_*^{\frac{1}{3}} \rangle^{\frac{3}{4}} \frac{m Y_i \tau^{\frac{1}{2}}}{M_{\rm Pl}^{\frac{1}{2}}} . \tag{2.65}$$

The cosmic temperature just after the decay is

$$H(\tau)^2 \sim \frac{1}{4\tau^2} \sim \frac{1}{3M_{\rm Pl}^2}\frac{\pi^2}{30} g_* T_{\rm R}^4 , \quad T_{\rm R} \sim 0.8 \times g_*^{-\frac{1}{4}} \left(\frac{M_{\rm Pl}}{\tau}\right)^{\frac{1}{2}} . \tag{2.66}$$

2.2.4 Reheating

We apply the discussion of the entropy production to the beginning of the Big-Bang Universe. The inflaton, which finished the role of driving inflation, should pass its energy to standard model particles. This process is called reheating of the Universe, often described as energy dissipation of the homogeneous oscillation of the inflaton. Inflaton reaches the bottom of the potential at the end of inflation and begins oscillation around there. Therefore the equation of motion becomes

$$\frac{d^2}{dt^2}\phi + 3H\frac{d}{dt}\phi + m^2\phi = 0 , \tag{2.67}$$

where m represents the curvature of the potential. From this equation we can see that the energy density of this coherent oscillation decreases as $\rho_\phi \propto a^{-3}$, which is the same as that of non-relativistic matter.

If we simply assume that the inflaton energy is converted into radiation with dissipation rate Γ_ϕ, that is,

$$\frac{d\rho_\phi}{dt} = -3H\rho_\phi - \Gamma_\phi \rho_\phi , \tag{2.68}$$

$$\frac{d\rho_{\rm rad}}{dt} = -4H\rho_{\rm rad} + \Gamma_\phi \rho_\phi , \tag{2.69}$$

the time evolution of each energy component becomes

$$\rho_\phi(t) = \rho_\phi(t_{\rm end}) \left(\frac{a(t)}{a(t_{\rm end})}\right)^{-3} e^{-\Gamma_\phi (t - t_{\rm end})} , \tag{2.70}$$

$$\rho_{\rm rad}(t) = \Gamma_\phi a^{-4}(t) \int_{t_{\rm end}}^{t} dt' a^4(t') \rho_\phi(t') , \tag{2.71}$$

[2)] Though the dominant contribution comes from $t < \tau$ and we can roughly evaluate the integral using the functional form $a \propto t^{3/2}$, the numerical factor 1.09 is obtained after solving the evolution of the scale factor numerically.

where $t_{\rm end}$ represents the moment of the end of inflation.

The reheating temperature is defined as the temperature when the energy density of the relativistic particles exceeds that of the inflaton oscillation. As we saw before, this alternation happens at $t \sim \Gamma_\phi^{-1}$ and the reheating temperature is roughly given by

$$T_{\rm R} \sim 0.8 \times g_*^{-\frac{1}{4}} \left(\Gamma_\phi M_{\rm Pl}\right)^{\frac{1}{2}} . \tag{2.72}$$

From this moment the Universe enter the radiation-dominated era.

2.3 Phase Transitions

In this section, we briefly review the phase transitions in the early Universe. We focus on the two phase transitions in the standard model and other possible ones.

Electroweak Phase Transition

The discovery of Higgs boson in the Large Hadron Collider in 2013 verifies that the standard model based on gauge principle is at least a working model for describing physics up to $O(100\text{GeV})$. The change of vacuum expectation value of Higgs field causes electroweak phase transition, after which the weak interaction and electromagnetic interaction were split up. To be precise, the nonzero vev of Higgs field breaks the SU(2) subgroup of the $\mathrm{SU_L}(2) \times \mathrm{U_Y}(1)$ but leaves the subgroup $\mathrm{U_{em}}(1)$ unbroken. The vev of Higgs field makes the gauge bosons of weak interaction massive, but the photon is still massless and electromagnetic interaction is still long-range interactions.

Quark-Hadron Phase Transition

Hadrons such as protons and neutrons are not the elementary particles but composite particles made of quarks and gluons. Though we cannot see the single quarks around us, they were not confined before the QCD phase transition.

One of the models of this phase transition is called the bag model [29]. In this model a hadron is modeled by a bag containing quarks in vacuum, which has the energy proportional to the volume. In addition to this volume energy, the kinetic energy of quarks, which are assumed to freely move inside the bag, is taken into account. Since the smaller size of the bag leads to larger kinetic energy of quarks, the radius of a bag can be determined by minimizing the total energy. The total energy of hadrons can be expressed as

$$E_{\rm H} = K + \frac{4\pi r^3}{3} B , \tag{2.73}$$

where B is the constant energy density called bag constant. Assuming the form of the kinetic energy as $K \propto 1/r$, we can express the total energy of hadrons as

$$E_{\rm H} = \frac{16\pi}{3} r^3 B\,, \tag{2.74}$$

which indicates $B^{\frac{1}{4}} \sim O(100\text{MeV})$ since the total energy or the mass of hadrons are $O(100\text{MeV})$ and $O(1\text{fm}) \sim (O(100\text{MeV}))^{-1}$ for their radii. To estimate the critical temperature, we have to use thermodynamics for the kinetic term. For massless degrees of freedom the pressure is calculated as $p = \frac{\pi^2}{90} g_* T^4$ (we discuss more in detain in later). In the quark-gluon plasma phase it is evaluated as

$$p_{\rm QGP} = -B + \frac{\pi^2}{90} T^4 \times (2 \times 8 + \frac{7}{8} \times 3 \times 2 \times 2 \times 2)\,, \tag{2.75}$$

where we include 2×8 gluon degrees of freedom and light quark (up and down). In the hadron phase, we consider 3 pion degrees of freedom. Equating these two pressures leads to

$$T = \left(\frac{45}{17\pi^2} B\right)^{\frac{1}{4}} = 0.72 B^{\frac{1}{4}}\,, \tag{2.76}$$

from which we can estimate the critical temperature.

Theoretical Prediction

The only scalar boson in particle contents of the standard model is Higgs particle. However, in the theory of supersymmetry (SUSY), we have bosonic fields as much as fermionic fields. Therefore we expect the phase transition is ubiquitous in many SUSY models, which also provides a theoretical basis in building models of inflation.

The theoretical reason to expect the existence of supersymmetry is related to the mass of Higgs boson [30]. The quantum loop correction to the mass of Higgs particle is so large that we believe of some theoretical reason to keep it as small as the experimental value naturally. This is known as the hierarchy problem. In SUSY we have the bosonic superpartner of each fermion who cancels the mass correction from fermion. Though SUSY is an elegant theory it should be broken if it really existed since we have never seen the superpartners whose masses are exactly same as the particles in the standard model. In so-called soft SUSY breaking, the mass scale introduced to break SUSY is expected to be TeV scale in order to give a natural solution of the hierarchy problem [31].

Topological Defects

Most of the phase transitions in the early hot Universe are triggered by the temperature change. Therefore huge spatial regions larger than horizon scale at that time undergo the phase transition and at some points scalar fields cannot move to the vev and forms so-called topological

defects. There are several kinds of topological defects, which are determined by the mathematical structure of the broken symmetry. A comprehensive study on these topological defects are found in Ref.[32]. Monopoles, which are the particle like defects, are generally predicted in GUT theory. In the Big-Bang cosmology the generation of them cannot be avoided and this is called monopole problem. One-dimensional defects are called cosmic strings. Their most attractive property is that the network of cosmic strings satisfies the scaling rule and they never dominate the Universe. A part of the energy of long strings is transferred to loops and eventually converted to the gravitational waves, which provides a way to observationally probe the high energy physics through cosmic strings. Other topological defects, called domain walls and textures, are also produced in the corresponding phase transitions.

Chapter 3

Finite-Temperature Field Theory

3.1 Basic Formalism

We summarize the basic method of finite-temperature field theory in this section, following Ref. [33, 34] to prepare tools in treating interacting systems perturbatively.

3.1.1 From Statistical Mechanics to Quantum Mechanics

In statistical mechanics, expectation values in a thermal state are calculated as

$$\langle O \rangle_\beta = \sum_i O_i P_i = \frac{\sum_i O_i \exp[-\beta E_i]}{\sum_i \exp[-\beta E_i]}\,, \tag{3.1}$$

where O_i are eigenvalues of an operator $\hat{O}$,

$$O_i = \langle \psi_i | \hat{O} | \psi_i \rangle = \int dq\, \psi^*(q) \hat{O}(q) \psi(q)\,. \tag{3.2}$$

We can define the density matrix as

$$\rho(q) = \sum_i \exp[-\beta E_i] \psi_i^*(q) \psi_i(q)\,, \tag{3.3}$$

which enable us to express the thermal average as

$$\langle O \rangle_\beta = \int dq\, \hat{O}(q) \rho(q) = \mathrm{tr}(\rho\, O)\,. \tag{3.4}$$

Now we see the analogy between statistical mechanics and quantum mechanics more. The distribution function in statistical mechanics is given by

$$Z = \mathrm{tr}\left(e^{-\beta H}\right) = \int dq \langle q | e^{-\beta H} | q \rangle\,. \tag{3.5}$$

On the other hand, the transition amplitude for a particle from position q (at time t) to q' (at time t') in quantum mechanics is given by

$$\mathcal{A}(q', t'; q, t) = \langle q'|e^{-i\hat{H}(t'-t)}|q\rangle\,, \tag{3.6}$$

where $e^{-i\hat{H}t}$ is a time evolution operator for quantum states. Comparing eq.(3.5) and eq.(3.6) and regarding $e^{-\beta H}$ as a time evolution operator of $\Delta t = -i\tau = -i\beta$, we can express the distribution function in a form of path integral.

$$\begin{aligned} Z &= \int dq \mathcal{A}(q, -i\beta; q, 0) \\ &= \int \mathcal{D}q\, \exp\left[-\int_0^\beta d\tau \left(\frac{1}{2}m\dot{q}^2(\tau) + V(q)\right)\right] \\ &= \int \mathcal{D}q\, \exp\left[-S_{\mathrm{E}}\right]\,, \end{aligned} \tag{3.7}$$

where S_{E} is the Euclidean action. Note that the boundary conditions of this path integral is $q(\beta) = q(0)$, which is different from ones in quantum mechanics where we have $q(t) = q'$ and $q(0) = q$.

Using this condition we find

$$\langle Tq(-i\beta)q(-i\tau)\rangle_\beta = \langle Tq(0)q(-i\tau)\rangle_\beta\,. \tag{3.8}$$

Let us consider the two-point function furthermore. Generally it is convenient to write the T-product as

$$\Delta(\tau) = \langle Tq(-i\tau)q(0)\rangle_\beta\,. \tag{3.9}$$

The T-product can be expressed as a combination of the following two-point functions,

$$D^>(t, t') = \langle q(t)q(t')\rangle_\beta\,, \tag{3.10}$$

$$D^<(t, t') = \langle q(t')q(t)\rangle_\beta\,. \tag{3.11}$$

We can obtain the following representation by inserting a complete set of energy eigenstate $1 = \sum_n |n\rangle\langle n|$,

$$D^>(t, t') = \frac{1}{Z}\sum_{n,m} e^{-\beta E_n - iE_n(t-t')}e^{+iE_m(t-t')}\,|\langle n|q(0)|m\rangle|^2\,. \tag{3.12}$$

From this expression we expect that the exponential factors determine the convergence of the state summation, so that the function $D^>(t - t')$ is well defined for

$$-\beta < \mathrm{Im}(t - t') < 0\,, \tag{3.13}$$

Similarly the function $D^<(t - t')$ is defined for

$$0 < \mathrm{Im}(t - t') < \beta\,. \tag{3.14}$$

So far we see the two-point function $\langle Tq(t)q(t')\rangle_\beta$ for $-\beta < \tau < \beta$. Remembering that thermally-averaged quantities can be calculated by performing traces, we can derive the Kubo-Martin-Schwinger relation

$$D^>(t,t') = D^<(t+i\beta,t')\,, \tag{3.15}$$

or

$$\Delta(\tau) = D^>(-i\tau,0) = D^<(-i\tau+i\beta,0) = \Delta(\tau-\beta)\,, \tag{3.16}$$

which gives a periodic condition and enables us to define the time-ordering product for any real time variables as

$$D(t-t') = \theta(t-t')D^>(t,t') + \theta(t'-t)D^<(t,t')\,. \tag{3.17}$$

In order to calculate thermally-averaged quantities, it is convenient to define the generating functional as

$$Z[J] = \int \mathcal{D}q \exp\left[-S_{\rm E} + \int_0^\beta d\tau J(\tau)q(\tau)\right], \tag{3.18}$$

which actually gives thermal quantities. Namely, we can formally express thermal quantities like

$$\langle f(q)\rangle_\beta = \frac{1}{Z[J]} f\left(\frac{\delta}{\delta J(\tau)}\right) Z[J]\bigg|_{J=0}\,. \tag{3.19}$$

In particular, we can perform the $q-$integral for a harmonic oscillator with $V = \frac{1}{2}\omega^2 q^2$ to obtain

$$Z[J] = (\text{const.}) \times \exp\left[\frac{1}{2}\int d\tau d\tau' J(\tau)K(\tau-\tau')J(\tau)\right], \tag{3.20}$$

where K is equivalent to

$$K(\tau-\tau') = \langle \mathrm{T}(q(-i(\tau-\tau'))q(0))\rangle = \Delta(\tau-\tau')\,, \tag{3.21}$$

and satisfy

$$\left(-\frac{d^2}{d\tau^2}+\omega^2\right)K(\tau-\tau') = \delta(\tau-\tau')\,. \tag{3.22}$$

Using its periodic property eq. (3.16), we obtain

$$K(\tau) = \frac{1}{2\omega}\left[(1+n(\omega))e^{-\omega\tau} + n(\omega)e^{+\omega\tau}\right], \quad (0<\tau<\beta) \tag{3.23}$$

where

$$n(\omega) = \frac{1}{e^{\beta|\omega|}-1}\,. \tag{3.24}$$

3.1.2 Field Theory at Finite Temperature: Imaginary-Time Formalism

The generating functional is expressed as

$$Z = \int \mathcal{D}\phi \exp\left[-S_{\mathrm{E}} + \int_0^\beta d^4x J(x)\phi(x)\right], \quad \left(\int_0^\beta d^4x = \int_0^\beta d\tau \int_{-\infty}^{+\infty} d^3x\right) \tag{3.25}$$

where S_{E} is the Euclidean action for a scalar field

$$S_{\mathrm{E}} = \int_0^\beta d^4x \left(\frac{1}{2}\partial_\mu\phi\partial^\mu\phi + \frac{1}{2}m^2\phi^2 + V[\phi]\right). \tag{3.26}$$

For a free scalar field, the partition function becomes

$$Z[J] = (\text{const.}) \times \exp\left[\frac{1}{2}\int_0^\beta d^4x d^4x' J(x)\Delta(x-x')J(x')\right]. \tag{3.27}$$

In Fourier space, the two point function K can be written as

$$\Delta(\omega_n, k) = \frac{1}{\omega_n^2 + \omega_k^2}, \quad \left(\omega_n = \frac{2\pi n}{\beta}, \ \ \omega_k = \sqrt{|\vec{k}|^2 + m^2}\right) \tag{3.28}$$

which is known as Matsubara propagator. Note that the Fourier transformation with respect to τ becomes the Fourier series expansion due to the periodic property as follows.

$$\Delta(\tau) = \frac{1}{\beta}\sum_{n=-\infty}^{\infty} e^{-i\omega_n\tau}\Delta(i\omega_n), \tag{3.29}$$

$$\Delta(i\omega_n) = \int_0^\beta d\tau\, e^{i\omega_n\tau}\Delta(\tau). \tag{3.30}$$

We now compare the propagators at zero and finite temperature, and obtain a mathematical relation between them. In real (Euclidean) space, they can be expressed as

$$\Delta(\tau, \vec{x}, T=0) = \int \frac{d^4k}{(2\pi)^4}\frac{1}{k_0^2 + \omega_k^2}e^{-ik_0\tau + i\vec{k}\cdot\vec{x}}, \tag{3.31}$$

$$\Delta(\tau, \vec{x}, T) = \frac{1}{\beta}\sum_{n=-\infty}^{\infty}\int \frac{d^3k}{(2\pi)^3}\frac{1}{\omega_n^2 + \omega_k^2}e^{-i\omega_n\tau + i\vec{k}\cdot\vec{x}}. \tag{3.32}$$

First, we see that the propagator at finite temperature can be calculated as

$$\begin{aligned}
\Delta(\tau, \vec{x}, T) &= \frac{1}{\beta}\sum_{n=-\infty}^{\infty}\int \frac{d^3k}{(2\pi)^3}\frac{1}{\omega_n^2 + \omega_k^2}e^{-i\omega_n\tau + i\vec{k}\cdot\vec{x}} \\
&= \int \frac{d^3k}{(2\pi)^3}e^{-i\vec{k}\cdot\vec{x}}\frac{1}{\beta}\left[2\sum_{n=1}^{\infty}\frac{\cos\left(\frac{2\pi\tau}{\beta}n\right)}{\left(\frac{2\pi}{\beta}\right)^2 n^2 + \omega_k^2} + \frac{1}{\omega_k^2}\right] \\
&= \int \frac{d^3k}{(2\pi)^3}e^{-i\vec{k}\cdot\vec{x}}\frac{1}{2\omega_k}\left[(1+n(\omega_k))e^{-\omega_k\tau} + n(\omega_k)e^{\omega_k\tau}\right],
\end{aligned} \tag{3.33}$$

where we use a mathematical formula,

$$\sum_{n=1}^{\infty} \frac{\cos(nx)}{n^2+a^2} = \frac{\pi}{2a}\frac{\cosh(a\pi - ax)}{\sinh(a\pi)} - \frac{1}{2a^2}\,. \tag{3.34}$$

Second, we also see that a quantity related to zero-temperature propagator is calculated as

$$\begin{aligned}\sum_{n=-\infty}^{\infty} \Delta(\tau+n\beta,\vec{x},T=0) &= \sum_{n=-\infty}^{\infty}\int\frac{dk_0}{2\pi}\int\frac{d^3k}{(2\pi)^3}\frac{1}{k_0^2+\omega_k^2}e^{ik_0(\tau+n\beta)-i\vec{k}\cdot\vec{x}} \\ &= \int\frac{d^3k}{(2\pi)^3}e^{-i\vec{k}\cdot\vec{x}}\sum_{n=-\infty}^{\infty}\frac{1}{2\omega_k}e^{-\omega_k|\tau+n\beta|} \\ &= \int\frac{d^3k}{(2\pi)^3}e^{-i\vec{k}\cdot\vec{x}}\frac{1}{2\omega_k}\left[(1+n(\omega_k))e^{-\omega_k\tau}+n(\omega_k)e^{\omega_k\tau}\right]\,. \end{aligned} \tag{3.35}$$

From eq. (3.33) and eq. (3.35), we see that

$$\Delta(\tau,\vec{x},T) = \sum_{n=-\infty}^{\infty}\Delta(\tau+n\beta,\vec{x},T=0)\,. \tag{3.36}$$

Namely, the propagator at finite temperature can be expressed in terms of that of zero temperature.

3.1.3 Field Theory at Finite Temperature: Real-Time Formalism

In the so-called imaginary-time formalism, we have to perform analytic continuations to obtain physical quantities. In this subsection we review "real-time formalism", which enables us to directly calculate real-time quantities. In this formalism, however, we have some additional work in calculation.

As we saw before, we can take thermal average by generalizing the time variable to be complex-valued. We can directly calculate quantities of interest, such as correlation functions, if we take a part of the time path on real axis (Fig. 3.1).

We consider calculating n-point function,

$$G_c(x_1,x_2,\cdots x_n) = \langle \mathrm{T}_c\left(\hat{\phi}(x_1)\hat{\phi}(x_2)\cdots\hat{\phi}(x_n)\right)\rangle\,, \tag{3.37}$$

where the suffix c represents the path-ordering in place of time-ordering in usual QFT. This is because the time path we consider in finite-temperature field theory is defined on the complex plane. The generating functional of these correlation functions is given by

$$\begin{aligned} Z[J] &= \mathrm{tr}\left[e^{-\beta\hat{H}}T_c\exp\left(i\int d^4x J(x)\phi(x)\right)\right] \\ &= \int\mathcal{D}\phi\exp\left[i\int_c d^4x\left(\mathcal{L}+J(x)\phi(x)\right)\right]\,, \end{aligned} \tag{3.38}$$

where c means the time path from $t_\mathrm{i} = t$ to $t_\mathrm{f} = t - i\beta$ (see Fig. 3.1), and the boundary condition is $\phi(t, \vec{x}) = \phi(t - i\beta, \vec{x})$. Taking $t_\mathrm{i} \to -\infty$ allows us to neglect the C_3 and C_4 contribution [35]. Hereafter we call C_1 (C_2) path + (−) path. Namely, as the generating functional for free field we have

$$Z[J] = (\text{const.}) \times \exp\left[\frac{1}{2}\int_{-\infty}^{\infty} d^4x d^4x' J_\mathrm{a}(x) D_\mathrm{ab}(x - x') J_\mathrm{b}(x')\right], \quad (a,\, b = +,\, -) \tag{3.39}$$

and we have four propagators who can be simply expressed in Fourier space as

$$\begin{aligned}
D_{++}(k) &= \frac{i}{k^2 - m^2 + i\epsilon} + 2\pi n(k_0)\delta(k^2 - m^2)\,, \\
D_{--}(k) &= (D_{++}(k))^*\,, \\
D_{+-}(k) &= e^{+\sigma k_0}\left[n(k_0) + \theta(-k_0)\right] 2\pi\delta(k^2 - m^2)\,, \\
D_{-+}(k) &= e^{-\sigma k_0}\left[n(k_0) + \theta(k_0)\right] 2\pi\delta(k^2 - m^2)\,.
\end{aligned} \tag{3.40}$$

Since the choice of σ does not affect the final results, we choose $\sigma = 0$ hereafter.

With path integral representations we can evaluate interactions perturbatively. For a self-interaction Lagrangian $V(\phi)$ we can formally express

$$\begin{aligned}
Z = &\exp\left[-i\int_{-\infty}^{+\infty} d^4x \left(V\left(\frac{\delta}{i\delta J_+(x)}\right) - V\left(\frac{\delta}{i\delta J_-(x)}\right)\right)\right] \\
&\times \exp\left[-\frac{1}{2}\int_{-\infty}^{+\infty} d^4x d^4x' J_\mathrm{a}(x) D_\mathrm{ab}(x - x') J_\mathrm{b}(x')\right],
\end{aligned} \tag{3.41}$$

note that we have a term of $-V$ since we rewrite the "minus path" from $-\infty$ to $+\infty$.

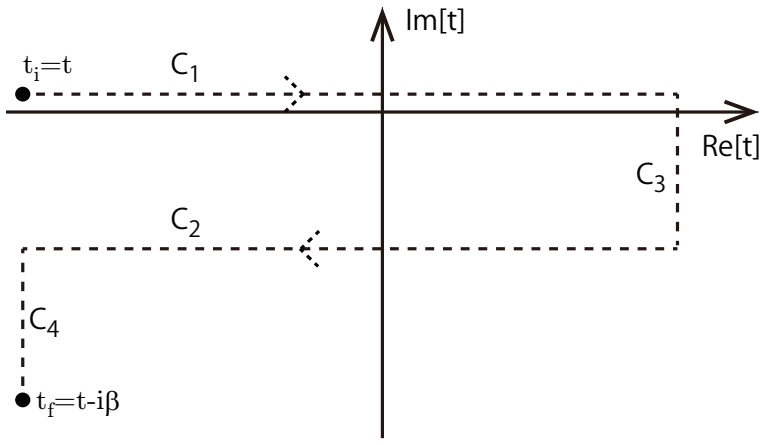

Figure 3.1: The time path used in the real-time formalism.

We briefly summarize the propagators for fermions here. In considering fermions we have to note that the commutation relation is different from that of bosons. Due to the equal-time

anti-commutation relations

$$\left\{\psi_\rho(t,\vec{x})\,,\ \psi^\dagger_\sigma(t,\vec{x}')\right\} = \delta_{\rho\sigma}\delta(\vec{x}-\vec{x}')\,, \tag{3.42}$$

it is convenient to define two-point functions as

$$S^>_{\rho\sigma}(x,x') = +\langle\psi_\rho(x)\bar{\psi}_\sigma(x')\rangle_\beta\,, \tag{3.43}$$
$$S^<_{\rho\sigma}(x,x') = -\langle\bar{\psi}_\sigma(x')\psi_\rho(x)\rangle_\beta\,. \tag{3.44}$$

The KMS relation is expressed as

$$S^>_{\rho\sigma}(t,\vec{x};t',\vec{x}') = -S^<_{\rho\sigma}(t+i\beta,\vec{x};t',\vec{x}')\,. \tag{3.45}$$

The Matsubara propagator in real space is given by

$$S_{\rho\sigma}(\tau,\vec{x};\tau',\vec{x}') = \langle T(\psi_\rho(-i\tau,\vec{x})\bar{\psi}_\sigma(-i\tau',\vec{x}'))\rangle_\beta \tag{3.46}$$
$$= \theta(\tau-\tau')S^>_{\rho\sigma}(\tau,\vec{x};\tau',\vec{x}') + \theta(\tau'-\tau)S^<_{\rho\sigma}(\tau,\vec{x};\tau',\vec{x}')\,, \tag{3.47}$$

and in Fourier space it becomes

$$S(-i\omega_n,\vec{p}) = \frac{m-\not{p}}{\omega_n^2+E_p^2} \tag{3.48}$$

where $\omega_n = (2n+1)\pi/\beta$ is the Matsubara frequency.

Propagators in real-time formalism are given by

$$\begin{aligned}
S_{++}(k) &= \frac{i}{\not{k}-m+i\epsilon} - 2\pi n(k_0)(\not{k}+m)\delta(k^2-m^2)\,,\\
S_{--}(k) &= \frac{-i}{\not{k}-m+i\epsilon} - 2\pi n(k_0)(\not{k}+m)\delta(k^2-m^2)\,,\\
S_{+-}(k) &= -\left[n(k_0)-\theta(-k_0)\right]2\pi(\not{k}+m)\delta(k^2-m^2)\,,\\
S_{-+}(k) &= -\left[n(k_0)-\theta(k_0)\right]2\pi(\not{k}+m)\delta(k^2-m^2)\,.
\end{aligned} \tag{3.49}$$

3.1.4 Renormalization Issue in Finite-Temperature Field Theory

One of the most complex calculations in quantum field theory is appropriate renormalization. We also encounter divergences in finite-temperature field theory, however, renormalization procedures are the same as that of zero-temperature. Intuitively, the effects of the finite temperature do not appear at much higher energy scale than temperature, so that ultraviolet divergences are not changed. Let us see this issue more qualitatively in imaginary-time method. We saw that the propagator at finite-temperature can be expressed as eq. (3.36),

$$\begin{aligned}
\Delta(\tau,\vec{x},T) &= \sum_{n=-\infty}^{\infty}\Delta(\tau+n\beta,\vec{x},T=0)\\
&= \Delta(\tau,\vec{x},T=0) + \sum_{n\neq 0}\Delta(\tau+n\beta,\vec{x},T=0)\,,
\end{aligned} \tag{3.50}$$

where the first term in the right hand side is just the zero-temperature propagator. From this expression, we see that the divergences related to a loop integral, which is τ, $\vec{x} \to 0$ limit, is the same as that at zero temperature.

In real-time formalism, we can also remove divergences by the similar way in zero-temperature theory. The explicit calculation is shown in Section 3.3, where we consider scalar QED.

3.2 Effective Action Method

In this section we review the definition of effective action and consider the resulting equation of motion. Practically, the effective action can be obtained from perturbative calculation with respect to coupling constants characterizing the strength of interactions. Namely, we first consider free theory at finite temperature and then perturbatively include interactions. Though the Universe as a whole should evolve unitarily, the system of our interest, a scalar field ϕ for example, is an open system which continuously exchange energy with other fields (e.g. a scalar field χ). As a result, the effective action for the system which includes effects of such interactions becomes a complex quantity. It is shown that the imaginary part of effective action can be rewritten as stochastic noise, which is connected to the friction term via the fluctuation-dissipation relation. This relation is derived on the assumption that both the system of interest ϕ and other fields (χ) interacting with ϕ are in (nearly) thermal equilibrium.

In particular, it is convenient to consider the homogeneous and static limit, in which the effective action reduces to effective potential. We also see the functional form of the one-loop effective potential at the end of this section.

3.2.1 Definition of Effective Action

The generating functional for connected diagrams, $W[J]$, is defined as

$$\exp\left(iW[J]\right) = Z[J] = \int \mathcal{D}\phi \exp\left[iS\left[\phi\right] + i\int d^4x J(x)\phi(x)\right]. \tag{3.51}$$

Let us briefly see that the above definition of $W[J]$ really gives the generating functional for connected diagrams [36]. Just for simplicity we consider in Euclidean space. The generating function Z is expanded as

$$\begin{aligned} Z[J] &= \int \mathcal{D}\phi \exp\left[\int d^4x S\left[\phi\right] + \int d^4x J(x)\phi(x)\right] \\ &= \sum_N \frac{1}{N!}\int d^4x_1 \cdots \int d^4x_N J(x_1)\cdots J(x_N)\langle\phi(x_1)\cdots\phi(x_N)\rangle \\ &\equiv \sum_N \frac{1}{N!}F_N\,, \end{aligned} \tag{3.52}$$

where we use $F_N = \langle (\int d^4x J(x)\phi(x))^N \rangle$. Generally the N-point function contains disconnected ones, which are Green functions satisfying $\langle \phi_1\phi_2\phi_3\phi_4 \rangle = \langle \phi_1\phi_2 \rangle \langle \phi_3\phi_4 \rangle$, for example. Therefore we can express a Green function by a linear combination of the products of connected functions. By considering dividing N particles into various boxes (the number of boxes containing k particles are defined n_k), we obtain

$$F_N = \sum_{\{n_k\}} N! \prod_s \frac{\left(\frac{1}{s!}F_s^{\mathrm{c}}\right)^{n_s}}{n_s!} \delta_{N,\sum_k k\cdot n_k}\,, \tag{3.53}$$

where F_s^{c} represents the s-point connected Green's function (integrated with weight $J(x)$) and $\{n_k\}$ means all the possible realization of the way of division. Remembering that the generating function $Z[J]$ contains the summation over N, we erase the Kronecker's delta to rewrite

$$\sum_N \sum_{\{n_k\}} \delta_{N,\sum_k k\cdot n_k} \prod_s = \prod_s \left(\sum_{n_s=0}^{\infty} \right), \tag{3.54}$$

then we find

$$\begin{aligned} Z[J] &= \sum_N \frac{1}{N!} \sum_{\{n_k\}} N! \prod_s \frac{\left(\frac{1}{s!}F_s^{\mathrm{c}}\right)^{n_s}}{n_s!} \delta_{N,\sum_k k\cdot n_k} \\ &= \prod_s \left(\sum_{n_s=0}^{\infty} \frac{\left(\frac{1}{s!}F_s^{\mathrm{c}}\right)^{n_s}}{n_s!} \right) \\ &= \prod_s \exp\left[\frac{F_s^{\mathrm{c}}}{s!} \right], \end{aligned} \tag{3.55}$$

from which we can see that the $W[J]$ is the generating function of the connected functions.

$$\begin{aligned} W[J] &= \log Z[J] \\ &= \sum_s \frac{1}{s!} F_s^{\mathrm{c}} \\ &= \sum_s \frac{1}{s!} \int d^4x_1 \cdots \int d^4x_s J(x_1)\cdots J(x_s) G^c(x_1, \cdots, x_s)\,. \end{aligned} \tag{3.56}$$

Actually $W[J]$ gives the vacuum expectation value of ϕ under the presence of an external field J as

$$\begin{aligned} \phi_J(x) &= \frac{1}{Z[J]} \int \mathcal{D}\phi\, \phi(x) \exp\left[iS[\phi] + i\int d^4y J(y)\phi(y) \right] \\ &= \frac{1}{Z[J]} \frac{\delta}{i\delta J(x)} Z[J] \\ &= \frac{\delta}{\delta J(x)} W[J]\,. \end{aligned} \tag{3.57}$$

We can interpret this equation gives the value of J which is required to obtain the expectation value of ϕ_J. Namely, to set the left hand side of eq. (3.57) as $\phi_J = \phi_*$, we have to determine the external field J to J_{ϕ_*} which satisfy $\phi_* = \delta W[J_{\phi_*}]/\delta J_{\phi_*}$.

Performing a Legendre transformation with respect to J, we obtain Γ as

$$\Gamma[\phi] = -\int d^4x\, \phi(x)J(x) + W[J]\,, \tag{3.58}$$

which consists of one-particle irreducible (1PI) diagrams. Γ is the quantum effective action since its variation gives a equation of motion for the expectation value of ϕ if we set $J = 0$ as

$$\frac{\delta\Gamma[\phi]}{\delta\phi(x)} = -J(x)\,. \tag{3.59}$$

3.2.2 Effective Action at Finite Temperature and Langevin equation

We now consider the effective action derived from finite-temperature field theory. Assuming both the system of interest, ϕ, and the relevant fields interacting with ϕ are in thermal equilibrium, we can perturbatively evaluate 1PI diagrams by using four propagators as we saw. Generally the effective action can be expressed as [18, 19, 20, 21]

$$\Gamma = S_0 + \Gamma_{\rm R} + \Gamma_{\rm I}\,, \tag{3.60}$$

where S_0 is the tree level action, and $\Gamma_{\rm R}$ and $\Gamma_{\rm I}$, respectively, represent the real and imaginary parts[1)] coming from interactions. In order to focus on the properties of the effective action, we postpone seeing practical procedures in evaluating effective action until the next section, where we consider scalar QED. Skipping calculations let us see specific examples studied in Ref. [20]. An interaction term $\mathcal{L}_{\rm int} = -\lambda^2\chi^2\phi^2$ leads to the 1PI diagrams shown in Fig. 3.2. Their contributions to the effective action are calculated as follows.

$$\begin{aligned}\Gamma_{\rm D1} =& -16\lambda^4\int d^4x_1 d^4x_2\, {\rm Im}\left[G_\phi^{++}(x_1-x_2)G_\chi^{++}(x_1-x_2)^2\right]\phi_\Delta(x_1)\phi_{\rm c}(x_2)\theta(t_1-t_2)\\ &+4i\lambda^4\int d^4x_1 d^4x_2\, {\rm Re}\left[G_\phi^{++}(x_1-x_2)G_\chi^{++}(x_1-x_2)^2\right]\phi_\Delta(x_1)\phi_\Delta(x_2)\,,\end{aligned} \tag{3.61}$$

$$\begin{aligned}\Gamma_{\rm D2} =& -8\lambda^4\int d^4x_1 d^4x_2\, {\rm Im}\left[G_\chi^{++}(x_1-x_2)^2\right]\times\left(\phi_\Delta(x_1)\phi_{\rm c}(x_1)\phi_{\rm c}^2(x_2)+\frac{1}{4}\phi_\Delta(x_1)\phi_{\rm c}(x_1)\phi_\Delta^2(x_2)\right)\theta(t_1-t_2)\\ &+4i\lambda^4\int d^4x_1 d^4x_2\, {\rm Re}\left[G_\chi^{++}(x_1-x_2)^2\right]\phi_\Delta(x_1)\phi_{\rm c}(x_1)\phi_\Delta(x_2)\phi_{\rm c}(x_2)\,,\end{aligned} \tag{3.62}$$

where we use new variables for convenience,

$$\phi_c = \frac{\phi_+ + \phi_-}{2}\,,\quad \phi_\Delta = \phi_+ - \phi_-\,. \tag{3.63}$$

[1)] $\Gamma_{\rm I}$ is purely imaginary.

$\Gamma_{\rm D1}$ ($\Gamma_{\rm D2}$) represents the contribution from the left (right) diagram in Fig. 3.2. The first (second) line contributes to the real (imaginary) part of the effective action. Not only for the interaction we saw, $\mathcal{L}_{\rm int} = -\lambda^2\chi^2\phi^2$, but for other interactions the basic structure[2)] of the effective action is expressed as

$$\begin{aligned}\Gamma = & S_0 \\ & - \int d^4x_1 d^4x_2\, B_{\rm a}(x_1 - x_2)\theta(t_1 - t_2)\phi_\Delta(x_1)\phi_{\rm c}(x_2) \\ & - \int d^4x_1 d^4x_2\, B_{\rm m}(x_1 - x_2)\theta(t_1 - t_2)\left(\phi_\Delta(x_1)\phi_{\rm c}(x_1)\phi_{\rm c}(x_2)^2 + \frac{1}{4}\phi_\Delta(x_1)\phi_{\rm c}(x_1)\phi_\Delta^2(x_2)\right) \\ & + \frac{i}{2}\int d^4x_1 d^4x_2\, A_{\rm a}(x_1 - x_2)\phi_\Delta(x_1)\phi_\Delta(x_2) \\ & + \frac{i}{2}\int d^4x_1 d^4x_2\, A_{\rm m}(x_1 - x_2)\phi_\Delta(x_1)\phi_{\rm c}(x_1)\phi_\Delta(x_2)\phi_{\rm c}(x_2)\,. \end{aligned} \tag{3.64}$$

Though functions $A(x)$ and $B(x)$ are obtained only after evaluating the effective action, the contribution from 1PI diagrams with two (four) external lines takes the above form. Therefore we proceed for a while without using specific forms of A and B, in order to make the consideration applicable to various interactions.

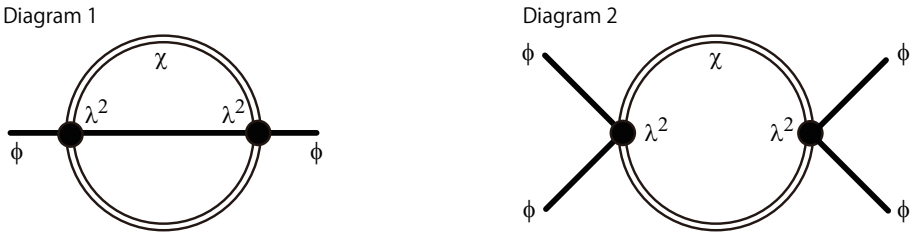

Figure 3.2: Two examples of 1PI diagrams coming from $\mathcal{L}_{\rm int} = -\lambda^2\chi^2\phi^2$ are shown. In Ref. [20] the contribution from the left (right) diagram to the effective action, $\Gamma_{\rm D1}$ ($\Gamma_{\rm D2}$), is evaluated.

Now we are ready for introducing stochastic noise term. Remembering the Gaussian integral

[2)] To be precise, we have local corrections in addition to non-local terms in eq. (3.64). Though we do not show them in eq. (3.64), they are included in $V_{\rm eff}$ in EoM, eq. (3.70).

formula,

$$\exp\left[-\int d^4x d^4y\, \varphi(x)M(x,y)\varphi(y)\right]$$
$$\propto \int \mathcal{D}\xi \exp\left[-\frac{1}{4}\int d^4x d^4y\, \xi(x)M^{-1}(x,y)\xi(y) + i\int d^4x\, \xi(x)\varphi(x)\right], \tag{3.65}$$

we can rewrite the imaginary part by introducing integrals over ξ as follows.

$$\begin{aligned}
&\exp\left[i\Gamma_{\rm I}\right] \\
&= \exp\left[-\frac{1}{2}\int d^4x_1 d^4x_2 A_{\rm a}(x_1-x_2)\phi_\Delta(x_1)\phi_\Delta(x_2) + A_{\rm m}(x_1-x_2)\phi_\Delta(x_1)\phi_\Delta(x_2)\phi_c(x_1)\phi_c(x_2)\right] \\
&= \int \mathcal{D}\xi_{\rm a}\mathcal{D}\xi_{\rm m}\, P[\xi_{\rm a}]P[\xi_{\rm m}] \exp\left[iS_{\rm noise}\right],
\end{aligned} \tag{3.66}$$

where

$$\begin{aligned}
P[\xi_{\rm a}] &\propto \exp\left[-\frac{1}{2}\int d^4x_1 d^4x_2\, \xi_{\rm a}(x_1)A_{\rm a}^{-1}(x_1-x_2)\xi_{\rm a}(x_2)\right], \\
P[\xi_{\rm m}] &\propto \exp\left[-\frac{1}{2}\int d^4x_1 d^4x_2\, \xi_{\rm m}(x_1)A_{\rm m}^{-1}(x_1-x_2)\xi_{\rm m}(x_2)\right], \\
S_{\rm noise} &= \int d^4x\, \left[\xi_{\rm a}(x)\phi_\Delta(x) + \xi_{\rm m}(x)\phi_\Delta(x)\phi_c(x)\right].
\end{aligned} \tag{3.67}$$

The new variables, $\xi_{\rm a}$ and $\xi_{\rm m}$, are introduced by considering Gaussian integrals. Though the above procedure is nothing but a mathematical transformation so far, we can interpret the new variables ξ as stochastic noise variables whose probability distributions are given by $P[\xi]$. The validity of this interpretation is discussed soon.

Though we do not use the specific form of $A(x)$ and $B(x)$, there is a necessary condition for function $A(x)$. Just like convergence of a one dimensional Gaussian integral, $\int dx\, \exp[-ax^2]$, requires $a > 0$, all of the eigenvalues of $A(x_1, x_2)$ should be positive. This requirement is understood more clearly in Fourier space,

$$\int d^4x d^4y\, \xi(x)A^{-1}(x,y)\xi(y) = \int \frac{d^4k}{(2\pi)^4}\tilde{A}^{-1}(k)|\tilde{\xi}(k)|^2, \tag{3.68}$$

then we see that $\tilde{A}(k)$ should be positive.

Combined with the real part, we now obtain

$$e^{i\Gamma} = \int \mathcal{D}\xi_{\rm a}\mathcal{D}\xi_{\rm m}\, P[\xi_{\rm a}]P[\xi_{\rm m}]\, e^{i\left(S_0 + \Gamma_{\rm R} + S_{\rm noise}\right)}. \tag{3.69}$$

Finally the equation of motion, which is the equation for ϕ_c obtained by varying the effective action with respect to ϕ_Δ, becomes a Langevin equation. Since the equation of motion, $\delta\Gamma/\delta\phi =$

0, is equivalent to $\delta e^{i\Gamma}/\delta\phi = 0$, we obtain

$$\Box\phi(x) + V'_{\rm eff}[\phi] + \int_{-\infty}^{t} dt' \int d^3x'\, B_{\rm a}(x-x')\phi(x') + \phi(x)\int_{-\infty}^{t} dt' \int d^3x'\, B_{\rm m}(x-x')\phi^2(x') = \xi_{\rm a}(x) + \xi_{\rm m}(x)\phi(x)\,. \tag{3.70}$$

The suffixes a (m) represents additive (multiplicative) noise.

The above treatment of the imaginary part of the effective action is not just a mathematical transformation but important steps to interpret the equation of motion. The right hand side, ξ and $\xi\phi$, kick or perturb the mean field ϕ and supply energy to it from the thermal bath. On the other hand, the non-local terms on the left hand side represent the friction, which dissipate energy of the mean field into the bath. In order for a system to achieve and keep thermal equilibrium, there is a necessary condition between noise terms and the memory terms, which is known as the fluctuation-dissipation relation.

For simplicity we concentrate on the additive noise term and the corresponding memory term. The similar discussion holds on the multiplicative noise and the memory term [20]. Since the fluctuation-dissipation relation can be seen simply in the Fourier space, we rewrite the equation of motion as

$$(-\omega^2 + |\vec{k}|^2 + m^2)\tilde{\phi}(\omega,\vec{k}) + \int \frac{d\omega'}{2\pi}\frac{\mathcal{P}}{\omega-\omega'} i\tilde{B}_{\rm a}(\omega,\vec{k}) + \frac{1}{2}\tilde{B}_{\rm a}(\omega,\vec{k})\tilde{\phi}(\omega,\vec{k}) = \tilde{\xi}(\omega,\vec{k})\,, \tag{3.71}$$

where $\mathcal{P}$ means its principle value. The noise correlation is given by

$$\langle \xi_{\rm a}(x_1)\xi_{\rm a}^{\dagger}(x_2)\rangle = A_{\rm a}(x_1 - x_2)\,. \tag{3.72}$$

Now the fluctuation-dissipation relation is written as

$$\frac{\tilde{A}_{\rm a}(\omega,\vec{k})}{\frac{-1}{\omega}{\rm Im}\tilde{B}_{\rm a}(\omega,\vec{k})} = \frac{\omega}{2}\frac{e^{\beta\omega}+1}{e^{\beta\omega}-1} = \omega\left(\frac{1}{2} + n_\omega\right). \tag{3.73}$$

For a variety of interactions we can check this relation. Explicit forms of non-local terms and noise correlations are found in Ref.[20]. This is the quantum fluctuation-dissipation relation [20, 21, 37, 38, 39]. In light of this fact, we conclude that the noise term introduced by rewriting the imaginary part of the effective action is not just a mathematical trick. In the high temperature limit, $\beta\omega \ll 1$, the right hand side of eq. (3.73) reduces to T.

Now let us explicitly see the fluctuation-dissipation relation by considering $\mathcal{L}_{\rm int} = -\lambda^2\chi^2\phi^2$. Functions A and B for additive noise and the correspondent non-local term in Fourier space are

calculated as

$$
\begin{aligned}
A_{\rm a}(\omega,\vec{k}) = -16\pi i\lambda^4 \int \frac{d^3q_1}{(2\pi)^3}\frac{d^3q_2}{(2\pi)^3}\frac{d^3q_3}{(2\pi)^3}(2\pi)^3\delta^3(\vec{q}_1+\vec{q}_2+\vec{q}_3-\vec{k})\frac{1}{8\omega_{q_1}\omega_{q_2}\omega_{q_3}} \\
\times\Big[\Big\{(1+n_{q_1})(1+n_{q_2})(1+n_{q_3})+n_{q_1}n_{q_2}n_{q_3}\Big\}\delta(\omega-\omega_{q_1}-\omega_{q_2}-\omega_{q_3}) \\
+\Big\{(1+n_{q_1})(1+n_{q_2})n_{q_3}+n_{q_1}n_{q_2}(1+n_{q_3})\Big\}\delta(\omega-\omega_{q_1}-\omega_{q_2}+\omega_{q_3}) \\
+\Big\{(1+n_{q_1})n_{q_2}(1+n_{q_3})+n_{q_1}(1+n_{q_2})n_{q_3}\Big\}\delta(\omega-\omega_{q_1}+\omega_{q_2}-\omega_{q_3}) \\
+\Big\{n_{q_1}(1+n_{q_2})(1+n_{q_3})+(1+n_{q_1})n_{q_2}n_{q_3}\Big\}\delta(\omega+\omega_{q_1}-\omega_{q_2}-\omega_{q_3}) \\
+\Big\{(1+n_{q_1})n_{q_2}n_{q_3}+n_{q_1}(1+n_{q_2})(1+n_{q_3})\Big\}\delta(\omega-\omega_{q_1}+\omega_{q_2}+\omega_{q_3}) \\
+\Big\{n_{q_1}(1+n_{q_2})n_{q_3}+(1+n_{q_1})n_{q_2}(1+n_{q_3})\Big\}\delta(\omega+\omega_{q_1}-\omega_{q_2}+\omega_{q_3}) \\
+\Big\{n_{q_1}n_{q_2}(1+n_{q_3})+(1+n_{q_1})(1+n_{q_2})n_{q_3}\Big\}\delta(\omega+\omega_{q_1}-\omega_{q_2}+\omega_{q_3}) \\
+\Big\{n_{q_1}n_{q_2}n_{q_3}+(1+n_{q_1})(1+n_{q_2})(1+n_{q_3})\Big\}\delta(\omega+\omega_{q_1}+\omega_{q_2}+\omega_{q_3})\Big],
\end{aligned}
\tag{3.74}
$$

$$
\begin{aligned}
B_{\rm a}(\omega,\vec{k}) = 8\pi\lambda^4 \int \frac{d^3q_1}{(2\pi)^3}\frac{d^3q_2}{(2\pi)^3}\frac{d^3q_3}{(2\pi)^3}(2\pi)^3\delta^3(\vec{q}_1+\vec{q}_2+\vec{q}_3-\vec{k})\frac{1}{8\omega_{q_1}\omega_{q_2}\omega_{q_3}} \\
\times\Big[\Big\{(1+n_{q_1})(1+n_{q_2})(1+n_{q_3})-n_{q_1}n_{q_2}n_{q_3}\Big\}\delta(\omega-\omega_{q_1}-\omega_{q_2}-\omega_{q_3}) \\
+\Big\{(1+n_{q_1})(1+n_{q_2})n_{q_3}-n_{q_1}n_{q_2}(1+n_{q_3})\Big\}\delta(\omega-\omega_{q_1}-\omega_{q_2}+\omega_{q_3}) \\
+\Big\{(1+n_{q_1})n_{q_2}(1+n_{q_3})-n_{q_1}(1+n_{q_2})n_{q_3}\Big\}\delta(\omega-\omega_{q_1}+\omega_{q_2}-\omega_{q_3}) \\
+\Big\{n_{q_1}(1+n_{q_2})(1+n_{q_3})-(1+n_{q_1})n_{q_2}n_{q_3}\Big\}\delta(\omega+\omega_{q_1}-\omega_{q_2}-\omega_{q_3}) \\
+\Big\{(1+n_{q_1})n_{q_2}n_{q_3}-n_{q_1}(1+n_{q_2})(1+n_{q_3})\Big\}\delta(\omega-\omega_{q_1}+\omega_{q_2}+\omega_{q_3}) \\
+\Big\{n_{q_1}(1+n_{q_2})n_{q_3}-(1+n_{q_1})n_{q_2}(1+n_{q_3})\Big\}\delta(\omega+\omega_{q_1}-\omega_{q_2}+\omega_{q_3}) \\
+\Big\{n_{q_1}n_{q_2}(1+n_{q_3})-(1+n_{q_1})(1+n_{q_2})n_{q_3}\Big\}\delta(\omega+\omega_{q_1}-\omega_{q_2}+\omega_{q_3}) \\
+\Big\{n_{q_1}n_{q_2}n_{q_3}-(1+n_{q_1})(1+n_{q_2})(1+n_{q_3})\Big\}\delta(\omega+\omega_{q_1}+\omega_{q_2}+\omega_{q_3})\Big],
\end{aligned}
\tag{3.75}
$$

where $\omega_{q_1} = \sqrt{|\vec{q}_1|^2+m_\chi^2}$, $\omega_{q_2} = \sqrt{|\vec{q}_2|^2+m_\chi^2}$, $\omega_{q_3} = \sqrt{|\vec{q}_3|^2+m_\phi^2}$, and $n_{q_i} = \frac{1}{e^{\beta\omega_{q_i}}-1}$. We can explicitly see that the fluctuation-dissipation relation shown as eq. (3.73) holds.

Finally we comment on the functional form of the fluctuation-dissipation relation given by eq. (3.73). We consider the following equation of motion

$$
(-\omega^2+\vec{k}^2+\mathcal{M}^2)\tilde{\phi}(\omega,\vec{k})+\tilde{b}(\omega,\vec{k})\tilde{\phi}(\omega,\vec{k}) = \tilde{\xi}(\omega,\vec{k}), \tag{3.76}
$$

where $\mathcal{M}$ is the effective mass including corrections from interactions. $\tilde{b}(\omega,\vec{k})$ is defined as

$$
\tilde{b}(\omega,\vec{k}) = \int_0^\infty dt\, e^{i\omega t}B(t,\vec{k}). \tag{3.77}
$$

This expression enables us to connect the thermal average of the scalar field and that of noise term.

$$\langle\tilde{\phi}(\omega,\vec{k})\tilde{\phi}^{\dagger}(\omega',\vec{k'})\rangle = \frac{\langle\tilde{\xi}(\omega,\vec{k})\tilde{\xi}^{\dagger}(\omega',\vec{k'})\rangle}{\left(-\omega^2+\vec{k}^2+\mathcal{M}^2+\tilde{b}(\omega,\vec{k})\right)\left(-\omega'^2+\vec{k'}^2+\mathcal{M}^2+\tilde{b}^*(\omega',\vec{k'})\right)} \tag{3.78}$$

First, the ϕ in the left hand side is not an operator but a c-number, we may evaluate the left hand side as a Fourier transform of a symmetric propagator $\langle\{\hat{\phi}(t,\vec{x}),\hat{\phi}^{\dagger}(t',\vec{y})\}\rangle/2$ which corresponds to half of the Hadamard propagator. The Hadamard propagator G^1 can be expressed as

$$G^1(x,x') = G^{++}(x,x') + G^{--}(x,x')\,, \tag{3.79}$$

since G^{++} is an expectation value of T-product (Feynman propagator), and G^{--} is that of anti T-product (Dyson propagator). The right hand side becomes

$$\begin{aligned}
&\langle\phi(\omega,\vec{k})\phi^{\dagger}(\omega',\vec{k'})\rangle \\
&= \int dtdt'\, e^{i\omega t}e^{-i\omega' t'}(-i)\frac{1}{2}\left[G_k^{++}(t',t)+G_k^{--}(t',t)\right](2\pi)^3\delta^{(3)}(\vec{k}-\vec{k'}) \\
&= \int d\tau dt'\, e^{i\omega\tau}e^{i(\omega-\omega')t'}\frac{1}{2\omega_k}\Big[(1+2n_k)\left(e^{-i\omega_k\tau}+e^{i\omega_k\tau}\right)\Big](2\pi)^3\delta^{(3)}(\vec{k}-\vec{k'}) \quad (\tau\equiv t-t') \\
&= \frac{1}{2\omega_k}(1+2n_k)\Big[2\pi\delta(\omega-\omega_k)+2\pi\delta(\omega+\omega_k)\Big](2\pi)^4\delta(\omega-\omega')\delta^{(3)}(\vec{k}-\vec{k'}) \\
&= (1+2n_k)(2\pi)\delta(\omega^2-\omega_k^2)(2\pi)^4\delta(\omega-\omega')\delta^{(3)}(\vec{k}-\vec{k'})
\end{aligned} \tag{3.80}$$

Second, the noise correlation in k-space is

$$\langle\tilde{\xi}(\omega,\vec{k})\tilde{\xi}^{\dagger}(\omega',\vec{k'})\rangle = \tilde{A}(\omega,\vec{k})(2\pi)^4\delta(\omega-\omega')\delta^{(3)}(\vec{k}-\vec{k'})\,. \tag{3.81}$$

The right hand side of eq. (3.78) can be written as

$$\begin{aligned}
&(2\pi)^4\delta(\omega-\omega')\delta^{(3)}(\vec{k}-\vec{k'})\frac{\tilde{A}(\omega,\vec{k})}{\left(\omega^2+\vec{k}^2+\mathcal{M}^2+\tilde{b}(\omega,\vec{k})\right)\left(-\omega^2+\vec{k}^2+\mathcal{M}^2+\tilde{b}^*(-\omega,\vec{k})\right)} \\
=&(2\pi)^4\delta(\omega-\omega')\delta^{(3)}(\vec{k}-\vec{k'})\frac{\tilde{A}(\omega,\vec{k})}{-2i\mathrm{Im}\tilde{b}(\omega,\vec{k})}\left[\frac{1}{-\omega^2+\vec{k}^2+\mathcal{M}^2+\tilde{b}(\omega,\vec{k})}-\frac{1}{-\omega^2+\vec{k}^2+\mathcal{M}^2+\tilde{b}^*(\omega,\vec{k})}\right].
\end{aligned} \tag{3.82}$$

We further decompose the fraction like

$$\frac{1}{-\omega^2+\vec{k}^2+\mathcal{M}^2+\tilde{b}(\omega,\vec{k})} = \frac{1}{2\omega_k}\left(\frac{1}{\omega+\omega_k-\frac{i\mathrm{Im}\tilde{b}(\omega,\vec{k})}{2\omega}}-\frac{1}{\omega-\omega_k-\frac{i\mathrm{Im}\tilde{b}(\omega,\vec{k})}{2\omega}}\right). \tag{3.83}$$

Since b appears from interactions, in taking small-coupling limit we can rewrite them with delta functions by applying a formula

$$\lim_{\epsilon\to+0}\frac{1}{x\pm i\epsilon}=\frac{\mathcal{P}}{x}\mp i\pi\delta(x)\,. \tag{3.84}$$

Note that, to use this formula, signs of $\mathrm{Im}b_{\vec{k}}(\omega)$ at $\omega=\pm\omega_k$ are important. Let us assume $B(\vec{x},t)$ is an even function of $\vec{x}$. Of course it should be real so that the action is real. Under these conditions, $\mathrm{Im}\tilde{b}(\omega,\vec{k})$ becomes an odd function of ω. Furthermore, since $A(\vec{x},t)$ is expected to be an even function of t, $\tilde{A}_{\vec{k}}(\omega)$ is an even function of ω. Taking these considerations into account, we can express the right hand side of eq. (3.78) evaluated at free limit as

$$\pi\frac{\tilde{A}(+\omega_k,\vec{k})}{|\mathrm{Im}\tilde{b}(+\omega_k,\vec{k})|}\delta(\omega^2-\omega_k^2)(2\pi)^4\delta(\omega-\omega')\delta^{(3)}(\vec{k}-\vec{k}')\,. \tag{3.85}$$

By equating eq. (3.80) and eq. (3.85), we obtain the fluctuation-dissipation relation

$$\frac{\tilde{A}(+\omega_k,\vec{k})}{|\frac{2}{\omega_k}\mathrm{Im}\tilde{b}(+\omega_k,\vec{k})|}=\omega_k\left(\frac{1}{2}+n_k\right)=\frac{\omega_k}{2}\frac{e^{\beta\omega_k}+1}{e^{\beta\omega_k}-1}\,. \tag{3.86}$$

This is consistent with previous studies.

3.2.3 Effective Potential

In practice the effective potential is more useful than the effective action. Effective potential V_{eff} is defined as

$$\Gamma[\phi(x)=\varphi]=\int d^4x\,(-V_{\mathrm{eff}}[\varphi])\ ,\ \text{or}\quad V_{\mathrm{eff}}[\varphi]=\frac{-1}{V_4}\Gamma[\phi(x)=\varphi]\,, \tag{3.87}$$

where $V_4=\int d^4x$ is the spacetime volume and φ is a constant independent of spacetime coordinate x. Namely, the effective action, which is a functional of any field configurations $\phi(x)$, reduces to the effective potential up to the factor $-V_4$.

The 1-loop correction of the effective potential is expressed as

$$V_{\mathrm{eff}}^{1-\mathrm{loop}}[\phi]=\frac{1}{2}\int\frac{d^4k}{(2\pi)^4}\log\left[iG^{-1}(k,\phi)\right]\,, \tag{3.88}$$

where ϕ_{cl} is the solution of the classical equation of motion and

$$iG^{-1}(k,\phi)=\left.\frac{\delta^2\mathcal{L}(\phi_{\mathrm{cl}}+\phi)}{\delta\phi^2}\right|_{\phi=0}\,. \tag{3.89}$$

Writing $iG^{-1}(k,\phi)=k^2+m^2(\phi)$, we can perform the k_0-integral and obtain

$$V_{\mathrm{eff}}^{1-\mathrm{loop}}[\phi]=\frac{1}{2}\int\frac{d^3k}{(2\pi)^3}\sqrt{|\vec{k}|^2+m^2(\phi)}\,. \tag{3.90}$$

At finite temperature, the effective potential becomes

$$V_{\rm eff}[\phi] = \frac{1}{2\beta}\sum_{n=-\infty}^{+\infty}\int\frac{d^3k}{(2\pi)^3}\log\left[\left(\frac{2\pi n}{\beta}\right)^2 + |\vec{k}|^2 + m^2(\phi)\right] \tag{3.91}$$

Evaluation of this expression is a bit technical [34]. We would like to calculate

$$v_{\rm b}(E) \equiv \sum_{n=-\infty}^{+\infty}\log\left[\left(\frac{2\pi n}{\beta}\right)^2 + E^2\right], \tag{3.92}$$

which is diverging. However, we can extract the ϕ-dependent part by performing differentiation and integration with respect to E to impose the divergence on the integration constant.

$$\begin{aligned}\frac{\partial v_{\rm b}}{\partial E} &= \sum_{n=-\infty}^{\infty}\frac{2E}{\left(\frac{2\pi n}{\beta}\right)^2 + E^2} = \beta\coth\frac{\beta E}{2}\,,\\ v_{\rm b}(E) &= \int dE\frac{\partial v_{\rm b}}{\partial E} = \beta E + 2\log\left(1 - e^{-\beta E}\right).\end{aligned} \tag{3.93}$$

The above treatment leads to

$$V_{\rm eff}[\phi] = \int\frac{d^3k}{(2\pi)^3}\left[\frac{1}{2}\sqrt{|\vec{k}|^2 + m^2(\phi)} + \frac{1}{\beta}\log\left[1 - e^{-\beta\sqrt{|\vec{k}|^2+m^2(\phi)}}\right]\right] + (\text{const.})\,, \tag{3.94}$$

where the finite-temperature correction appears as the second term in the integrand.

The effective potential coming from interactions with fermions are calculated in the same way.

$$V_{\rm eff}[\phi] = -\frac{2}{\beta}\sum_{n=-\infty}^{+\infty}\int\frac{d^3k}{(2\pi)^3}\log\left[\left(\frac{(2n+1)\pi}{\beta}\right)^2 + |\vec{k}|^2 + m^2(\phi)\right] \tag{3.95}$$

We also evaluate the following quantity

$$v_{\rm f}(E) \equiv \sum_{n=-\infty}^{+\infty}\log\left[\left(\frac{(2n+1)\pi}{\beta}\right)^2 + E^2\right], \tag{3.96}$$

by a set of differentiation and integration as

$$\begin{aligned}\frac{\partial v_{\rm f}}{\partial E} &= \sum_{n=-\infty}^{\infty}\frac{2E}{\left(\frac{(2n+1)\pi}{\beta}\right)^2 + E^2} = \frac{4\beta}{\pi}\sum_{n:\text{odd}}\frac{\frac{\beta E}{\pi}}{n^2 + \left(\frac{\beta E}{\pi}\right)^2} = \beta\tanh\frac{\beta E}{2}\,,\\ v_{\rm f}(E) &= \int dE\frac{\partial v_{\rm f}}{\partial E} = \beta E + 2\log\left(1 + e^{-\beta E}\right).\end{aligned} \tag{3.97}$$

Then the effective potential from interactions with fermion becomes

$$V_{\rm eff}[\phi] = -\int\frac{d^3k}{(2\pi)^3}\left[\frac{1}{2}\sqrt{|\vec{k}|^2 + m^2(\phi)} + \frac{1}{\beta}\log\left[1 + e^{-\beta\sqrt{|\vec{k}|^2+m^2(\phi)}}\right]\right] + (\text{const.})\,. \tag{3.98}$$

3.3 Extension to Gauged Scalar Field

So far, the effective action and the resultant equation of motion of a scalar field has been studied in models where it has self-interaction and interactions with other fermions and scalar bosons [19, 20]. Therefore it is interesting to extend the previous studies to include interactions with gauge fields. In this section we consider the effects from gauge interactions on the effective action of scalar fields by analyzing scalar QED [40]. This consideration would help us to complete the field theory at finite temperature.

3.3.1 Settings

The Lagrangian density of Scalar QED is given by

$$\begin{aligned}\mathcal{L} =& D_\mu \Phi^\dagger D^\mu \Phi - m^2 \Phi^\dagger \Phi - \frac{1}{4} F_{\mu\nu} F^{\mu\nu} \\ =& \partial_\mu \Phi^\dagger \partial^\mu \Phi - m^2 \Phi^\dagger \Phi - \frac{1}{4} F_{\mu\nu} F^{\mu\nu} \\ &+ ieA_\mu (\Phi^\dagger \partial^\mu \Phi - \Phi \partial^\mu \Phi^\dagger) + e^2 A_\mu A^\mu \Phi^\dagger \Phi \,. \end{aligned} \tag{3.99}$$

In considering physical quantities we impose the Coulomb gauge condition $\vec{\nabla} \cdot \vec{A} = 0$, which enable us to rewrite the Lagrangian as

$$\begin{aligned}\mathcal{L} =& \partial_\mu \Phi^\dagger \partial^\mu \Phi - m^2 \Phi^\dagger \Phi + \frac{1}{2} \partial_\mu \vec{A}_T \cdot \partial^\mu \vec{A}_T \\ &- ie\vec{A}_T (\Phi \vec{\nabla} \Phi^\dagger - \Phi^\dagger \vec{\nabla} \Phi) - e^2 \vec{A}_T \cdot \vec{A}_T \Phi^\dagger \Phi \\ &+ \frac{1}{2} (\vec{\nabla} A_0)^2 - ieA_0 (\Phi \dot{\Phi}^\dagger - \Phi^\dagger \dot{\Phi}) + e^2 A_0^2 \Phi^\dagger \Phi \,, \end{aligned} \tag{3.100}$$

where $\vec{A}_{\mathrm{T}}$ represents the transverse components, which satisfy $\vec{\nabla} \cdot \vec{A}_{\mathrm{T}} = 0$. Though we use the Coulomb gauge, other choices of gauge, such as axial gauge or Lorenz gauge, should also be possible in principle [3)]. Although the equation of motion may be gauge dependent, physical quantities calculated from it should be gauge invariant. We discuss this issue in Appendix by showing that the dissipation rate is independent on the choice of gauge.

Following Boyanovsky *et al.* [41], thermal propagators for the scalar field Φ and gauge field $\vec{A}_{\mathrm{T}}$ are expressed as follows.

Propagators for the scalar field:

$$\langle \Phi^{(a)\dagger}(\vec{x}, t) \Phi^{(b)}(\vec{x'}, t') \rangle = -i \int \frac{d^3k}{(2\pi)^3} G_k^{ab}(t, t') e^{-i\vec{k} \cdot (\vec{x} - \vec{x'})} \tag{3.101}$$

[3)] In addition to these conditions, we come up with the so-called covariant gauge. While it is often convenient to use it, we should note that it has a different meaning from other gauge conditions, namely, we do not specify the gauge-fixing condition in the covariant gauge. In calculating effective action, this gauge is inappropriate since it is useful only in the problems where physical quantities such as the S-matrix elements can be directly calculated.

$$G_k^{++}(t,t') = G_k^{>}(t,t')\Theta(t-t') + G_k^{<}(t,t')\Theta(t'-t) \tag{3.102}$$
$$G_k^{--}(t,t') = G_k^{>}(t,t')\Theta(t'-t) + G_k^{<}(t,t')\Theta(t-t') \tag{3.103}$$
$$G_k^{+-}(t,t') = -G_k^{<}(t,t') \tag{3.104}$$
$$G_k^{-+}(t,t') = -G_k^{>}(t,t') \tag{3.105}$$

$$G_k^{>}(t,t') = \frac{i}{2\omega_k}\Big[(1+n_k)e^{-i\omega_k(t-t')} + n_k e^{+i\omega_k(t-t')}\Big] \tag{3.106}$$
$$G_k^{<}(t,t') = \frac{i}{2\omega_k}\Big[n_k e^{-i\omega_k(t-t')} + (1+n_k)e^{+i\omega_k(t-t')}\Big] \tag{3.107}$$

$$\omega_k = \sqrt{|\vec{k}|^2 + m^2},\ n_k = \frac{1}{e^{\beta\omega_k} - 1} \tag{3.108}$$

Although we have already seen these propagators before, it is convenient to use the expression in $(t, \vec{k})$ space.

Propagators for the gauge field:

$$\langle A_{Ti}^{(a)}(\vec{x},t) A_{Tj}^{(b)}(\vec{x'},t')\rangle = -i\int \frac{d^3k}{(2\pi)^3}\mathcal{G}_{k\,ij}^{ab}(t,t')e^{-i\vec{k}\cdot(\vec{x}-\vec{x'})} \tag{3.109}$$

$$\mathcal{G}_{k\,ij}^{++}(t,t') = \mathcal{P}_{ij}(\vec{k})\Big[g_k^{>}(t,t')\Theta(t-t') + g_k^{<}(t,t')\Theta(t'-t)\Big] \tag{3.110}$$
$$\mathcal{G}_{k\,ij}^{--}(t,t') = \mathcal{P}_{ij}(\vec{k})\Big[g_k^{>}(t,t')\Theta(t'-t) + g_k^{<}(t,t')\Theta(t-t')\Big] \tag{3.111}$$
$$\mathcal{G}_{k\,ij}^{+-}(t,t') = -\mathcal{P}_{ij}(\vec{k})g_k^{<}(t,t') \tag{3.112}$$
$$\mathcal{G}_{k\,ij}^{-+}(t,t') = -\mathcal{P}_{ij}(\vec{k})g_k^{>}(t,t') \tag{3.113}$$

$$g_k^{>}(t,t') = \frac{i}{2k}\Big[(1+N_k)e^{-ik(t-t')} + N_k e^{+ik(t-t')}\Big] \tag{3.114}$$
$$g_k^{<}(t,t') = \frac{i}{2k}\Big[N_k e^{-ik(t-t')} + (1+N_k)e^{+ik(t-t')}\Big] \tag{3.115}$$

$$k = \sqrt{|\vec{k}|^2},\quad N_k = \frac{1}{e^{\beta k}-1},\quad \mathcal{P}_{ij}(\vec{k}) = \delta_{ij} - \frac{k_i k_j}{k^2} \tag{3.116}$$

The generating functional of the Green's function, $Z[J^{(+)}, J^{(-)}]$, is

$$Z[J^{(+)},J^{(-)}] = \int \mathcal{D}\vec{A}_T\mathcal{D}\Phi\mathcal{D}\Phi^{\dagger}\exp\left[i(S^{(+)}-S^{(-)}) + i\int d^4x\,\left\{J^{(+)}(x)\Phi^{(+)}(x) - J^{(-)}(x)\Phi^{(-)}(x)\right\}\right], \tag{3.117}$$

where

$$S^{(\pm)} = \int d^4x \mathcal{L}[\vec{A}_T^{(\pm)},\ \Phi^{(\pm)},\ \Phi^{\dagger(\pm)}]\,. \tag{3.118}$$

3.3.2 Effective Action and Langevin equation

As we saw before, calculating the effective action corresponds to the summation of one-particle-irreducible (1PI) diagrams. Practically, though, effective action can be obtained only by means of a perturbative expansion in terms of the gauge coupling constant e. The lowest nontrivial contributions to the effective action appear at the second order of coupling constant e. At this order, there are two relevant diagrams, which are shown in Fig. 3.3.

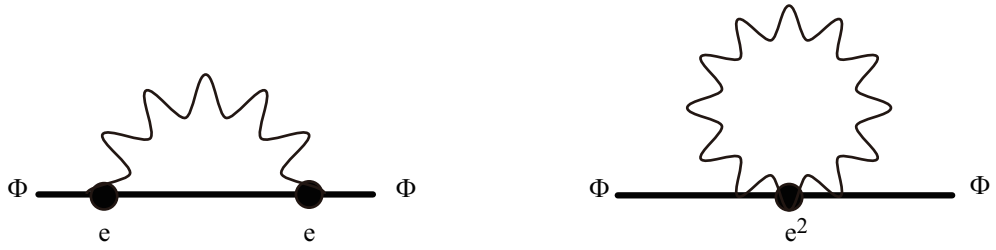

Figure 3.3: $O(e^2)$ 1PI diagrams. The solid/wavy line represents the scalar/photon propagator, respectively. The left diagram generates nonlocal terms in the effective action. The right diagram produces a thermal correction to the mass term, which is proportional to T^2.

In addition to these 1PI diagrams, we have to rewrite A_0 using its Euler-Lagrange equation as

$$A_0(x) = -\frac{1}{\Delta}\rho(x) + O(e^2) \tag{3.119}$$

$$\rho \equiv ie(\Phi\dot{\Phi}^\dagger - \Phi^\dagger\dot{\Phi}) \tag{3.120}$$

and take the following interaction into account:

$$\frac{1}{2}(\vec{\nabla}A_0)^2 \overset{\text{td}}{=} -\frac{1}{2}A_0\Delta A_0 = \frac{1}{2}\rho\frac{1}{\Delta}\rho = \frac{e^2}{8\pi}\int d^3y \frac{(\Phi\dot{\Phi}^\dagger - \Phi^\dagger\dot{\Phi})(\vec{x},t)(\Phi\dot{\Phi}^\dagger - \Phi^\dagger\dot{\Phi})(\vec{y},t)}{|\vec{x}-\vec{y}|} \tag{3.121}$$

Here $\overset{\text{td}}{=}$ means an equality up to a total derivative term. Obviously this represents the Coulomb potential. Although the meaning of this interaction is clearly seen in real space, we can treat it more easily in Fourier space. The action corresponding to this term is given by

$$S \supset \frac{e^2}{2}\int dt \int \frac{d^3k}{(2\pi)^3}\int \frac{d^3p}{(2\pi)^3}\int \frac{d^3q}{(2\pi)^3}\,\frac{1}{\vec{k}^2}\left(\tilde{\Phi}(t,\vec{p})\dot{\tilde{\Phi}}^\dagger(t,\vec{p}-\vec{k}) - \dot{\tilde{\Phi}}(t,\vec{p})\tilde{\Phi}^\dagger(t,\vec{p}-\vec{k})\right) \times\left(\tilde{\Phi}(t,\vec{q})\dot{\tilde{\Phi}}^\dagger(t,\vec{k}+\vec{q}) - \dot{\tilde{\Phi}}(t,\vec{q})\tilde{\Phi}^\dagger(t,\vec{k}+\vec{q})\right), \tag{3.122}$$

where $\tilde{\Phi}(t,\vec{p})$ is the spatial Fourier transformation of $\Phi(t,\vec{x})$, defined as

$$\tilde{\Phi}(t,\vec{p}) \equiv \int d^3x\, e^{i\vec{p}\cdot\vec{x}}\Phi(t,\vec{x})\,. \tag{3.123}$$

The contribution of the left diagram in Fig. 3.3 to the effective action Γ is

$$\begin{aligned}\Gamma \supset &+ 4ie^2 \int d^4x_1 d^4x_2 \left\langle A^{(+)}_{Ti}(x_1) A^{(+)}_{Tj}(x_2) \right\rangle \left\langle \partial_i \Phi^{\dagger(+)}(x_1) \partial_j \Phi^{(+)}(x_2) \right\rangle \Phi^{\dagger(+)}(x_2) \Phi^{(+)}(x_1) \\ &+ 4ie^2 \int d^4x_1 d^4x_2 \left\langle A^{(-)}_{Ti}(x_1) A^{(-)}_{Tj}(x_2) \right\rangle \left\langle \partial_i \Phi^{\dagger(-)}(x_1) \partial_j \Phi^{(-)}(x_2) \right\rangle \Phi^{\dagger(-)}(x_2) \Phi^{(-)}(x_1) \\ &- 4ie^2 \int d^4x_1 d^4x_2 \left\langle A^{(-)}_{Ti}(x_1) A^{(+)}_{Tj}(x_2) \right\rangle \left\langle \partial_i \Phi^{\dagger(-)}(x_1) \partial_j \Phi^{(+)}(x_2) \right\rangle \Phi^{\dagger(+)}(x_2) \Phi^{(-)}(x_1) \\ &- 4ie^2 \int d^4x_1 d^4x_2 \left\langle A^{(+)}_{Ti}(x_1) A^{(-)}_{Tj}(x_2) \right\rangle \left\langle \partial_i \Phi^{\dagger(+)}(x_1) \partial_j \Phi^{(-)}(x_2) \right\rangle \Phi^{\dagger(-)}(x_2) \Phi^{(+)}(x_1) \,, \end{aligned} \tag{3.124}$$

and the right diagram gives the following contribution,

$$\Gamma \supset -e^2 \int d^4x \Big[\left\langle A^{(+)}_{Ti}(x) A^{(+)}_{Ti}(x) \right\rangle \Phi^{\dagger(+)}(x) \Phi^{(+)}(x) - \left\langle A^{(-)}_{Ti}(x) A^{(-)}_{Ti}(x) \right\rangle \Phi^{\dagger(-)}(x) \Phi^{(-)}(x) \Big] \,. \tag{3.125}$$

The propagators of gauge field are calculated as

$$\left\langle A^{(+)}_{Ti}(x) A^{(+)}_{Ti}(x) \right\rangle = \left\langle A^{(-)}_{Ti}(x) A^{(-)}_{Ti}(x) \right\rangle = \int \frac{d^3k}{(2\pi)^3} \frac{2}{k} \left(\frac{1}{2} + N_k \right) , \tag{3.126}$$

where the first term in the bracket in the right hand side contains divergence, which should be removed by the same counter term as that in zero temperature. Therefore we only focus on the finite-temperature correction, which becomes

$$\left\langle A^{(+)}_{Ti}(x) A^{(+)}_{Ti}(x) \right\rangle = \left\langle A^{(-)}_{Ti}(x) A^{(-)}_{Ti}(x) \right\rangle = \frac{T^2}{6} \,. \tag{3.127}$$

As for the Coulomb potential term (3.122), although it does not have diagrammatic correspondence, we implement the same procedure as the previous interaction terms. After taking contractions except for two field variables which correspond to external lines, we have

$$\begin{aligned}\Gamma \supset -ie^2 \int dt \int \frac{d^3k}{(2\pi)^3} \frac{d^3p}{(2\pi)^3} \frac{1}{|\vec{k}-\vec{p}|^2} \Big[&-G^{++}_p(t,t) \left(\dot{\tilde{\Phi}}^{(+)} \dot{\tilde{\Phi}}^{\dagger(+)} - \dot{\tilde{\Phi}}^{\dagger(-)} \dot{\tilde{\Phi}}^{\dagger(-)} \right)(t,\vec{k}) \\ &+ \ddot{G}^{++}_p(t,t) \left(\tilde{\Phi}^{(+)} \tilde{\Phi}^{\dagger(+)} - \tilde{\Phi}^{\dagger(-)} \tilde{\Phi}^{\dagger(-)} \right)(t,\vec{k}) \Big] \,. \end{aligned} \tag{3.128}$$

Now it is convenient to introduce new variables and replace $\Phi^{(\pm)}$ with them,

$$\Phi^{(\pm)} = \phi_c \pm \frac{1}{2} \phi_\Delta \,. \tag{3.129}$$

Finally we obtain the effective action Γ, incorporating these two diagrams and A_0 terms up

to the second order in e, as

$$\begin{aligned}
\Gamma = & \int d^4x \left[\phi_\Delta^\dagger(x)\left(-\partial_\mu\partial^\mu - m^2 - e^2\frac{T^2}{6}\right)\phi_c(x)\right. \\
& \left. + \phi_\Delta(x)\left(-\partial_\mu\partial^\mu - m^2 - e^2\frac{T^2}{6}\right)\phi_c(x)^\dagger\right] \\
& - 4ie^2\int d^4x_1 d^4x_2 \int \frac{d^3p_1}{(2\pi)^3}\frac{d^3p_2}{(2\pi)^3} e^{-i(\vec{p_1}+\vec{p_2})\cdot(\vec{x_1}-\vec{x_2})}\mathcal{P}_{ij}(\vec{p_1})p_{2i}p_{2j}\Theta(t_2-t_1) \\
& \quad [g^<_{p_1}(t_1,t_2)G^<_{p_2}(t_1,t_2) - g^>_{p_1}(t_1,t_2)G^>_{p_2}(t_1,t_2)]\left(\phi_c^\dagger(x_1)\phi_\Delta(x_2) + \phi_c(x_1)\phi_\Delta^\dagger(x_2)\right) \\
& - 2ie^2\int d^4x_1 d^4x_2 \int \frac{d^3p_1}{(2\pi)^3}\frac{d^3p_2}{(2\pi)^3} e^{-i(\vec{p_1}+\vec{p_2})\cdot(\vec{x_1}-\vec{x_2})}\mathcal{P}_{ij}(\vec{p_1})p_{2i}p_{2j} \\
& \quad [g^<_{p_1}(t_1,t_2)G^<_{p_2}(t_1,t_2) + g^>_{p_1}(t_1,t_2)G^>_{p_2}(t_1,t_2)]\phi_\Delta^\dagger(x_1)\phi_\Delta(x_2) \\
& + \Gamma_{A_0}\,,
\end{aligned} \tag{3.130}$$

$$\begin{aligned}
\Gamma_{A_0} = & -e^2\int \frac{d^4k}{(2\pi)^4}\frac{d^3p}{(2\pi)^3}\frac{1}{|\vec{k}-\vec{q}|^2}\cdot\left(\frac{1}{2}+n_p\right)\cdot\left(\frac{\omega^2}{\omega_p}+\omega_p\right) \\
& \times\left(\tilde{\phi_c}(k)\tilde{\phi_\Delta}^\dagger(k) + \tilde{\phi_\Delta}(k)\tilde{\phi_c}^\dagger(k)\right) \\
\equiv & \int \frac{d^4k}{(2\pi)^4}\left(\tilde{\phi_c}(k)\tilde{\phi_\Delta}^\dagger(k) + \tilde{\phi_\Delta}(k)\tilde{\phi_c}^\dagger(k)\right)\tilde{f}_{A_0}(k)\,.
\end{aligned} \tag{3.131}$$

Γ_{A_0} comes from the Coulomb potential term, which gives corrections to the dispersion relation as well as the thermal mass term.

Let us show that the non-local terms which come from diagrams in Fig. 3.3 have a non-zero imaginary part. First, both of the integrands are invariant under replacements $\vec{p}_1 \to -\vec{p}_1$ and $\vec{p}_2 \to -\vec{p}_2$ respectively. This property allows us to replace $e^{-i(\vec{p}_1+\vec{p}_2)\cdot(\vec{x}_1-\vec{x}_2)}$ with $\cos\left[(\vec{p}_1+\vec{p}_2)\cdot(\vec{x}_1-\vec{x}_2)\right]$. Second, from Eqs. (3.106), (3.107), (3.114), and (3.115), we note that $g^<G^< - g^>G^>$ is purely imaginary and $g^<G^< + g^>G^>$ is real. Thus, the first non-local term is real and the second one is purely imaginary.

The imaginary part of the effective action is

$$i\Gamma \supset -\int d^4x_1 d^4x_2\, \mathcal{N}(x_1-x_2)\left(\phi_{\Delta\mathrm{R}}(x_1)\phi_{\Delta\mathrm{R}}(x_2) + \phi_{\Delta\mathrm{I}}(x_1)\phi_{\Delta\mathrm{I}}(x_2)\right)\,, \tag{3.132}$$

where

$$\begin{aligned}
\mathcal{N}(x_1-x_2) = & -2e^2\int \frac{d^3p_1}{(2\pi)^3}\frac{d^3p_2}{(2\pi)^3} e^{-i(\vec{p_1}+\vec{p_2})\cdot(\vec{x_1}-\vec{x_2})}\mathcal{P}_{ij}(\vec{p_1})p_{2i}p_{2j} \\
& [g^<_{p_1}(t_1,t_2)G^<_{p_2}(t_1,t_2) + g^>_{p_1}(t_1,t_2)G^>_{p_2}(t_1,t_2)]\,.
\end{aligned} \tag{3.133}$$

$\phi_{\Delta\mathrm{R/I}}$ are the real/imaginary part of ϕ_Δ, respectively.

The Fourier transformation of $\mathcal{N}$ with respect to $t-t'$ and $\vec{x}-\vec{x}'$ is

$$\begin{aligned}\tilde{\mathcal{N}}(\omega,\vec{k}) =& 2e^2\int\frac{d^3p_1}{(2\pi)^3}\frac{d^3p_2}{(2\pi)^3}\mathcal{P}_{ij}(\vec{p_1})p_{2i}p_{2j}(2\pi)^3\delta(\vec{k}-\vec{p_1}-\vec{p_2})\\ &\frac{2\pi}{2p_1 2\omega_{p_2}}\Big[\{(1+N_{p_1})(1+n_{p_2})+N_{p_1}n_{p_2}\}\delta(\omega-p_1-\omega_{p_2})\\ &+\{(1+N_{p_1})n_{p_2}+N_{p_1}(1+n_{p_2})\}\delta(\omega-p_1+\omega_{p_2})\\ &+\{N_{p_1}(1+n_{p_2})+(1+N_{p_1})n_{p_2}\}\delta(\omega+p_1-\omega_{p_2})\\ &+\{N_{p_1}n_{p_2}+(1+N_{p_1})(1+n_{p_2})\}\delta(\omega+p_1+\omega_{p_2})\Big]. \end{aligned}\tag{3.134}$$

Clearly, this is positive for any $(\omega,\vec{k})$, and thus this expression ensures us that we can use the formula (3.65) and rewrite the effective action with stochastic noise terms.

Now we obtain a real effective action S_{eff} by introducing noise terms. To derive an equation of motion for the physical variable ϕ_c in the closed time-path formalism we take a variation with respect to ϕ_Δ and set it to zero. The equation of motion of the physical variable $\phi_c(x)$, which is obtained after taking a variation with respect to ϕ_Δ and setting it to zero, is

$$\begin{aligned}&\left(\Box+m^2+e^2\frac{T^2}{6}\right)\phi_c(x)-\int d^4x'\,f_{A_0}(x-x')\phi_c(x')\\ &+4ie^2\int_{-\infty}^{t}dt'\int d^3x'\int\frac{d^3p_1}{(2\pi)^3}\frac{d^3p_2}{(2\pi)^3}e^{-i(\vec{p_1}+\vec{p_2})\cdot(\vec{x'}-\vec{x})}\mathcal{P}_{ij}(\vec{p_1})p_{2i}p_{2j}\\ &\quad[g^<_{p_1}(t',t)G^<_{p_2}(t',t)-g^>_{p_1}(t',t)G^>_{p_2}(t',t)]\phi_c(t',\vec{x'})\\ &=\xi(x)\,. \end{aligned}\tag{3.135}$$

By writing the non-local memory term as

$$\int_{-\infty}^{t}dt'\int d^3x\,C(x-x')\phi(x')\,,\tag{3.136}$$

The equation of motion in the Fourier space is

$$\begin{aligned}&(-\omega^2+k^2+m^2)\tilde{\phi}(\omega,\vec{k})\\ &+\left(e^2\frac{T^2}{6}-\tilde{f}_{A_0}(\omega,\vec{k})+\int\frac{d\omega'}{2\pi}\frac{\mathcal{P}}{\omega-\omega'}i\tilde{C}(\omega',\vec{k})\right)\tilde{\phi}(\omega,\vec{k})\\ &+\frac{1}{2}\tilde{C}(\omega,\vec{k})\tilde{\phi}(\omega,\vec{k})=\tilde{\xi}(\omega,\vec{k})\,. \end{aligned}\tag{3.137}$$

Note that $\tilde{C}$ is purely imaginary and $\tilde{f}_{A_0}$ is real, hence all the coefficients of $\tilde{\phi}$ in the second line are real. They can be interpreted as corrections to the free part, i.e., the first line. The terms in the third line can be interpreted as dissipation and fluctuation.

The imaginary part of the Fourier transformation of the memory kernel $C(t,\vec{x})$ is

$$\begin{aligned}\mathrm{Im}\tilde{C}(\omega,\vec{k}) = -4e^2\int\frac{d^3p_1}{(2\pi)^3}\frac{d^3p_2}{(2\pi)^3}\mathcal{P}_{ij}(\vec{p_1})p_{2i}p_{2j}(2\pi)^3\delta^{(3)}(\vec{k}-\vec{p_1}-\vec{p_2})\\ \times\frac{2\pi}{2p_1 2\omega_{p_2}}\Big[\{(1+N_{p_1})(1+n_{p_2})-N_{p_1}n_{p_2}\}\delta(\omega-p_1-\omega_{p_2})\\ +\{(1+N_{p_1})n_{p_2}-N_{p_1}(1+n_{p_2})\}\delta(\omega-p_1+\omega_{p_2})\\ +\{N_{p_1}(1+n_{p_2})-(1+N_{p_1})n_{p_2}\}\delta(\omega+p_1-\omega_{p_2})\\ +\{N_{p_1}n_{p_2}-(1+N_{p_1})(1+n_{p_2})\}\delta(\omega+p_1+\omega_{p_2})\Big]. \quad (3.138)\end{aligned}$$

Therefore the fluctuation-dissipation relation also holds in Scalar QED.

$$\frac{\tilde{\mathcal{N}}(\omega,\vec{k})}{\frac{-1}{\omega}\mathrm{Im}\tilde{C}(\omega,\vec{k})} = \frac{\omega}{2}\frac{e^{\beta\omega}+1}{e^{\beta\omega}-1} = \omega\left(\frac{1}{2}+n_\omega\right). \quad (3.139)$$

3.3.3 Properties of the Stochastic Noise

We see that the equal-time noise correlation is expressed as

$$\begin{aligned}&\langle\xi(\vec{x_1},t)\xi^\dagger(\vec{x_2},t)\rangle\\ =&\frac{e^2}{2}\int\frac{d^3p_1}{(2\pi)^3}\int\frac{d^3p_2}{(2\pi)^3}e^{-i(\vec{p_1}+\vec{p_2})\cdot(\vec{x_1}-\vec{x_2})}\mathcal{P}_{ij}(\vec{p_1})p_{2i}p_{2j}\frac{1}{p_1\omega_{p_2}}(1+2N_{p_1})(1+2n_{p_2}).\end{aligned} \quad (3.140)$$

It is convenient to divide it as

$$\begin{aligned}\langle\xi(\vec{x_1},t)\xi^\dagger(\vec{x_2},t)\rangle =&\frac{e^2}{2}(\alpha_{ij}-\beta_{ij})\gamma_{ij}\\ =&\frac{e^2}{2}\Big[-\alpha(r)\left(\gamma''(r)+\frac{2}{r}\gamma'(r)\right)-\frac{2}{r^2}\beta'(r)\gamma'(r)-\beta''(r)\gamma''(r)\Big],\end{aligned} \quad (3.141)$$

where

$$\alpha_{ij} = \int\frac{d^3p_1}{(2\pi)^3}e^{-i\vec{p_1}\cdot\vec{r}}\frac{1}{p_1}\left(1+\frac{2}{e^{\beta p_1}-1}\right)\delta_{ij}\equiv\alpha(r)\delta_{ij}, \quad (3.142)$$

$$\beta_{ij} = \int\frac{d^3p_1}{(2\pi)^3}e^{-i\vec{p_1}\cdot\vec{r}}\frac{p_{1i}p_{1j}}{p_1^3}\left(1+\frac{2}{e^{\beta p_1}-1}\right)\equiv-\frac{\partial}{\partial r_i}\frac{\partial}{\partial r_j}\beta(r), \quad (3.143)$$

$$\gamma_{ij} = \int\frac{d^3p_2}{(2\pi)^3}e^{-i\vec{p_2}\cdot\vec{r}}\frac{p_{2i}p_{2j}}{\omega_{p_2}}\left(1+\frac{2}{e^{\beta\omega_{p_2}}-1}\right)\equiv-\frac{\partial}{\partial r_i}\frac{\partial}{\partial r_j}\gamma(r), \quad (3.144)$$

and we use $r=|\vec{r}|=|\vec{x_1}-\vec{x_2}|$.

The functions α, β, γ and their derivatives can be expressed as follows.

$$\alpha(r) = \frac{1}{2\pi r\beta}\coth\left(\frac{r}{\beta}\pi\right) \tag{3.145}$$

$$\beta'(r) = -\frac{1}{2\pi^2 r} + \sum_{n=1}^{\infty}\frac{-r + n\beta\,\mathrm{Arccot}(\frac{n\beta}{r})}{\pi^2 r^2} \tag{3.146}$$

$$\beta''(r) = \frac{1}{\pi^2 r^2} - \frac{1}{2\pi r\beta}\coth(\frac{r}{\beta}\pi) + \sum_{n=1}^{\infty}\frac{2}{\pi^2 r^3}\Big[r - n\beta\,\mathrm{Arccot}(\frac{n\beta}{r})\Big] \tag{3.147}$$

$$\gamma'(r) = -\frac{m^2}{2\pi^2 r}K_2(mr) - \frac{m^2 r}{\pi^2}\sum_{n=1}^{\infty}\frac{1}{r^2+n^2\beta^2}K_2(m\sqrt{r^2+n^2\beta^2}) \tag{3.148}$$

$$\begin{aligned}\gamma''(r) = &-\frac{m^2}{2\pi^2}\Big[\frac{1}{r^2}K_2(mr) - \frac{m}{r}K_3(mr)\Big] \\ &-\frac{m^2}{\pi^2}\sum_{n=1}^{\infty}\Big[\frac{1}{r^2+n^2\beta^2}K_2(m\sqrt{r^2+n^2\beta^2}) - \frac{mr^2}{(r^2+n^2\beta^2)^{3/2}}K_3(m\sqrt{r^2+n^2\beta^2})\Big]\end{aligned} \tag{3.149}$$

$K_\nu(z)$ is the modified Bessel function of the νth order.

As can be seen from the above expressions, they are so complicated. Then we consider simpler form in some limiting case. First, in the short-distance limit, the correlation function reduces to

$$\langle\xi(\vec{x_1},t)\xi^\dagger(\vec{x_2},t)\rangle \simeq -\frac{3e^2}{2\pi^4 r^6}\Theta(r) + \frac{e^2}{4\pi^4 r^5}\delta(r)\,. \tag{3.150}$$

For the derivation of this expression, see Appendix B. Here we define the step function as

$$\Theta(x) = \begin{cases} 0 & x \le 0\,, \\ 1 & x > 0\,. \end{cases} \tag{3.151}$$

On the other hand, in the long distance limit $r \gg \beta, \frac{1}{m}$, it becomes

$$\langle\xi(\vec{x_1},t)\xi^\dagger(\vec{x_2},t)\rangle \simeq -\frac{e^2m^2}{8\pi^2\beta^2 r^2}e^{-mr}\,. \tag{3.152}$$

For the massless scalar field, we obtain

$$\langle\xi(\vec{x_1},t)\xi^\dagger(\vec{x_2},t)\rangle \simeq -\frac{e^2}{8\pi^2\beta^2 r^4}\,. \tag{3.153}$$

For the derivation of these expressions, see Appendix B.

We show the spatial correlation for various masses in Fig. 3.4. As the approximate expression (3.152) shows, the noise correlation is exponentially suppressed at $r \gtrsim \frac{1}{m}$ and monotonically approaches zero. Asymptotically, the noise correlation obtained by numerical evaluation is consistent with the above simple expressions that were obtained analytically. We see that the noise in this model shows anticorrelation, which is different from the previous study [19].

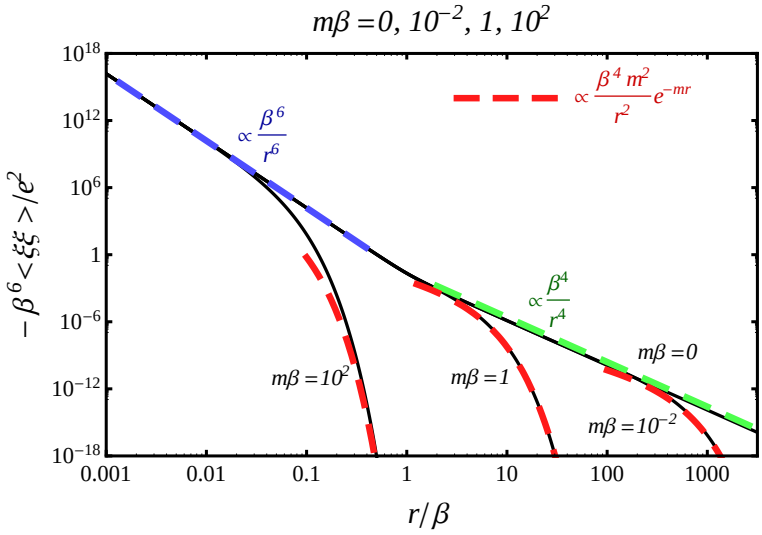

Figure 3.4: Noise spatial correlations for various mass values. The solid black line represents the exact expression (3.141) with Eqs. (3.145) ~ (3.149). The dashed blue, red, and green lines correspond to the analytical approximations (3.150), (3.152), and (3.153), respectively. For $r < \frac{1}{m}$, correlations obey power-law decay. They start to decay exponentially when r exceeds $\frac{1}{m}$.

3.3.4 Dissipation Rate

Let us evaluate the dissipation rate of the scalar field. As the equation of motion for the k mode oscillation of a scalar field, we consider

$$(-\omega^2 + M_{k,\omega}^2)\tilde{\phi}(\omega,\vec{k}) + \frac{1}{2}\tilde{C}(\omega,\vec{k})\tilde{\phi}(\omega,\vec{k}) = \tilde{\xi}(\omega,\vec{k})\,. \tag{3.154}$$

We assume the ω and nontrivial k dependence of $M_{k,\omega}$ is negligibly small, that is

$$M_{k,\omega}^2 = k^2 + M_0^2\,, \tag{3.155}$$

where M_0 is a constant. Under this assumption the dissipation rate of the k mode is given by

$$\Gamma_{\rm D}(\vec{k}) = -{\rm Im}\tilde{C}(\vec{k}, M_{k,\omega})/2M_{k,\omega}\,. \tag{3.156}$$

From the previous consideration, $M_{k,\omega}$ is given by

$$M_{k,\omega}^2 = k^2 + m^2 + e^2\frac{T^2}{6} - \tilde{f}_{A_0}(\omega,\vec{k}) + \int\frac{d\omega'}{2\pi}{\rm P}\frac{1}{\omega-\omega'}i\tilde{C}_{\vec{k}}(\omega')\,. \tag{3.157}$$

Both $\tilde{f}_{A_0}$ and the principal value integral are divergent, however, we can remove them by renormalizing the scalar field strength. In other words, we can cancel out this divergence by adding a counter term which is proportional to the kinetic term. The details are shown in Appendix.

Although the k and ω dependences of $M_{k,\omega}$ are nontrivial, such corrections are proportional to e^2 hence we can neglect them in small-coupling limit. Assuming $M_{k,\omega}$ is given by Eq. (3.155), we find

$$\begin{aligned}\Gamma_{\rm D}(\vec{k}) =& \frac{e^2}{4\pi}\frac{k}{\sqrt{M_0^2+k^2}}\int_{p_i}^{p_f} dp\left(1+\frac{1}{e^{\beta p}-1}-\frac{1}{e^{\beta(\sqrt{M_0^2+k^2}-p)}-1}\right)\\ &\times\left[-\frac{M_0^2}{k^2}+\frac{(M_0^2-m^2)\sqrt{M_0^2+k^2}}{k^2 p}-\frac{(M_0^2-m^2)^2}{4k^2p^2}\right]\\ p_i =& \frac{M_0^2-m^2}{2(\sqrt{M_0^2+k^2}+k)}, \quad p_f = \frac{M_0^2-m^2}{2(\sqrt{M_0^2+k^2}-k)}\end{aligned} \tag{3.158}$$

Though we derive this expression assuming $M_0 > m$, it is finite even in the limit of $M_0 \to m$. In this limit, we can obtain

$$\Gamma_{\rm D}(\vec{k}) = \begin{cases} \frac{e^2}{3\pi\beta}\frac{k^2}{m^2} & k \ll m \\ \frac{e^2}{2\pi\beta} & k \gg m\,. \end{cases} \tag{3.159}$$

We can see the physical processes related to dissipation and fluctuation by cutting the diagram into two pieces [42] since both the dissipation and fluctuation are derived from the left diagram in Fig. 3.3. Considering the fact that due to energy and momentum conservation a scalar boson cannot decay into a scalar boson of the same species and a massless gauge boson, it may be doubtful that Eq. (3.158) really expresses the physical dissipation rate. Though the calculated quantity is expressed as an integral over the loop momentum, only the $\vec{p} = \vec{0}$, or a soft-photon loop, contributes to the resultant finite value [4)]. A mathematical explanation is that it results from a cancellation between the divergent contribution from the bosonic distribution function and the vanishment of the phase space, like $\int_0 p^2 dp \times \frac{1}{p^2}\delta(p)$. If we include higher-order corrections, for example, by using dressed propagators instead of free ones, gauge fields acquire a plasmon mass. Therefore the bosonic distribution function at zero momentum becomes finite, so that the dissipation rate from this diagram vanishes. In this case Eq. (3.134) would also vanish, as it should.

The necessity of higher-order corrections to obtain a physical dissipation rate is also explained by another consideration. Since the contribution of the zero-mode seems important, we have considered the same problem in a finite box having a spatial volume V with a periodic boundary condition, by which we discretize the momentum and isolate the zero-mode. We can see that the zero mode contribution contains the thermal average of the field value squared which evidently diverges since no particular field value is energetically favored. As a result, the

[4)] We can see this more explicitly by going back to Eq. (3.138), which is related to the dissipation rate by Eq. (3.156). After performing p_2 integral, one can see that only the first and the third delta function can contribute to the p_1-integral at $\vec{p}_1 = 0$ for on-shell scalar field.

contribution to Eq. (3.158) scales as Φ_Λ^2/V, where Φ_Λ is a cutoff of the zero-mode field amplitude. Thus, the zero-mode contribution has an ambiguity arising from its dependence on the order of taking the limit $\Phi_\Lambda \to \infty$ and $V \to \infty$. Hence we may not trust the finite value obtained in Eq. (3.158) which is obtained by the particular continuum calculation. Indeed Eq. (3.158) itself would vanish, if we incorporate a plasmon mass into the gauge field using a dressed propagator or simply a mass term generated by a finite value of ϕ. In this case Eq. (3.134) would also vanish, as it should.

Thus the dissipation arises from higher order diagrams with respect to the coupling constant e, which is shown in Fig. 3.5 corresponding to the interaction $e^2 A_\mu A^\mu \Phi^\dagger \Phi$. In this case, the noise becomes the multiplicative-type. As the nonlocal memory term in the effective action, we obtain

$$\begin{aligned}\Gamma \supset & -4ie^4 \int d^4x_1 d^4x_2 \left[\phi_{\mathrm{cR}}(x_1)\phi_{\Delta\mathrm{R}}(x_1) + \phi_{\mathrm{cI}}(x_1)\phi_{\Delta\mathrm{I}}(x_1)\right]\left[|\phi_{\mathrm{c}}(x_2)|^2 + \frac{1}{4}|\phi_\Delta(x_2)|^2\right] \\ & \times \int \frac{d^3k_1}{(2\pi)^3}\frac{d^3k_2}{(2\pi)^3} e^{-i(\vec{k_1}+\vec{k_2})\cdot(\vec{x_1}-\vec{x_2})} \mathcal{P}_{ij}(\vec{k_1})\mathcal{P}_{ij}(\vec{k_2}) \\ & \left[g^>_{k_1}(t_1,t_2)g^>_{k_2}(t_1,t_2) - g^<_{k_1}(t_1,t_2)g^<_{k_2}(t_1,t_2)\right]\Theta(t_1-t_2)\,. \end{aligned} \tag{3.160}$$

In Ref. [20] the dissipation rate corresponding to multiplicative noise cases is also studied. We can evaluate the dissipation rate for the homogeneous field configuration [5)] as

$$\Gamma_{\mathrm{D}} = \frac{\tilde{C}_{\mathrm{m}}(\vec{k}=\vec{0}, 2M)}{2iM}|\phi(t)|^2 = \frac{e^4|\phi(t)|^2}{4\pi M}(1+2N_M)\,, \tag{3.161}$$

where M is the angular frequency of the coherent oscillation and $|\phi(t)|^2$ is a mean square amplitude around the time t. We now see that even the coherent oscillation has nonzero dissipation at this order. The function $\tilde{C}_{\mathrm{m}}$ is the Fourier transformation of the following function.

$$\begin{aligned} C_{\mathrm{m}}(x-x') \equiv & 4ie^4 \int \frac{d^3k_1}{(2\pi)^3}\frac{d^3k_2}{(2\pi)^3} e^{-i(\vec{k_1}+\vec{k_2})\cdot(\vec{x}-\vec{x'})} \mathcal{P}_{ij}(\vec{k_1})\mathcal{P}_{ij}(\vec{k_2}) \\ & \left[g^>_{k_1}(t,t')g^>_{k_2}(t,t') - g^<_{k_1}(t,t')g^<_{k_2}(t,t')\right]\,. \end{aligned} \tag{3.162}$$

3.3.5 Summary

In Section 3.3, we studied the role of gauge fields in the effective action for the scalar field by considering the scalar QED theory. As can be expected from previous studies, the effective action we obtained contains an imaginary part. We rewrote it by applying the Gaussian functional integral formula, and interpreted the integral over the variable ξ as ensemble averaging.

[5)] Here we focus on the dissipation rate in the configuration which is essentially equivalent to the single field dynamics (both the real and imaginary part are oscillating with the same phase).

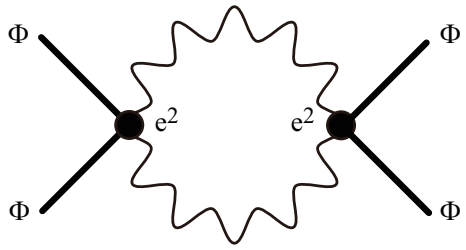

Figure 3.5: 1PI diagram relevant to the multiplicative noise. This $O(e^4)$ diagram leads to the nonzero dissipation rate for the coherently oscillating scalar field.

The validity of this arrangement is confirmed by the fluctuation-dissipation relation between the memory term and the introduced noise term. Then we analyzed the spatial correlation of the noise, and found that the noise shows anticorrelation, which is different from the case of scalar and fermionic interactions. The origin of this anticorrelation is due to the existence of derivative interactions between the scalar and gauge fields. We also considered the dissipation rate of the scalar field. Though we obtained a finite dissipation rate, it comes from a soft photon in the loop. It would vanish if we incorporated a finite mass which may be generated from higher-order loops. Furthermore since the dissipation we have obtained comes from derivative interactions, the dissipation rate for the coherent oscillation vanishes. On the other hand, higher order diagrams, consisting of a nonderivative interaction as depicted in Fig. 3.5, gives a nonzero dissipation rate.

Considering that gauge coupling constants are generally larger than Yukawa coupling constants, the absolute value of the noise correlation function for the massless case [Eqs. (3.150) and (3.153)] can be larger than that of fermionic noise studied by Ref. [19]. It would be interesting to study the phase transitions numerically with our results included. Another possible extension is to apply our results to non-Abelian gauge theories in order to treat the realistic phenomena in the early Universe.

Chapter 4

Phase Transitions in the Early Universe

4.1 Generalities on Cosmological Phase Transitions

4.1.1 Types of Phase Transitions

Phase transitions described by an effective potential with more than two local minima during the phase transition are called first-order phase transition. On the other hand, we say the phase transition is second order if the place of the local minimum continuously varies to the zero-temperature value. In the first-order phase transition, the field value is determined by the false vacuum and there appears a true vacuum with lower energy when the temperature drops below the critical value. Since the true vacuum is energetically favored, phase transitions proceeds by bubble formation, that is, in some spatial regions field values changes to the value of true vacuum. This happens around the Universe over the Hubble volume since the values of temperature are almost the same over huge spatial regions due to the inflation. The bubbles of the true vacuum expands and finally the Universe transits to the true vacuum. In the second-order phase transition there are no bubble creation and the field value gradually transit to the true vacuum.

Though the potential shape indicates a first-order phase transition, there is so-called phase mixing case. If the height of the potential barrier between the false vacuum and the true vacuum is low, the field value changes many times between false/true vacuum. In such a case the transition is called weakly first-order and cannot be described by critical bubble formation.

4.1.2 Bubble Physics

Here we consider a decay of false vacuum by tunneling following Ref.[43]. The false vacuum is a local minimum of the potential at $\phi = 0$ and the true vacuum is the global minimum at $\phi = \phi_{\rm vev}$.

The tunneling rate for unit volume per unit time is expressed as

$$\Gamma = Ae^{-S_4}, \tag{4.1}$$

where the coefficient A and the exponent S_4 are

$$A = \left(\frac{S_4}{2\pi}\right)^2 \left(\frac{\det'[-\Box + V''(\phi)]}{\det[-\Box + V''(0)]}\right)^{-\frac{1}{2}}, \tag{4.2}$$

$$S_4 = \int d^4x \left(\frac{1}{2}\left(\frac{d\phi}{dt}\right)^2 + \frac{1}{2}(\nabla\phi)^2 + V(\phi)\right). \tag{4.3}$$

The $\det'$ means neglecting the zero-eigenvalue part in calculating the determinant. In order to evaluate the Euclidean action S_4, we have to solve the equation of motion

$$\frac{d^2\phi}{dt^2} + \vec{\nabla}^2\phi - \frac{dV}{d\phi} = 0 \tag{4.4}$$

with boundary condition $\phi = 0|_{t^2+|\vec{x}|^2\to\infty}$. Though all the solution of this equation contribute to the Euclidean action S_4, it is often considered to be sufficient to use only the O(4)-symmetric solution since it minimize the action and give the largest contribution to the rate Γ. In considering the O(4)-symmetric solution, we have to solve

$$\frac{d^2\phi}{dr^2} + \frac{3}{r}\frac{d\phi}{dr} - \frac{dV}{d\phi} = 0\,, \tag{4.5}$$

where $r = \sqrt{t^2 + |\vec{x}|^2}$ and the boundary conditions are $\phi(r=\infty) = 0$, $\frac{d\phi}{dr}\big|_{r=0} = 0$.

Next let us consider the above tunneling argument in a finite-temperature state. As we see in Section 3.1, the finite temperature theory is described with an imaginary time which has a periodicity of $1/T$. Therefore we can replace the time integral in S_4 by a factor of $1/T$ and obtain $S_4 = S_3/T$. By a simple dimensional analysis one can estimate the tunneling rate as

$$\Gamma \approx T^4 e^{-\frac{S_3}{T}}, \tag{4.6}$$

where

$$S_3 = \int d^3x \left(\frac{1}{2}(\nabla\phi)^2 + V(\phi)\right). \tag{4.7}$$

The dominant contribution comes from the solution of the equation of motion

$$\frac{d^2\phi}{dr^2} + \frac{2}{r}\frac{d\phi}{dr} - \frac{dV}{d\phi} = 0\,, \tag{4.8}$$

under the boundary condition $\phi(r=\infty) = 0$, $\frac{d\phi}{dr}\big|_{r=0} = 0$. In this equation $r = |\vec{x}|$.

We know that this equation describes the one-dimensional motion of a point mass whose position at "time" r is $\phi(r)$. Note that the potential of this "particle" is $-V$. The solution with boundary conditions $\phi(r=\infty) = 0$, $\frac{d\phi}{dr}\big|_{r=0} = 0$ satisfies $\phi(0) > \phi_\star$ since the equation of motion contains the friction term which always gives a decelerating force.

We briefly explain the strategy of evaluating the bubble action S_3. Due to the initial condition $\phi'(0) = 0$, we expand ϕ around $r = 0$ as

$$\phi(r) = \phi_0 + \phi_2 \cdot r^2 + \cdots , \tag{4.9}$$

where ϕ_0 and ϕ_2 are constants. Inserting this expression into eq. (4.8), we obtain

$$6\phi_2 - \left.\frac{dV}{d\phi}\right|_{\phi=\phi_0} = 0 , \tag{4.10}$$

which fixes the value of ϕ_2 as a function of ϕ_0. Then we search the value of ϕ_0 which leads to a solution satisfying $\phi(r = \infty) = 0$. If we choose a too large value of ϕ_0, the field value ϕ overshoots the origin at some r . On the other hand, with a too small ϕ_0, $\phi(r)$ remains positive and never reaches the origin. In this way we can find the appropriate initial value and the corresponding solution of $\phi(r)$.

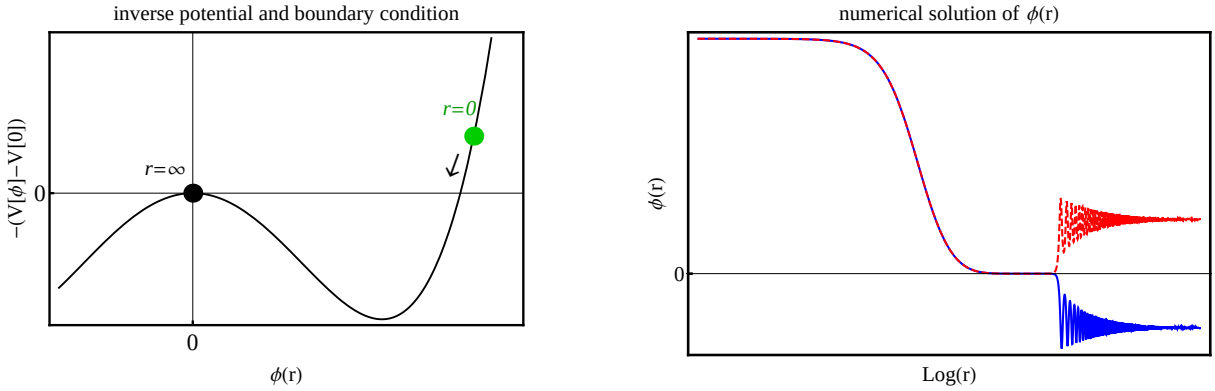

Figure 4.1: An example of the inverse potential and corresponding solution of $\phi(r)$. By choosing the "initial" position of $\phi(r)$ (the green point in the left panel), we can find the solution which satisfy $\phi(r = \infty) = 0$. If we choose too large (small) value, the solution becomes like one shown with blue(red) line in the right panel.

The spatial fraction of the regions occupied by bubbles are evaluated as [44]

$$F(t) = 1 - e^{-P(t)} , \tag{4.11}$$

where

$$P(t) = \frac{4\pi}{3} \int^t dt' \, \Gamma(t') a(t')^3 \left(\int_{t'}^t dt'' \frac{1}{a(t'')} \right)^3 . \tag{4.12}$$

4.1.3 Gravitational Waves from Bubble Collisions

Here we comment on the gravitational wave production by collisions of bubbles. There are many studies on the gravitational waves from strong first-order phase transition [12, 13, 14].

According to Ref. [14], the peak frequency of the gravitational waves produced by bubble collisions and its density parameter $\Omega_{\rm GW} = \frac{1}{\rho_{\rm tot}} \frac{d\rho_{\rm GW}}{d\ln\omega}$ are estimated as follows. We parameterize the bubble nucleation rate (at the phase transition) as

$$\Gamma = \Gamma_0 e^{Bt} \,. \tag{4.13}$$

In other words, $B = \frac{d}{dt} \ln \Gamma$ parameterizes typical quantities. We expect that the duration of the phase transition is characterized by B^{-1} and the typical bubble radius is B^{-1}, whose percolation produces gravitational waves with typical frequency $\omega \sim B$. Using eq. (4.6), we obtain

$$\frac{B}{H} = T \frac{d}{dT} \left(\frac{S_3}{T} \right) - 4 \,, \tag{4.14}$$

where we use T rather than t, since the effective potential and the corresponding value of S_3 are computed as functions of T. The value of $\Omega_{\rm GW}$ at this frequency is estimated as

$$\Omega_{\rm GW} = O(0.01) \times \frac{H^2}{B^2} \kappa^2 \frac{A^2}{(1+A)^2} \,, \tag{4.15}$$

where κ is the efficiency factor representing the conversion rate of the energy from the vacuum energy to the kinetic energy of bubbles. The parameter A is the ratio of vacuum energy in the false vacuum to the radiation energy. In order to calculate the current frequency and the density parameter, we have to specify the history of the Universe after the phase transition. In the following sections we consider the phase transition at the end of thermal inflation. The gravitational waves in this scenario is studied in Ref. [12]. The current peak frequency is

$$f_0 \approx 0.7 {\rm Hz} \left(\frac{B/H_{\rm p}}{1000} \right) \left(\frac{V_{\rm TI}^{1/4}}{10^6 \,{\rm GeV}} \right)^{\frac{2}{3}} \left(\frac{T_{\rm R,TI}}{100 \,{\rm GeV}} \right)^{1/3} \left(\frac{V_{\rm TI}^{1/3} a_{\rm p}}{\rho_{R,TI}^{1/3} a_{\rm R,TI}} \right) , \tag{4.16}$$

and the current density parameter at this frequency is

$$\Omega_{\rm GW} h^2 = 5 \times 10^{-18} \left(\frac{B/H_{\rm p}}{1000} \right)^{-2} \left(\frac{V_{\rm TI}^{1/4}}{10^6 \,{\rm GeV}} \right)^{-\frac{4}{3}} \left(\frac{T_{\rm R,TI}}{100 \,{\rm GeV}} \right)^{4/3} \left(\frac{V_{\rm TI}^{1/3} a_{\rm p}}{\rho_{R,TI}^{1/3} a_{\rm R,TI}} \right)^4 , \tag{4.17}$$

where the suffix "p" represents the value at the percolation. Other parameters like $V_{\rm TI}$ and $T_{\rm R,TI}$ are defined later. This expression tells us that the gravitational waves produced by the phase transition at the end of thermal inflation may be detectable by future experiments such as DECIGO [15, 45]. However, the above arguments are based on the assumption that thermal inflation ends with a strong first-order phase transition, which is described by bubble formation. We consider its validity later.

4.2 Thermal Inflation and Thermal Effects

Now we apply the finite-temperature field theory to phase transitions in the early Universe. We focus on the so-called thermal inflation, which occurs in the presence of a thermal bath. In this thesis we consider the phase transition related to thermal inflation [6, 7], however, it has other interesting properties. For example, thermal inflation provides a mechanism for baryogenesis. Though it washes out the baryon number generated before thermal inflation, mechanisms for generating baryon asymmetry at the end of thermal inflation are studied in Refs. [46]. Effects of thermal inflation on the primordial density fluctuations are also studied in Ref. [47].

4.2.1 Outline of Thermal Inflation

We briefly review the scenario of thermal inflation in this section. In considering the dynamics of thermal inflation, we often use the thermal effective potential. Since thermal inflation occurs after primordial inflation and reheating, there is a hot thermal bath and interactions between the flaton and the fields in the bath lead to thermal corrections to the flaton potential. The flaton is kept at the origin of the potential owing to this correction and the potential energy at the origin drives thermal inflation. One example of the flaton potential at zero temperature is

$$V_0(\phi) = V_{\rm TI} - \frac{1}{2}m_\phi^2\phi^2 + \lambda_6\phi^6, \tag{4.18}$$

where the second term represents a tachyonic mass term, whose value is assumed to be set by the soft SUSY breaking scale, $m_\phi \approx m_{\rm soft} \approx 10^3$GeV. The energy scale of thermal inflation is determined by the constant term $V_{\rm TI}$. The exactly flat potential is curved due to SUSY breaking, and stabilized by unrenormalizable terms [1)]. By requiring the potential energy at the bottom of the potential to be zero, we obtain $\lambda_6 = \frac{m_\phi^6}{54V_{\rm TI}^2}$ and $\phi_{\rm vev} = \sqrt{3V_{\rm TI}}/m_\phi$, where $\phi_{\rm vev}$ is the vacuum expectation value of the flaton.

Let us move on to the thermal corrections. The one-loop effective potential arising from thermal corrections is given by

$$V_T^{1-\rm loop}(\phi) = T^4 \sum_p g_p J_p\left(\frac{m_p(\phi,T)}{T}\right), \tag{4.19}$$

where p labels both the bosonic and fermionic degrees of freedom and the function J_p is expressed in terms of an integral as

$$J_\pm(y) = \pm\frac{1}{2\pi^2}\int_0^\infty dx\, x^2 \ln\left(1 \mp e^{-\sqrt{x^2+y^2}}\right), \tag{4.20}$$

[1)] The exact form of the third term and possible higher order terms are unimportant for our study.

for bosons and fermions, respectively. Following Ref.[12], the effective mass squared for fields in the bath are

$$m_p^2(\phi, T) \approx \begin{cases} m_{\rm b}^2 + \frac{1}{2}\lambda_{\rm b}^2\phi^2 + (\frac{1}{4}\lambda_{\rm b}^2 + \frac{2}{3}g_{\rm b}^2)T^2 & \text{boson}\,, \\ \frac{1}{2}\lambda_{\rm f}^2\phi^2 + \frac{1}{6}g_{\rm f}^2T^2 & \text{fermion}\,. \end{cases} \tag{4.21}$$

Here we consider Yukawa couplings between the flaton and scalar boson and fermion, with coupling constants $\lambda_{\rm b}$ and $\lambda_{\rm f}$, respectively. The coupling constants $g_{\rm b}$ and $g_{\rm f}$ are associated with the gauge interactions of the scalar boson and fermion, respectively. We assume that the masses of other bosons are also determined by $m_{\rm soft} \approx 10^3$GeV and that fermions are massless at tree level. Since these corrections lower the potential by $O(T^4/10)$ around $|\phi| \lesssim T$, there appears a small dip at the origin, which traps the flaton to drive thermal inflation. We show an example flaton potential in Fig.4.2.

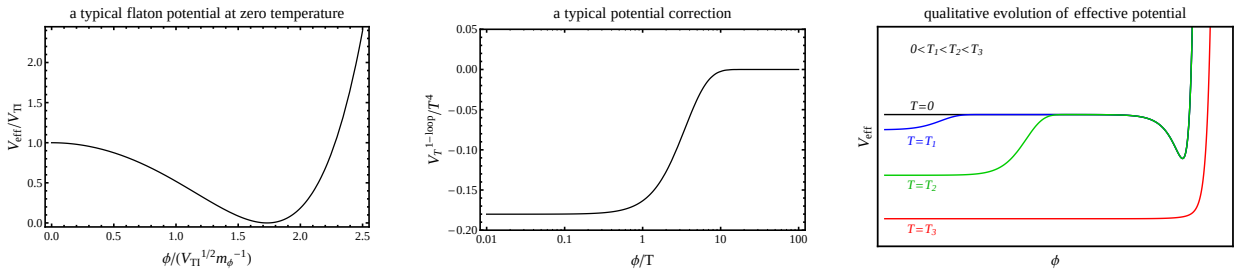

Figure 4.2: The zero-temperature potential of the flaton and its finite-temperature correction.

The thermal inflation begins when the energy density of other components decays to be as small as the potential energy of the flaton, $V_{\rm TI}$. Therefore we can tune the onset by changing the value of $V_{\rm TI}$. We discuss the onset of the thermal inflation later.

During thermal inflation, the potential energy of the false vacuum phase around the origin is larger than that of the true vacuum, meaning that we might expect tunneling from the false to the true vacuum. However, the tunneling rate is so small [7] that the flaton is assumed to be fixed at the origin until the dip almost disappears. Since the order of the curvature of the dip is determined by the temperature as $V''_{\rm eff} \sim O(T^2)$, thermal inflation ends when the temperature becomes as small as $m_\phi \approx m_{\rm soft}$. Therefore, by choosing $V_{\rm TI}$ and m_ϕ, one can tune the duration of thermal inflation.

4.2.2 Onset of Thermal Inflation

Thermal inflation begins when the potential energy density of the flaton dominates the energy density of other components. After the primordial inflation, there are several possible scenarios of the evolution of the Universe. Though one of the motivations of thermal inflation is to

solve the cosmological moduli problem, first let us assume there are no (dangerous) moduli. In this case the Universe evolves from the oscillating-inflaton-dominated era to the radiation-dominated (RD) era. If thermal inflation begins after reheating, $T_{\rm begin}$ can be simply determined as

$$T_{\rm begin} = \left(\frac{\pi^2}{30} g_*\right)^{-\frac{1}{4}} V_{\rm TI}^{\frac{1}{4}} . \tag{4.22}$$

Second, we take the possible moduli into account. Hereafter we use Φ to represent one of the moduli fields. Its mass and initial amplitude of oscillation are denoted by m_Φ and Φ_0, respectively. If the reheating temperature is much high, the Hubble parameter becomes as small as m_Φ after reheating and the moduli start oscillation in the RD Universe. Since the Hubble parameter at reheating is $H_{\rm R} = \left(\frac{\pi^2}{90} g_*\right)^{1/2} \frac{T_{\rm R}^2}{M_{\rm Pl}}$, the reheating temperature determines whether the oscillation of moduli starts

A. before reheating, if $T_{\rm R} < \left(\frac{\pi^2}{90} g_*\right)^{-1/4} m_\Phi^{1/2} M_{\rm Pl}^{1/2}$,

B. after reheating, if $T_{\rm R} > \left(\frac{\pi^2}{90} g_*\right)^{-1/4} m_\Phi^{1/2} M_{\rm Pl}^{1/2}$.

As for the onset of thermal inflation, there are three possible era, namely,

1. the era before reheating, when the oscillating inflaton dominates the Universe,
2. the RD era,
3. the era when the oscillating moduli becomes dominant after reheating.

Therefore from now we consider 6 possibilities.

scenario A-1

If the energy density of the flaton is larger than that of radiation at reheating, this is the case. The condition is given by

$$V_{\rm TI} > \frac{\pi^2}{30} g_* T_{\rm R}^4 . \tag{4.23}$$

scenario A-2

In order for the moduli to begin oscillation after reheating, the condition $V_{\rm TI} > \frac{\pi^2}{30} g_* T_{\rm R}^4$ is required. Now we consider radiation-moduli equality time. Since the moduli start oscillation before reheating, its energy density at reheating can be evaluated as

$$\rho_\Phi(\text{at reheating}) = \frac{1}{2} m_\Phi^2 \Phi_0^2 \times \left(\frac{a_{\rm osc}}{a_{\rm R}}\right)^3 = \frac{1}{2} m_\Phi^2 \Phi_0^2 \times \left(\frac{H_{\rm R}}{H_{\rm osc}}\right)^2 = \frac{1}{2} \Phi_0^2 H_{\rm R}^2 . \tag{4.24}$$

The temperature of radiation-moduli equality, $T_{\rm eq}$, is determined as

$$3M_{\rm Pl}^2 H_R^2 \times \left(\frac{T_{\rm R}}{T_{\rm eq}}\right)^{-4} = \frac{1}{2}\Phi_0^2 H_{\rm R}^2 \times \left(\frac{T_{\rm R}}{T_{\rm eq}}\right)^{-3}, \text{ or } \quad \left(\frac{T_{\rm R}}{T_{\rm eq}}\right)^{-1} = \frac{\Phi_0^2}{6M_{\rm Pl}^2}. \tag{4.25}$$

Then the energy density other than the flaton at $T = T_{\rm eq}$ is $\rho_{\rm r} + \rho_\Phi = \frac{1}{6^3}\frac{\pi^2}{90} g_* \frac{\Phi_0^8}{M_{\rm Pl}^8} T_{\rm R}^4$, the condition that thermal inflation begins during RD era is

$$V_{\rm TI} > \frac{1}{6^3}\frac{\pi^2}{90} g_* \frac{\Phi_0^8}{M_{\rm Pl}^8} T_{\rm R}^4 . \tag{4.26}$$

Since thermal inflation is assumed to begin in the RD Universe, $T_{\rm begin}$ is the same as eq.(4.22).

scenario A-3

The condition of this scenario is

$$V_{\rm TI} < \frac{1}{6^3}\frac{\pi^2}{90} g_* \frac{\Phi_0^8}{M_{\rm Pl}^8} T_{\rm R}^4 . \tag{4.27}$$

Since in this case thermal inflation begins when the energy density of moduli becomes equal to the flaton energy density, $T_{\rm begin}$ is determined by

$$\frac{1}{2}\Phi_0^2 H_{\rm R}^2 \times \left(\frac{T_{\rm begin}}{T_{\rm R}}\right)^3 = V_{\rm TI} , \tag{4.28}$$

which becomes

$$\begin{aligned} T_{\rm begin} &= \left(\frac{180}{\pi^2}\right)^{1/3} g_*^{1/3} V_{\rm TI}^{1/3} \Phi_0^{-2/3} T_{\rm R}^{-4/3} M_{\rm Pl}^{2/3} \\ &= 9.7 \times 10^5 \,{\rm GeV} \left(\frac{g_*}{200}\right)^{-1/3} \left(\frac{T_{\rm R}}{10^9\,{\rm GeV}}\right)^{-1/3} \left(\frac{V_{\rm TI}^{1/4}}{10^7\,{\rm GeV}}\right)^{4/3} \left(\frac{\Phi_0}{M_{\rm Pl}}\right)^{2/3} . \end{aligned} \tag{4.29}$$

scenario B-1

In this scenario, thermal inflation begins before reheating and before the moduli start oscillation. Therefore thermal inflation cannot decrease the energy density of moduli, in other words, it cannot serve as a solution to the cosmological moduli problem.

scenario B-2

In this scenario we again need to evaluate the radiation-moduli equality time. Since the moduli start oscillation after reheating at $T = T_{\rm osc}$, or

$$m_\Phi^2 = H_{\rm osc}^2 = \frac{\pi^2}{90} g_* \frac{T_{\rm osc}^4}{M_{\rm Pl}^2} , \tag{4.30}$$

is satisfied. Using this expression, the equality temperature becomes

$$T_{\rm eq} = \frac{3^{-3/4}}{2}\left(\frac{\pi^2}{30}g_*\right)^{-1/4} m_\Phi^{1/2} M_{\rm Pl}^{1/2}\left(\frac{\Phi_0}{M_{\rm Pl}}\right)^2 . \tag{4.31}$$

Then the total energy density other than the flaton at $T = T_{\rm eq}$ becomes $6^{-3} m_\Phi^2 M_{\rm Pl}^2 \left(\frac{\Phi_0}{M_{\rm Pl}}\right)^8$, which gives the condition for this scenario as

$$V_{\rm TI} > 6^{-3} m_\Phi^2 M_{\rm Pl}^2 \left(\frac{\Phi_0}{M_{\rm Pl}}\right)^8 . \tag{4.32}$$

Since we consider the scenario that thermal inflation begins in the RD Universe, $T_{\rm begin}$ is the same as eq.(4.22).

scenario B-3

The condition is given by

$$V_{\rm TI} < 6^{-3} m_\Phi^2 M_{\rm Pl}^2 \left(\frac{\Phi_0}{M_{\rm Pl}}\right)^8 . \tag{4.33}$$

$T_{\rm begin}$ is the temperature at which the energy density of moduli becomes equal to that of the flaton. Namely,

$$\frac{1}{2} m_\Phi^2 \Phi_0^2 \times \left(\frac{T_{\rm begin}}{T_{\rm osc}}\right)^3 = V_{\rm TI} , \tag{4.34}$$

where the temperature $T_{\rm osc}$ is given by eq. (4.30). We obtain

$$\begin{aligned} T_{\rm begin} &= 2^{1/3}\left(\frac{\pi^2}{90}\right)^{-1/4} g_*^{-1/4} m_\Phi^{-1/6} M_{\rm Pl}^{1/2} V_{\rm TI}^{1/3} \Phi_0^{-2/3} \\ &= 3.4 \times 10^5\,{\rm GeV}\left(\frac{g_*}{200}\right)^{-1/4}\left(\frac{V_{\rm TI}^{1/4}}{10^7\,{\rm GeV}}\right)^{4/3}\left(\frac{\Phi_0}{M_{\rm Pl}}\right)^{-2/3}\left(\frac{m_\Phi}{1\,{\rm TeV}}\right)^{-1/6} . \end{aligned} \tag{4.35}$$

The condition for each scenario are summarized in Fig.4.3.

4.2.3 Entropy Production after Thermal Inflation

In this subsection, we consider the entropy production by the flaton decay after thermal inflation. The entropy density at the end of thermal inflation, before flaton decay, is given by,

$$s_{\rm before} = \frac{2\pi^2}{45} g_*(T_{\rm end}) T_{\rm end}^3 , \tag{4.36}$$

as usual. Then the energy density of the flaton, $V_{\rm TI}$ is converted to radiation to reheat the Universe with temperature $T = T_{\rm R,\,TI}$. This decay leads to the following entropy density,

$$s_{\rm after} = \frac{4}{3}\frac{V_{\rm TI}}{T_{\rm R,\,TI}} , \tag{4.37}$$

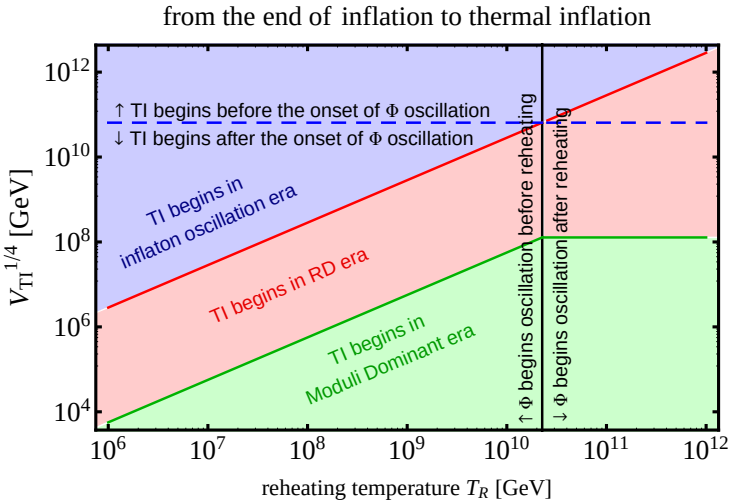

Figure 4.3: The cosmic scenario after the primordial inflation to the onset of thermal inflation. In this figure we set $\Phi_0/M_{\rm Pl} = 0.1$, $g_* = 200$, and $m_\Phi = 10^3$ GeV. The height of green line is proportional to $(\Phi_0/M_{\rm Pl})^2$. The region filled with blue corresponds to eq. (4.23). The boundary between red and green regions are given by eq. (4.26) and eq. (4.32). The vertical black line is the boundary between scenario A and B.

that is, the ratio of the entropy densities before and after the flaton decay becomes

$$\frac{s_{\rm after}}{s_{\rm before}} = \frac{\frac{4}{3}\frac{V_{\rm TI}}{T_{\rm R,TI}}}{\frac{2\pi^2}{45}g_*(T_{\rm end})T_{\rm end}^3} = 1.5\times 10^{17}\left(\frac{V_{\rm TI}^{\frac{1}{4}}}{10^7\,{\rm GeV}}\right)^4\left(\frac{T_{\rm R,TI}}{1\,{\rm GeV}}\right)^{-1}\left(\frac{T_{\rm end}}{\rm TeV}\right)^{-3}\left(\frac{g_*}{200}\right)^{-1}. \tag{4.38}$$

Here we implicitly assume the reheating temperature after thermal inflation as $T_{\rm R,TI} \sim 1\,{\rm GeV}$. This value strongly depends on the details of the model parameter of thermal inflation. We do not explicitly build a model but note that we have to assume at least two kinds of interactions to realize both thermal inflation itself and the subsequent reheating. As an example, let us focus on a Yukawa-type interaction between the flaton ϕ and a real scalar field χ like $\mathcal{L}_{\rm int} = g\phi^2\chi^2$. First, the flaton should have non-suppressed interactions ($g \sim 1$) to drive thermal inflation in order for the thermal effective potential to keep the flaton at the origin of the potential. Second, particles which interacts only weakly with the flaton should be exist in order to reheat the Universe by the flaton decay. After thermal inflation, the flaton settles down to the bottom of the potential to have a larger VEV ($\equiv M$) than its tachyonic mass (m_ϕ) at the origin. The mass of the flaton around the VEV is the same order of this tachyonic mass. The particles interacting with the flaton acquire the mass through the VEV of the flaton, like $\Delta m_\chi \sim \sqrt{g}M$. Therefore the fields strongly interacting with flaton become heavier than the

flaton, which are not (directly) reheated by the decay of the flaton. On the other hand, fields which interact with flaton via very small couplings, like $g \ll (m_\phi/M)^2$, still remains lighter than the flaton hence the flaton can decay to produce such particles and reheat the Universe. If we assume $g \sim (m_\phi/M)^2$, the reheating temperature after thermal inflation via the interaction $\mathcal{L}_{\rm int} = 2gM\delta\phi\chi^2$ (where we decomposed the field as $\phi = M + \delta\phi$) is roughly given by $T_{\rm R,TI} \sim \sqrt{M_{\rm Pl} m_\phi^3/M^2} \sim 100{\rm GeV} \times (m_\phi/10^3{\rm GeV})^{3/2}(M/10^{11}{\rm GeV})^{-1}$.

4.2.4 Gravitino Problem

The gravitino, a fermionic partner of the graviton with spin 3/2, appears in the theory of supergravity. Its number density per comoving volume is proportional to the reheating temperature after inflation [8]. Therefore, if the reheating temperature is high, the gravitinos are abundantly produced, so that their role in cosmology should be seriously considered. The mass of the gravitino depends on models of SUSY breaking [48, 49]. The lifetime of the gravitino is estimated as

$$\tau \sim \frac{8\pi M_{\rm Pl}^2}{m_{3/2}^3} \sim 10^5\,{\rm sec}\left(\frac{m_{3/2}}{1{\rm TeV}}\right)^{-3} . \tag{4.39}$$

If the gravitino mass takes a value $m_{3/2} = 1$TeV, they decay after Big-Bang Nucleosynthesis (BBN) due to their very weak interactions. Subsequently, the decay products of gravitinos spoil the light elements after BBN [50, 51]. Or if the gravitino is the lightest superparticle, it cannot decay to others. In Ref. [52] it is shown that to avoid the overclosure by such stable gravitinos, the reheating temperature is required to be low enough. These are called the gravitino problem.

Let us consider a simple estimation of the initial abundance of gravitinos by integrating eq. (2.52) from reheating. We simply replace $\langle\sigma v\rangle$ with $\alpha M_{\rm Pl}^{-2}$, where α is the gauge coupling constant. Since the abundance Y is much smaller than its equilibrium value, we neglect Y^2 in the right hand side. Then we obtain

$$Y \sim \alpha g_*^{1/2}\frac{T_{\rm R}}{M_{\rm Pl}}Y_{\rm eq}^2 \sim 10^{-9}\times\alpha\left(\frac{T_{\rm R}}{10^{10}\,{\rm GeV}}\right), \tag{4.40}$$

where we used $g_* = g_{*s} = 200$. A more precise estimation is shown in Ref. [51]. In order not to contradict the observations, we need a mechanism to decrease Y if the reheating temperature is high. Thermal inflation is the very phenomenon to solve the gravitino problem. It dilutes gravitinos by a short accelerated period followed by entropy production due to the flaton decay.

4.2.5 Cosmological Moduli Problem

Using the same mechanism to solve the gravitino problem, thermal inflation serve as a solution for the cosmological moduli problem. The scalar fields called moduli, with Planck-suppressed couplings, are also dangerous in a similar way [9, 10]. The masses of the moduli are expected

to be the same order of that of gravitino [10]. They start to oscillate when the Hubble parameter becomes as small as their mass and soon dominate the Universe, since the initial amplitude of such oscillations is expected to be on the order of $M_{\rm Pl}$. Driven by the coherent oscillations of the moduli fields the Universe evolves like a matter-dominated one, until the moduli decay to reheat the Universe. The moduli fields are coupled very weakly with other fields, and as a result of their long lifetime the reheating temperature is so low that BBN does not work. Furthermore, in Ref. [53] it is shown that the energy density of moduli is also constrained by X(γ)-ray observations, requiring that the theoretical prediction does not exceed the observed backgrounds.

Assuming the moduli start oscillating before reheating, during the era when the energy density associated with the coherent oscillations of the inflaton dominate the Universe, the moduli abundance before flaton decay is evaluated as

$$Y_\Phi = \frac{\frac{1}{m_\Phi}\frac{1}{2}\Phi_0^2 H_{\rm R}^2}{\frac{4}{3T_{\rm R}} \times 3M_{\rm Pl}^2 H_{\rm R}^2} = \frac{1}{8}\frac{T_{\rm R}}{m_\Phi}\left(\frac{\Phi_0}{M_{\rm Pl}}\right)^2 , \tag{4.41}$$

where we use eq. (4.24) and assume that there is no entropy production after reheating. After the flaton decays, by using eq. (4.38), Y_Φ becomes

$$\begin{aligned} Y_{\Phi,\,\rm after} &\approx \frac{\pi^2}{240} g_*(T_{\rm end}) \left(\frac{\Phi_0}{M_{\rm Pl}}\right)^2 \frac{T_{\rm R} T_{\rm R,TI} T_{\rm end}^3}{m_\Phi V_{\rm TI}} \\ &= 8.2 \times 10^{-13} \left(\frac{V_{\rm TI}^{\frac{1}{4}}}{10^7\,{\rm GeV}}\right)^{-4} \left(\frac{T_{\rm R}}{10^9\,{\rm GeV}}\right)\left(\frac{T_{\rm R,TI}}{1\,{\rm GeV}}\right)\left(\frac{T_{\rm end}}{m_\Phi}\right)^3 \left(\frac{m_\Phi}{1\,{\rm TeV}}\right)\left(\frac{\Phi_0}{M_{\rm Pl}}\right)^2 \left(\frac{g_*(T_{\rm end})}{200}\right) . \end{aligned} \tag{4.42}$$

Therefore, with appropriate parameters, thermal inflation can make Y_Φ small enough for successful BBN.

4.3 Consequences of the Existence of Thermal Fluctuations

4.3.1 Flaton Dynamics in a Thermal Bath

In this subsection, we consider the flaton dynamics based on the finite-temperature field theory. In order to describe the dynamics of the expectation values of quantum fields in a thermal bath, we use the effective action method as we consider in Chapter 3. The equation of motion of the flaton field ϕ becomes a Langevin equation like

$$\begin{aligned} &\Box\phi(x) + V'_{\rm eff}[\phi] + \int_{-\infty}^{t} dt' \int d^3x'\, B_{\rm a}(x-x')\phi(x') + \phi(x)\int_{-\infty}^{t} dt' \int d^3x'\, B_{\rm m}(x-x')\phi^2(x') \\ =&\xi_{\rm a}(x) + \xi_{\rm m}(x)\phi(x) . \end{aligned} \tag{4.43}$$

Though the noise terms generally consist of both additive noise, $\xi_{\rm a}$, and multiplicative noise, $\xi_{\rm m}\phi$, we focus on the additive noise term since the former is more important to trigger phase transition. Again, this noise term is related to the "friction" term though the fluctuation-dissipation relation as we saw in subsection 3.2.1,

$$\frac{\text{noise correlation}}{\text{dissipation coefficient}} = \frac{A_{\rm a}(\omega,\vec{k})}{iB_{\rm a}(\omega,\vec{k})/2\omega} = \omega\frac{e^{\omega/T}+1}{e^{\omega/T}-1} \to 2T \ (T \gg \omega)\,. \tag{4.44}$$

In Ref. [19] it was shown that the damping scale of the fermionic noise correlation is independent of the mass of the fermion, which is different from the bosonic noise whose correlation damps exponentially above the mass scale. Therefore, in the high-temperature regime $T \gg m$, the dominant noise component comes from interactions with fermions. More quantitatively, the correlation function for fermionic noise can be expressed as

$$\langle\xi(t,\vec{x})\xi(t,\vec{x}')\rangle \propto \frac{T^4}{r^2}e^{-2\pi rT}\,, \quad \text{for } r \gg \frac{1}{\pi T}\,, \quad (r = |\vec{x}-\vec{x}'|)\,. \tag{4.45}$$

From this expression we take the correlation length of thermal noise as $(\pi T)^{-1}$. This length scale is very important in estimating the typical value of the flaton at finite temperature. Here let us take a quick look at this typical field value, as this will help us to understand the results of numerical simulations later. The form of the effective potential is too complicated to be well approximated by a simple polynomial function, so for simplicity let us neglect the potential here. Following Ref. [54], the mean square value of the coarse-grained field ϕ over the spatial scale R is given by

$$\langle\phi^2\rangle_{\rm R} = \frac{1}{2\pi^2}\int_0^\infty dk\,k\left(\frac{1}{2}+\frac{1}{e^{\frac{k}{T}}-1}\right)W(k,R)^2\,, \tag{4.46}$$

where $W(k,R)$ is the coarse-graining window function. As an example, if we take the Gaussian function

$$W(k,R) = e^{-\frac{1}{2}k^2R^2}\,, \tag{4.47}$$

we obtain $\sqrt{\langle\phi^2\rangle} \approx 0.43T$ for $R = (\pi T)^{-1}$.

Since the correlation length of the noise is $\sim (\pi T)^{-1}$, we can treat the noise as being uncorrelated on larger scales. The same is true for the temporal noise correlation, since it is suppressed exponentially for $\Delta t > (\pi T)^{-1}$. As such, the noise term can be approximated by a white, Gaussian random variable when we consider dynamics on spatial and temporal scales that are larger than the above correlation length. In other words, the noise correlation function is approximated by a delta function as far as we consider larger scales than $\sim (\pi T)^{-1}$. Then the function $A_{\rm a}(\omega,\vec{k})$ in the fluctuation-dissipation relation (eq. (4.44)) becomes a constant, which means the function $B_{\rm a}/\omega$ is also a constant at high temperature limit. This is realized by a local friction term, $\eta\dot{\phi}(x)$, since it leads to $B(\omega,\vec{k}) = -2i\eta\omega$ after performing Fourier transformation. In addition, following Ref. [55], this approximation is also well-justified if we consider the nearly homogeneous

field configuration and assume that it changes more slowly than non-local kernel $B(t)$. Namely, we approximate the field configuration in the integrand in eq. (4.43) as

$$\phi(t') \approx \phi(t) + \dot{\phi}(t) \times (t - t')\,, \tag{4.48}$$

then the first term can be approximately absorbed in the (derivative of) effective potential part and the second term leads to the following local quantity.

$$\dot{\phi} \int_0^\infty d\tau \int d^3x'\, B(\tau, \vec{x}')\tau = \left(\frac{-i}{2} \lim_{k\to 0} \frac{\partial}{\partial k_0} \tilde{B}(k) \right) \dot{\phi} = \eta\dot{\phi}\,, \quad (\tau \equiv t - t') \tag{4.49}$$

where $\tilde{B}(k)$ is the Fourier transformation of $B(x)$.

Hence we use the following simple EoM.

$$\ddot{\phi}(\vec{x}, t) - \vec{\nabla}^2\phi(\vec{x}, t) + \eta\dot{\phi}(\vec{x}, t) + V'_{\rm eff}[\phi] = \xi(\vec{x}, t)\,, \tag{4.50}$$

where the correlation function of the noise term is

$$\langle \xi(\vec{x}, t)\xi(\vec{x}', t') \rangle = D\delta(t - t')\delta^3(\vec{x} - \vec{x}')\,. \tag{4.51}$$

The fluctuation-dissipation relation in this simple EoM is

$$\frac{D}{\eta} = 2T\,. \tag{4.52}$$

Due to the fluctuation-dissipation relation, equilibrium values do not depend on the friction coefficient η. Its value is related with the decay rate of ϕ particle if ϕ is oscillating [18, 20, 21]. On dimensional grounds we can take $\Gamma \propto T$. Since the value of η only determines the time scale on which the system approaches equilibrium, here we simply take $\eta = T$ as strong enough couplings between the flaton and the thermal bath are required for successful thermal inflation. Then the ratio of the equilibration timescale to the cosmic expansion timescale is

$$\frac{\text{equilibration timescale}}{\text{Hubble time}} \sim \frac{\eta^{-1}}{H^{-1}} = \frac{T^{-1}}{H^{-1}} \sim \begin{cases} \frac{T}{M_{\rm Pl}} & \text{(RD era)}\,, \\ \\ \frac{V_{\rm TI}^{\frac{1}{2}}}{M_{\rm Pl}\, T} & \text{(during thermal inflation)}\,. \end{cases} \tag{4.53}$$

We see that this ratio is much smaller than unity in both the RD era and the period of thermal inflation, from which we can conclude that the equilibration time is still much shorter than the Hubble time even if we take other choices for the value of η. This huge difference between the two timescales allows us to safely ignore the Hubble expansion in simulations we show later .

4.3.2 Setup of Numerical Simulations

In this subsection we summarize the details of our three-dimensional lattice simulation. We solved the equation of motion given by eq. (4.50) by the second-order explicit Runge-Kutta method with the second-order finite differences approximating the spatial derivatives. The basic setup is the same as in Ref.[19]. In numerical calculations we use dimensionless variables like $\tilde{x} = Tx$, $\tilde{t} = Tt$, $\tilde{\phi} = \phi/T$, and $\tilde{\xi} = \xi/T^3$ since the scale of interest is deeply related to the temperature.

The noise correlation function on the lattice becomes

$$\langle \xi(\vec{x}_i, t_m)\xi(\vec{x}_j, t_n)\rangle = 2\eta\delta(t_m - t_n)\delta^3(\vec{x}_i - \vec{x}_j) \to \frac{2\eta}{\Delta t(\Delta x)^3}\delta_{m,n}\delta_{i,j}\,, \tag{4.54}$$

since on the lattice the delta functions are properly replaced as $\delta(t_m - t_n) \to (\Delta t)^{-1}\delta_{m,n}$ and $\delta^3(\vec{x}_i - \vec{x}_j) \to (\Delta x)^{-3}\delta_{i,j}$. The value of noise variable on each lattice is given by

$$\xi(\vec{x}_i, t_m) = \left(\frac{2\eta}{\Delta t(\Delta x)^3}\right)^{\frac{1}{2}} \mathcal{G}_{i,m}\,, \tag{4.55}$$

where $\mathcal{G}$ is a standard Gaussian random variable.

We also define approximation function of the potential term, which is shown in Appendix. As can be seen later, the quantitative shape of the effective potential is very sensitive to the temperature, especially at the end of thermal inflation. Therefore we use the above approximation function both in the lattice simulation and semi-analytic calculation.

We choose the initial condition for simulations as

$$\phi(\vec{x}, t = 0) = \dot{\phi}(\vec{x}, t = 0) = 0\,. \tag{4.56}$$

Although this is an admittedly unrealistic initial condition, we have confirmed that the field quickly reaches the thermal configuration compared to the typical duration of simulation time and the timescale of the temperature variation.

With the above settings we use the 256^3 lattice points and m_ϕ (and $m_{\rm b}$ in eq. (4.21))= 10^3 and 10^2 GeV, but the qualitative results do not depend on these mass values.

4.3.3 Results of Numerical Simulations

phase 1: before thermal inflation

A necessary initial condition for the flaton to drive thermal inflation is that the field value of the flaton should be homogeneously close to zero before thermal inflation begins. However, the form of the 1-loop effective potential suggests that there is more than one local minimum, and if the flaton field is trapped in the true vacuum in some spatial regions, the thermal inflation scenario does not work. In order to determine whether or not this problem is encountered, we

simulated the time evolution of the flaton from a very high temperature, T_0, to the temperature at which thermal inflation begins.

The "high" temperature T_0 is determined by the following consideration. In order to realize a situation where the typical value of the flaton is $\phi_{\rm vev}$ ($\equiv \sqrt{3V_{\rm TI}}/m_\phi$, the vacuum expectation value at $T = 0$), we first perform a simulation at $T = \phi_{\rm vev}$, expecting $\sqrt{\langle\phi^2\rangle} \approx T \approx \phi_{\rm vev}$.[2)] At this temperature the shape of the effective potential becomes like the potential labelled "$T = T_1$" in the right panel of Fig.4.2. We then perform a second simulation, setting the temperature to half of that in the previous simulation and using the final configuration of the previous simulation to determine the initial conditions. Since we fix the gridsize of the simulation and the value of the lattice spacing normalized by the temperature, the physical size of the second simulation box is larger than that of the previous, hotter simulation. We therefore use periodic boundary conditions and define the initial condition for ϕ and $\dot{\phi}$ as averaged quantities of the previous values of close grids on each new grids. Repeating this procedures N times we can follow the flaton dynamics from $T = T_0$ to $T = T_0 \times 2^{-N} \sim T_{\rm begin}$.

In the numerical simulations we consider corrections to the potential coming from a single bosonic and single fermionic degree of freedom. In order to try and establish the importance of the thermal effects we perform simulations with two choices of the coupling constants appearing in eq. (4.21). Hereafter we refer to these two choices as the strongly and weakly coupled cases, and they correspond to taking $\lambda_{\rm b} = g_{\rm b} = \lambda_{\rm f} = g_{\rm f} = 1$ and $\lambda_{\rm b} = g_{\rm b} = \lambda_{\rm f} = g_{\rm f} = 0.1$ respectively. We also consider two different scenarios. In the first scenario thermal inflation is preceded by moduli domination (MD→TI) and in the second scenario thermal inflation is preceded by radiation domination (RD→TI). The results of simulations are shown in Fig.4.4. For the form of effective potential used in this study, we confirm that the typical value of the flaton is $\sqrt{\langle\phi^2\rangle} \approx T$, regardless of the temperature before thermal inflation. In other words, we do not see any spatial regions where the field value remains so large that the flaton potential energy becomes inhomogeneous and ruins the thermal inflation scenario.

We close this subsection with comments on the validity of our multistage simulation. The result shown in Fig. 4.4 confirms us that we properly follow the dynamics of the flaton from a high temperature to $T_{\rm begin}$, with multistage simulation. Since the equilibration timescale ($\sim \eta^{-1}$) is much shorter than that of temperature change ($\sim H^{-1}$), the system approaches the equilibrium rapidly enough in each simulation with a fixed temperature. In other words, even though we impose out-of-equilibrium initial condition which is simply connected by the previous simulation where the temperature is set twice as hot, we can realize the equilibrium distribution ($\sqrt{\langle\phi^2\rangle} \sim T$) by performing a simulation for a longer time than η^{-1} (but much shorter than

[2)] Note that the VEV of the zero-temperature potential also depends on $V_{\rm TI}$ as $\phi_{\rm vev} = \sqrt{3V_{\rm TI}}/m_\phi$. Since the temperature at the beginning of thermal inflation, $T_{\rm begin}$, is controlled by $V_{\rm TI}$ (see subsection 4.2.2), we choose the value of $V_{\rm TI}$ such that the number of e-folds of thermal inflation becomes about 6. In order to calculate the number of e-folds we also need to know the temperature at the end of thermal inflation, and this can be determined once we have fixed the coupling constants.

H^{-1}). Therefore repetitive simulations enable us to consider a system in quasi-equilibrium state for a longer time than Hubble time without including the exact change in temperature. The smooth change of the root mean square (RMS) value obtained in Fig. 4.4 justifies a factor of 2 change of the temperature at each step is small enough to warrant the adiabatic change of the temperature in the sequential simulations. As for the maximum value, we note that for random 256^3 realization of Gaussian distribution, the probability the maximum exceeds 6.2σ (5.6T) is 1 % and that it lies lower than 5.2 σ (4.6T) is also 1%. Although the field value at each point is correlated with nearby points, we find one-point distribution function is close to a Gaussian distribution. Hence we may conclude the observed maximum values in Fig. 4.4 are also in accordance with the entire distribution.

scenario	couplings	$T_{\rm begin}$[GeV]	$\phi_{\rm vev}(=T_0)$[GeV]
MD → TI	strong	2.1×10^{6}	3.7×10^{12}
MD → TI	weak	1.7×10^{7}	8.3×10^{13}
RD → TI	strong	2.1×10^{6}	6.0×10^{10}
RD → TI	weak	1.7×10^{7}	3.9×10^{12}

Table 4.1: The temperature at the beginning of thermal inflation and VEV of the flaton. Since the ratio of these values are $O(10^6) \sim 2^{20}$, we performed about 20 simulations to follow the flaton dynamics from T_0 to $T_{\rm begin}$.

phase 2: at the end of thermal inflation

It is believed that thermal inflation ends with a first-order phase transition accompanied by the formation of bubbles, and that the collision of these bubbles then leads to gravitational wave production. Here we briefly review the theory of tunneling at a finite temperature and define the percolation temperature at which the bubbles collide and start generating gravitational waves.

As we consider in subsection 4.1.2, the fraction of spatial regions occupied by bubbles can be written as [44]

$$F(t) = 1 - e^{-P(t)}\,, \tag{4.57}$$

where the function $P(t)$ is given by

$$\begin{aligned} P(t) =& \int^t dt'\,\Gamma(t')\frac{4\pi}{3}\left(\int_{t'}^t dt''\,\frac{a(t)}{a(t'')}\right)^3 \\ =& \frac{4\pi}{3}\int^t dt'\,\Gamma(t')\frac{1}{H^3}\left(e^{H(t-t')}-1\right)^3\,. \end{aligned} \tag{4.58}$$

Making use of eq.(4.6) we can rewrite this in terms of temperature as

$$P(T) = \frac{4\pi}{3}\int_T^\infty dT'\,\frac{T'^3}{H^4}\left(\frac{T'}{T}-1\right)^3 e^{-\frac{S_3(T')}{T'}}\,. \tag{4.59}$$

In this study we define the percolation temperature as $F(T = T_{\rm p}) = 0.5$ [3)] . Note that since the exponential factor $\exp[-S_3(T)/T]$ is very sensitive to the temperature and quickly becomes small when we take a large value of T, it is sufficient to take the upper limit of the integral to be some finite value. For example, it is enough to take it as $2T_{\rm curv}$, where $T_{\rm curv}$ is the temperature at which the curvature of the potential becomes zero. After evaluating the above quantities numerically, we find that the difference between the percolation temperature $T_{\rm p}$ and $T_{\rm curv}$ is tiny, so that the Universe becomes filled with critical bubbles almost immediately after bubble formation effectively begins.

From the above consideration based on the shape of the flaton effective potential, we may expect that thermal inflation ends with a first-order phase transition characterized by critical bubble formation. However, this description is based on the assumption that the flaton is well within the false vacuum phase before bubble nucleation occurs.

We see from Fig.4.5 that around the percolation temperature the potential barrier is located at $\phi \ll T$ and the height of the barrier is much smaller than T^4. Taking thermal fluctuations into account, since the width of the field distribution is $\sqrt{\langle\phi^2\rangle} \approx T$, we conclude that the small potential barrier cannot trap the flaton in the false vacuum phase until the temperature becomes as small as the temperature at which critical bubble nucleation occurs. This means that the two phases coexist well before the percolation epoch in the bubble nucleation picture, and the phase transition proceeds with phase-mixing. As such, the standard description of the end of thermal inflation in terms of a strong first-order phase transition which is accompanied with bubble formation is inappropriate.

Now let us investigate more quantitatively the failure of critical bubble formation as a description of the end of thermal inflation. The width of the wall trapping the flaton is broad at high temperatures and gradually becomes thin as the temperature drops. We define the width in field space, $\phi_{\rm wid}$, at temperature T, as

$$V_{\rm eff}[\phi = \phi_{\rm wid}, T] = V_{\rm eff}[\phi = 0, T]\,. \tag{4.60}$$

Since the shape of the effective potential depends on temperature, we obtain $\phi_{\rm wid}(T)$ by solving the above equation. As a typical temperature at which phase-mixing occurs, we define the temperature $T_{\rm sub}$ as

$$\phi_{\rm wid}(T = T_{\rm sub}) = T_{\rm sub}\,, \tag{4.61}$$

i.e. $T_{\rm sub}$ is the temperature at which the width of the potential wall becomes as small as the temperature. As we see from the simulations in the previous subsections and the analytical estimation (eq.4.46), the typical value of ϕ is as large as T. Therefore, at $T = T_{\rm sub}$, and if the height of the potential barrier is small enough, spatial regions in which the flaton lies outside of the potential dip are ubiquitous in the Universe. We call such regions subcritical bubbles, which

[3)] The qualitative conclusion ($T_{\rm curv} \approx T_{\rm p} < T_{\rm sub}$) remains unchanged if we employ other definitions such as $F(T_{\rm p}) = 0.01$ or 0.99.

are continuously created and destroyed by thermal fluctuations and hence differ from the critical bubbles which only grow after being nucleated by tunneling. For the effective potential we study in this thesis, the relations $T_{\rm sub} > T_{\rm p}$ and $F(T_{\rm sub}) \ll 1$ hold. Therefore, at $T = T_{\rm sub}$ the flaton is no longer trapped at the local minimum at the origin, meaning that there are practically no critical bubbles. Specific values are shown in Table 4.2 and 4.3. Field configurations for critical bubbles are also shown in Fig. 4.6. We would like to make a comment on the temperature at the end of thermal inflation, $T_{\rm end}$ quantitatively. From Table 4.2 and 4.3 we can see that $T_{\rm end}(\sim T_{\rm curv} \sim T_{\rm p} \sim T_{\rm sub})$ depends on the choice of parameters. In subsection 4.2.1 we simply estimated $T_{\rm end} \sim m_\phi$. Table 4.2 and 4.3, however, shows that while $T_{\rm curv}$, $T_{\rm p}$, and $T_{\rm sub}$ coincide with each other within 5% they deviate from m_ϕ by a factor of 0.5 - 40. Hence we should use $T_{\rm end} \sim T_{\rm sub}$ to estimate the proper duration of thermal inflation.

By performing numerical simulations at $T = T_{\rm sub}$ we were able to verify that the height of the potential barrier is small enough for the flaton to escape the local minimum. In some cases we found that the flaton rolls down to the bottom of the potential, which means that thermal inflation ends at $T > T_{\rm sub}$. The time evolution of the field value in this case is shown in Fig. 4.8. In other cases we found that the flaton remained around the origin, [4)] but with a distribution width that was broader than the potential well. The histogram of field values on lattice points is shown in Fig. 4.7, which tells us that even at this temperature the typical field value is as large as the temperature. We summarize the dependence of the potential shape on temperature in Fig. 4.9 schematically. We thus see that all cases deviate from the standard scenario in which thermal inflation ends as the result of a strong first-order phase transition.

scenario	couplings	$T_{\rm curv}$[GeV]	$T_{\rm p}$[GeV]	$T_{\rm sub}$[GeV]	$F(T_{\rm sub})$	simulated $\sqrt{\langle\phi^2\rangle}$ at $T_{\rm sub}$
MD → TI	strong	5230	5239 (2×10^{-3})	5502(5×10^{-2})	10^{-84}	$\phi_{\rm vev}$
MD → TI	weak	41216.96	41216.97(4×10^{-7})	41378(4×10^{-3})	less than 10^{-2000}	$0.91T$
RD → TI	strong	5230	5252 (4×10^{-3})	5502(5×10^{-2})	10^{-77}	$\phi_{\rm vev}$
RD → TI	weak	41216.96	41216.97(4×10^{-7})	41378(4×10^{-3})	less than 10^{-2000}	$0.91T$

Table 4.2: Specific temperature values for different parameters for $m_\phi = 1\,\text{TeV}$. Since the values themselves are almost the same, we also show the relative differences, $(T_{\rm p} - T_{\rm curv})/T_{\rm curv}$ and $(T_{\rm sub} - T_{\rm curv})/T_{\rm curv}$ in brackets. In evaluating $T_{\rm p}$ and $F(T)$, we fix the value of $V_{\rm TI}$ so that the thermal inflation begins at $T = T_{\rm curv} \times e^6$. The RMS values of ϕ at $T = T_{\rm sub}$, obtained by simulations with duration $t = 2000/T$ are also shown. In two cases the flaton leave the origin and settles in its VEV and in others it still stays at the origin, but its width is as broad as the barrier. Though the potential barrier is negligible, the potential force by the tachyonic mass term is also so weak that it may take a long time to distract the flaton from the origin.

[4)] This may be explained as an effect of surface tension, which is stronger than the potential force pulling the flaton away from the origin.

scenario	couplings	$T_{\rm curv}$[GeV]	$T_{\rm p}$[GeV]	$T_{\rm sub}$[GeV]	$F(T_{\rm sub})$	simulated $\sqrt{\langle\phi^2\rangle}$ at $T_{\rm sub}$
MD → TI	strong	522.97	525.07 (4×10^{-3})	550.2(5×10^{-2})	10^{-78}	$\phi_{\rm vev}$
MD → TI	weak	4121.689	4121.697 (2×10^{-6})	4137.8(4×10^{-3})	less than 10^{-2000}	$0.91T$
RD → TI	strong	522.97	527.14 (8×10^{-3})	550.2(5×10^{-2})	10^{-70}	$\phi_{\rm vev}$
RD → TI	weak	4121.689	4121.697(2×10^{-6})	4137.8(4×10^{-3})	less than 10^{-2000}	$0.91T$

Table 4.3: Specific temperature values for different parameters for $m_\phi = 100\,\text{GeV}$.

4.3.4 Summary

In Section 4.3, we studied the effect of thermal fluctuations on the thermal inflation scenario. Thermal inflation is a short period of accelerated expansion after reheating and provides a way to dilute dangerous moduli and gravitinos in order to make theories based on supersymmetry compatible with cosmological observations. Thermal inflation is driven by the flaton potential energy at the origin with the help of thermal corrections. Since the thermal environment gives rise to thermal fluctuations as well, we used lattice simulations to study the dynamics of the flaton taking into account the 1-loop effective potential, thermal fluctuations and the dissipation term. First we studied the effects of thermal fluctuations before thermal inflation. Though the effective potential contains multiple local minima during the course of the evolution of the Universe, the flaton settles at the origin before thermal inflation even when thermal fluctuations are taken into account. Therefore the scenario of thermal inflation may be feasible. Second, we find that thermal inflation ends with a weakly first-order phase transition. The tunneling rate of the flaton from the origin of the potential is so small that the tunneling does not occur until the position of the potential barrier becomes very close to the origin. However, since the height of the barrier is much smaller than T^4, the flaton can escape over the barrier before tunneling occurs. Though the form of the effective potential suggests that thermal inflation ends with a first-order phase transition accompanied by bubble formation, thermal fluctuations make the transition weakly first-order, which is characterized by subcritical bubbles. As such, we cannot expect critical bubble formation and the production of gravitational waves.

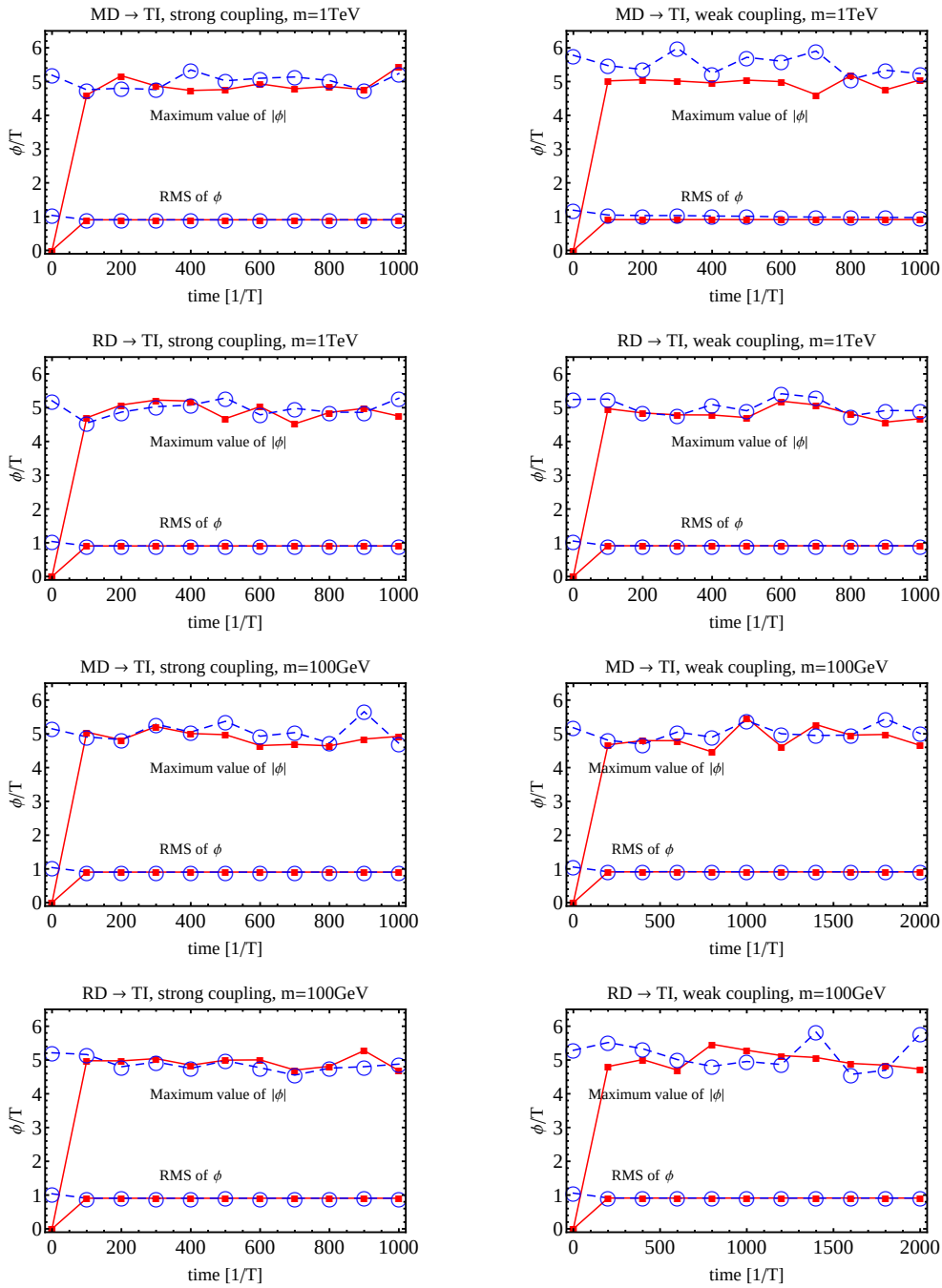

Figure 4.4: The results of multistage lattice simulations. The root mean square of ϕ and the maximum value of $|\phi|$, in the first and the last simulation at each reference time, are shown. The red lines with square vertices are the results of first (hot) simulation and the dashed blue lines with circular vertices are that of the last ($T \sim T_{\rm begin}$) simulation. Since we impose the initial condition $\phi = \dot{\phi} = 0$ in the first simulation and the following simulations starts with the previous, higher temperature results, the flaton distribution at each first reference time is not the equilibrium value.

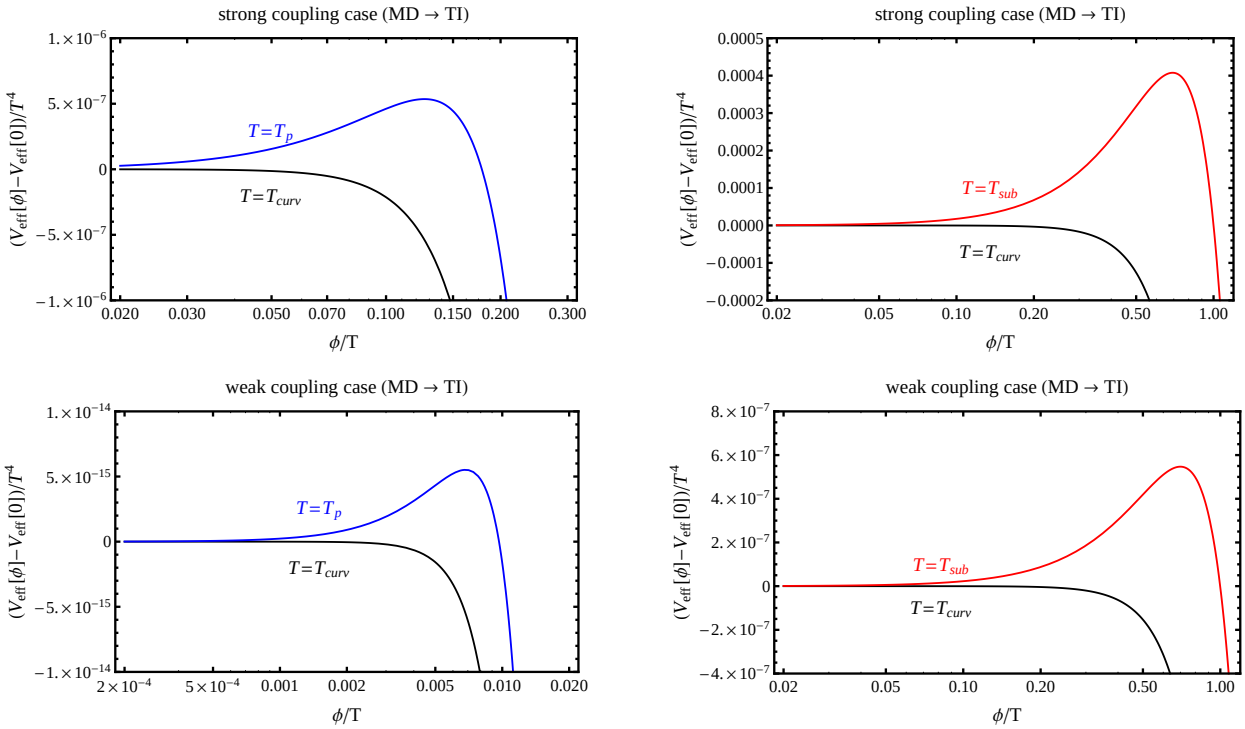

Figure 4.5: Some examples of the effective potential at $T = T_{\rm curv}$, $T_{\rm p}$, and $T_{\rm sub}$ are shown. Since at $T = T_{\rm p}$ the local maximum locates at $\phi < T$ and its height is much smaller than T^4, the flaton has already overflowed and critical bubble formation theory is not applicable.

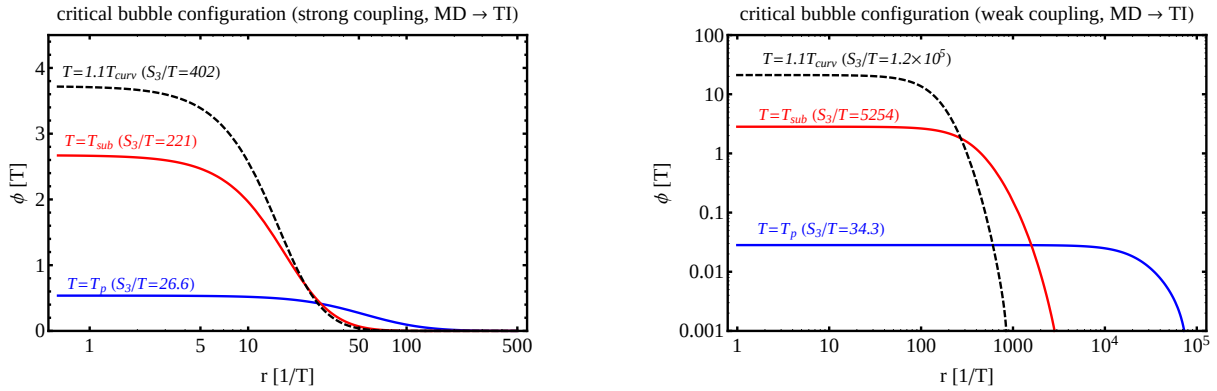

Figure 4.6: Critical bubble configurations at $T = T_{\rm p}$, $T_{\rm sub}$, and $1.1T_{\rm curv}$ are shown. We also mention the corresponding values of S_3/T, from which we can see that the tunneling rate is strongly suppressed at high temperature ($T > T_{\rm p}$).

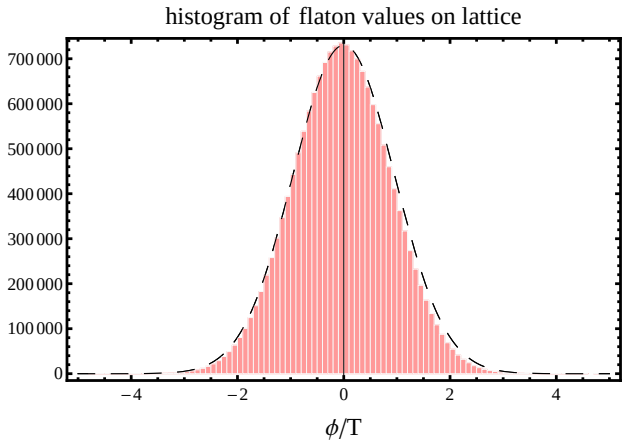

Figure 4.7: One of the histograms of the values of flaton on lattice, in a simulation in which we do not see the rolling of the flaton within the simulation time. The dashed line represents a gaussian function with $\sigma = 0.91$, which fits the data well.

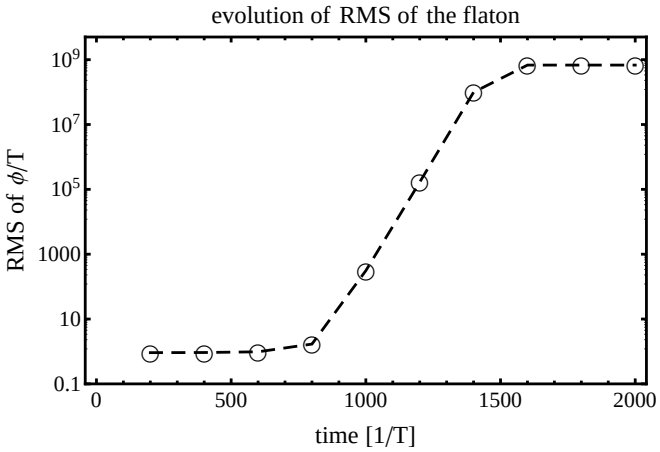

Figure 4.8: The time evolution of the root mean square of the flaton in a simulation. Since the size of simulation box is limited, the actual time of the onset of rolling may differ from this result. However, we can conclude that at least the broad distribution ($\sigma \sim T$) is also realized in this simulation hence the phase transition becomes cross over one.

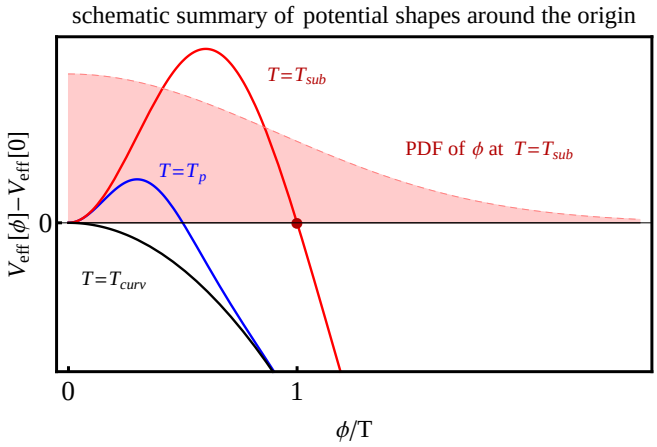

Figure 4.9: A schematic relation of the potential shapes at $T = T_{\rm sub}$, $T_{\rm p}$, and $T_{\rm curv}$. We also show the probability distribution function of the flaton at $T = T_{\rm sub}$, which indicates that the subcritical bubbles are abundant in the Universe at $T = T_{\rm sub}$.

Chapter 5

Conclusion

In this thesis we explore the hot early Universe, especially focusing on phase transitions. The hot Universe, which can be easily inferred from the fact of the ongoing expansion, has been a paradigm of modern cosmology as we overviewed in Chapter 2. The initial condition of the Big-Bang Universe is set by the preceding inflation, which is an accelerated expansion of the Universe. Though there are many models of inflation, a wide class of models assumes the potential energy of a scalar field called inflaton drives the inflation. It is also assumed that the inflaton field decays to other particles and realize the hot Universe. In addition to this background dynamics, the framework of inflation also provides a way of generating density perturbations, which grow to form rich structures of the Universe.

In order to consider micro physics in the early Universe in terms of quantum field theory, we reviewed basics and extended the effective action method in Chapter 3. Generally the equation of motion for a scalar field interacting with thermal bath becomes a Langevin-type equation. This equation is characterized by the noise term, which represents a kick from the bath particle. In addition to the noise term, there is a dissipation term, which is in general non-local in the equation of motion. The noise term and the dissipation term relate to each other through the fluctuation-dissipation relation. In addition to the Yukawa-type interactions which have been studied so far, we extended this method to gauge interactions. Though the gauge interaction contains derivative coupling, we confirmed that the fluctuation-dissipation relation also holds in this type of interaction.

The thermal fluctuations obtained by the above method play a fundamental role in phase transitions. They give the origin of inhomogeneities, which are important in considering the phase transitions since the process of phase transition is nothing less than the generation of inhomogeneities. Though the effective potential, which is a convenient quantity in determining the ideal value of fields, does not include this noisy effect. Since this noise generates inhomogeneity of the fields relevant to phase transitions, we consider the dynamics of the fields coarse-grained over this length scale.

We studied thermal inflation based on the above consideration in Chapter 4. Thermal in-

flation, which is a short inflationary period after the primordial one, has been studied to solve the gravitino problem and the cosmological moduli problem in the theory of supersymmetry. Though it is thought to end by a strong first-order phase transition so far, we found that the thermal fluctuations get the flaton out of the potential dip earlier, when there are no bubbles in the Universe. Therefore it ends by a cross over phase transition, which produces at least less gravitational waves than what is believed before.

In summary, the thermal fluctuations derived from the effective action method based on the finite-temperature field theory carry great significance, especially in considering dynamical phenomena like phase transitions. The fact that thermal fluctuations change the intensity of phase transitions implies that we have to take them into account seriously when trying to test hypothetical theories by observations related to gravitational waves.

Acknowledgements

First I would like to express my huge thanks to professor Jun'ichi Yokoyama. I could not have finished my research activities without his continuous help and encouragement. He gave me not only many suggestions as a supervisor but also some visionary comments as an experienced researcher of cosmology.

I also would like to thank Takashi Hiramatsu, Kohei Kamada, Hayato Motohashi, Teruaki Suyama, and Daisuke Yamauchi for exciting and fruitful collaborations. From the research activities with these coauthors I learned a lot on the attitude to approaching and solving problems. I also appreciate Matthew Lake and Jonathan White for their help to improve my English ability.

I appreciate discussions with the members of Research Center for the Early Universe (RESCEU) and the University of Tokyo Theoretical Astrophysics (UTAP). I obtained great benefit from the weekly seminars, meetings on recent papers, annual summer schools, and special lectures organized by RESCEU and UTAP. Administrative staff in RESCEU, Sayuri Nagano and Mieko Minamisawa also gave continuous support and encouragement.

My research was also supported by a fellowship for Young Scientists from Japan Society for the Promotion of Science (JSPS) for two years. Finally I appreciate my family for warm encouragement.

Appendix A

Gauge Invariance of the Dissipation Rate

We briefly discuss the gauge invariance of the dissipation rate. The generating functional $W_f[J]$ is defined by

$$e^{iW_f[J]} = \int \mathcal{D}A_\mu \mathcal{D}\phi^* \mathcal{D}\phi e^{iS[A,\phi]+i\int d^4x(J^\mu_A A_\mu+\phi J+\phi^* J^*)} B[f(A;x)] \det\left(\mathcal{F}_{x,y}\right), \tag{A.1}$$

where $f(A;x)$ is the gauge fixing condition and A_λ is the transformed gauge field by the gauge transformation specified by λ. The matrix $\mathcal{F}_{x,y}$ is defined by

$$\mathcal{F}_{x,y} = \left.\frac{\delta f(A_\lambda;x)}{\delta\lambda(y)}\right|_{\lambda=0}. \tag{A.2}$$

In the main text, we have been working in the Coulomb gauge for which we have

$$B[f(A;x)] = \prod_x \delta(f(A;x)), \qquad f(A;x) = \mathrm{div}\vec{A}(x). \tag{A.3}$$

The purpose of this appendix is to comment on the gauge dependence of the dissipation rate of ϕ on the gauge fixing condition. Although all the results in this note use the in-out formalism for notational simplicity, the same results hold for the case of the in-in formalism.

Under the slight change of the gauge fixing condition from f to $f+\Delta f$, W_f varies as [56]

$$W_{f+\Delta f}[J] - W_f[J] = \int_{x,y} \langle(\partial^\mu J_{A\mu}(x) + ie(\phi^*(x)J^*(x) - \phi(x)J(x)))\mathcal{F}^{-1}_{x,y}\Delta f(A;y)\rangle, \tag{A.4}$$

where $\langle O\rangle$ is defined by

$$\langle O\rangle = e^{-iW_f[J]} \int \mathcal{D}A_\mu \mathcal{D}\phi^* \mathcal{D}\phi\; e^{iS[A,\phi]+\int_x (J^\mu_A A_\mu+\phi J+\phi^* J^*)}\, O \det\left(\mathcal{F}_{x,y}\right). \tag{A.5}$$

Eq. (A.4) provides the transformation rule of $W_f[J]$ under the change of the gauge fixing condition.

From the definition of the generating functional, the expectation value of ϕ_f in the gauge f is given by

$$\phi_f(x) = \frac{\delta W_f[J]}{\delta J(x)}. \tag{A.6}$$

If we set $J = 0$ on the right hand side of the above equation, ϕ_f constitutes a solution of $\frac{\delta\Gamma_f}{\delta\phi} = 0$. From Eq. (A.4), we obtain the transformation rule of ϕ_f under the change of the gauge fixing condition as

$$\phi_{f+\Delta f}(x) - \phi_f(x) = \frac{\delta}{\delta J(x)} \int_{y,z} \langle (\partial^\mu J_{A\mu}(y) + ie(\phi^*(y)J^*(y) - \phi(y)J(y)))\mathcal{F}^{-1}_{y,z}\Delta f(A;z)\rangle. \tag{A.7}$$

In particular, for ϕ_f satisfying $\frac{\delta\Gamma_f}{\delta\phi} = 0$, we find

$$\phi_{f+\Delta f}(x) - \phi_f(x) = -\int_y \langle ie\phi(x)\mathcal{F}^{-1}_{x,y}\Delta f(A;y)\rangle = -ie\langle\phi(x)\Lambda(x)\rangle, \tag{A.8}$$

where Λ is the gauge transformation connecting two gauges f and $f + \Delta f$ and is related to Δf by

$$\Lambda(x) = \int_y \mathcal{F}^{-1}_{x,y}\Delta f(y). \tag{A.9}$$

In a similar way, we find

$$A^\mu_{f+\Delta f}(x) - A^\mu_f(x) = -\partial^\mu\langle\Lambda(x)\rangle. \tag{A.10}$$

From Eqs. (A.8) and (A.10), we find that gauge transformation of the expectation value of any field is given by expectation value of the gauge transformation for that field. We also find that $|\phi_f|$ is not gauge invariant in general. On the other hand, $F^{\mu\nu}_f = \partial^\mu A^\nu_f - \partial^\nu A^\mu_f$ is always gauge invariant.

If the path integral to compute the right hand side of Eq. (A.8) is dominated by the field configurations in close vicinity of ϕ_f, which is the case investigated in the main text, Eq. (A.8) approximately becomes

$$\phi_{f+\Delta f}(x) \approx (1 - ie\langle\Lambda(x)\rangle)\phi_f(x), \tag{A.11}$$

which means $|\phi_f(x)|^2$ is gauge invariant and hence the dissipation rate, too.

Appendix B

Noise correlation

We show some detailed behavior of noise correlation function.

short-range correlation

From (3.145)~(3.149), we obtain the following asymptotic form as $r \to 0$.

$$\begin{aligned} \alpha(r) &\to \frac{1}{2\pi^2 r^2} \\ \beta'(r) &\to -\frac{1}{2\pi^2 r}\,, \qquad \beta''(r) \to \frac{1}{2\pi^2 r^2} \\ \gamma'(r) &\to -\frac{1}{\pi^2 r^3}\,, \qquad \gamma''(r) \to \frac{3}{\pi^2 r^4} \end{aligned} \tag{B.1}$$

To derive these results, we have used the fact that modified Bessel functions $K_n(x)$ satisfy

$$\lim_{x\to 0} x^n K_n(x) = 2^{-1+n}\Gamma(n)\,. \tag{B.2}$$

Using the above expressions, the spatial noise correlation becomes

$$\langle \xi(\vec{x_1}, t)\xi^\dagger(\vec{x_2}, t)\rangle \;\simeq\; -\frac{3e^2}{2\pi^4 r^6}\,, \tag{B.3}$$

as r approaches zero.

Since the value at $r = 0$ corresponds to $\langle|\xi(\vec{x}, t)|^2\rangle$, the correlation function given by Eq. (B.3) being negative seems strange. We speculate that the origin of this apparent contradiction lies in the evaluation of γ_{ij}. To see the essence, we now consider the case where the scalar field is massless.

The divergence comes from the zero-temperature part.

$$\gamma'_{\rm zero} = \frac{1}{2\pi^2}\int_0^\infty dp\left(\frac{p\cos(pr)}{r} - \frac{\sin(pr)}{r^2}\right) \tag{B.4}$$

$$\gamma''_{\rm zero} = \frac{1}{2\pi^2}\int_0^\infty dp\left(\frac{-p^2\sin(pr)}{r} - 2\frac{p\cos(pr)}{r^2} + 2\frac{\sin(pr)}{r^3}\right) \tag{B.5}$$

These integrals are UV divergent. We regulate them by introducing a cutoff factor $e^{-p/\Lambda}$, getting

$$\gamma'_{\rm zero} = -\frac{1}{2\pi^2}\frac{2r\Lambda^4}{(1+r^2\Lambda^2)^2}\,, \tag{B.6}$$

$$\gamma''_{\rm zero} = \frac{1}{2\pi^2}\frac{2\Lambda^4(3r^2\Lambda^2-1)}{(1+r^2\Lambda^2)^3}\,. \tag{B.7}$$

If we evaluate the noise correlation with these regulated integral, the asymptotic form becomes

$$\langle\xi(\vec{x_1},t)\xi^\dagger(\vec{x_2},t)\rangle \simeq -\frac{e^2}{2\pi^4}\frac{\Lambda^4(3r^2\Lambda^2-1)}{r^2(1+r^2\Lambda^2)^3}\,. \tag{B.8}$$

When $r > 0$, taking $\Lambda \to \infty$ gives the same result as (B.3). On the other hand, if we keep Λ finite and take $r \to +0$, we see that the spatial noise correlation goes to $+\infty$. At $r = 0$, the dominant part is $\frac{e^2}{2\pi^4}\frac{\Lambda^4}{r^2(1+r^2\Lambda^2)^3}$. If we multiply it by r^5 and integrate from 0 to ∞, we obtain a finite value.

$$\int_0^\infty dr\,\frac{\Lambda^4}{r^2(1+r^2\Lambda^2)^3}\times r^5 = \frac{1}{4} \tag{B.9}$$

From this, we can write as follows.

$$\frac{e^2}{2\pi^4}\frac{\Lambda^4}{r^2(1+r^2\Lambda^2)^3} = \frac{e^2}{4\pi^4 r^5}\delta(r) \tag{B.10}$$

long-range correlation

We briefly show the long-range ($r \gg \beta,\ \frac{1}{m}$) behavior. In this limit, we obtain

$$\begin{aligned}
\alpha(r) &\to \frac{1}{2\pi\beta r}\\
\beta'(r) &\to -\frac{1}{4\pi\beta}\\
\beta''(r) &\to \frac{\beta}{12\pi r^3}\\
\gamma'(r) &\to \begin{cases} -\frac{1}{2\pi\beta r^2} & m=0\\ -\frac{m}{2\pi r\beta}e^{-mr} & m\neq 0\end{cases}\\
\gamma''(r) &\to \begin{cases} \frac{1}{\pi\beta r^3} & m=0\\ \frac{m^2}{2\pi r\beta}e^{-mr} & m\neq 0\end{cases}
\end{aligned} \tag{B.11}$$

In the evaluation of γ' and γ'', we used the asymptotic form for modified Bessel functions $K_n(x)$,

$$K_n(x) \to \sqrt{\frac{\pi}{2}}x^{-1/2}e^{-x} \quad \text{as } x\to\infty. \tag{B.12}$$

Appendix C

Scalar Field Strength Renormalization

In this appendix we consider a non-trivial renormalization issue. We show the divergent part of

$$-\tilde{f}_{A_0}(\omega,\vec{k})+\int\frac{d\omega'}{2\pi}\mathrm{P}\frac{1}{\omega-\omega'}i\tilde{C}_{\vec{k}}(\omega') \tag{C.1}$$

can be removed by renormalizing the field strength of the scalar field.

First, $\tilde{f}_{A_0}$ can be expressed as

$$-\tilde{f}_{A_0}(\omega,\vec{k})=\frac{e^2}{2}\int\frac{d^3q}{(2\pi)^3}\frac{\omega^2+\omega_q^2}{\omega_q|\vec{k}-\vec{q}|^2}(1+2n_q)\,. \tag{C.2}$$

This is an UV-divergent integral, whose divergence comes from zero temperature part. Sticking to massless case which does not loss generality of the analysis in this section, we find

$$-\tilde{f}_{A_0}(\omega,\vec{k})\to\frac{e^2}{16\pi^2k}\int_0^\infty dq(\omega^2+q^2)\ln\frac{(k+q)^2}{(k-q)^2}\,. \tag{C.3}$$

Now we use the dimensional regularization method. Changing the dimensions from 3 to $3+\epsilon$ in Eq. (C.2) enables us to extract the divergence as follows.

$$-\tilde{f}_{A_0}(\omega,\vec{k})=\frac{e^2}{12\pi^2}(3\omega^2+k^2)\frac{1}{\epsilon}+(\text{regular terms}) \tag{C.4}$$

Second, it is convenient to use another expression for the principal integral term,

$$\begin{aligned}
&\int\frac{d\omega'}{2\pi}\mathrm{P}\frac{1}{\omega-\omega'}i\tilde{C}_{\vec{k}}(\omega')\\
&=-\frac{e^2}{2}\int\frac{d^3p}{(2\pi)^3}\mathcal{P}_{ij}k_ik_j\frac{1}{p\,\omega_{k+p}}\\
&\quad\times\left[(1+2N_p)\left(\frac{\mathrm{P}}{\omega+p+\omega_{k+p}}-\frac{\mathrm{P}}{\omega-p-\omega_{k+p}}-\frac{\mathrm{P}}{\omega+p-\omega_{k+p}}+\frac{\mathrm{P}}{\omega-p+\omega_{k+p}}\right)\right.\\
&\qquad\left.+(1+2n_{k+p})\left(\frac{\mathrm{P}}{\omega+p+\omega_{k+p}}-\frac{\mathrm{P}}{\omega-p-\omega_{k+p}}-\frac{\mathrm{P}}{\omega-p+\omega_{k+p}}+\frac{\mathrm{P}}{\omega+p-\omega_{k+p}}\right)\right].
\end{aligned} \tag{C.5}$$

This is also UV divergent and we use the dimensional regularization method once more. The above integral at large p is simplified to

$$-\frac{e^2k^2}{3\pi}\int^{\infty} dp\, p^{-1+\epsilon} \to -\frac{e^2k^2}{3\pi^2}\frac{1}{\epsilon}\,. \tag{C.6}$$

Finally we find Eq.(C.1) diverges like $\frac{e^2}{4\pi^2}(\omega^2-k^2)\frac{1}{\epsilon}$. This combination of (ω^2-k^2) ensures that we can remove this divergence by the renormalization of the scalar field strength.

Appendix D

Constructing Approximation Functions of the Potential Term

In this appendix, we consider the approximation of Eq. (4.20), which determines the functional shape of the thermal correction to the flaton potential. Expanding the integrand of Eq. (4.20), we can perform the integration term by term,

$$\begin{aligned} J_{\pm}(y) &= \mp\frac{1}{2\pi^2}\sum_{n=1}^{\infty}\frac{(\pm 1)^n}{n}\int_0^{\infty} dx\, x^2 e^{-n\sqrt{x^2+y^2}}, \\ &= \mp\frac{y^2}{2\pi^2}\sum_{n=1}^{\infty}\frac{(\pm 1)^n}{n^2}K_2(ny), \end{aligned} \tag{D.1}$$

where $K_2(x)$ is the modified Bessel function of the second kind. The derivative of $J(y)$ with respect to y, which appears in the field equation, (4.50), is calculated as

$$\frac{dJ}{dy} = \pm\frac{y^2}{2\pi^2}\sum_{n=1}^{\infty}\frac{(\pm 1)^n}{n}K_1(ny). \tag{D.2}$$

For convenience, we define the shape function,

$$S_{\pm}(y) \equiv \sum_{n=1}^{\infty}\frac{(\pm 1)^n}{n}K_1(ny). \tag{D.3}$$

The modified Bessel function $K_1(z)$ for small z can be approximated as

$$K_1(z) \approx \frac{1}{z}. \tag{D.4}$$

Therefore, the shape function for small y becomes

$$S_{\pm}(y) \approx \frac{1}{y}\sum_{n=1}^{\infty}\frac{(\pm 1)^n}{n^2} = \frac{1}{y}\times\begin{cases}\zeta(2), & \text{for } + \\ -\dfrac{\zeta(2)}{2}. & \text{for } -\end{cases} \tag{D.5}$$

Away from $y = 0$ this approximation breaks down almost immediately. Moreover, it is difficult to achieve better accuracy by simply retaining more terms in the expansion in Eq. (D.4), since there are logarithmic terms like $\ln z$, meaning that we cannot take the infinite summation analytically. Instead, we use the following ansatz,

$$\widetilde{S}_{+}^{(0)}(y) = \frac{e^{-y}}{y}\left(\zeta(2) + a_1 y + a_2 y^2 + a_3 y^3\right), \tag{D.6}$$

$$\widetilde{S}_{-}^{(0)}(y) = \frac{e^{-y}}{y}\left(-\frac{\zeta(2)}{2} + b_1 y + b_2 y^2 + b_3 y^3 + b_4 y^4\right), \tag{D.7}$$

where a_i and b_i are determined by requiring a good fit with the shape function in the limited region $0 \le y \le 2$; we obtain $a_i = (0.146773, 0.106023, -0.0248936)$ and $b_i = (-0.772073, 0.163142, -0.0547415, 0.0107667)$.

In the opposite limit, for large y we can truncate the infinite summation in Eq. (D.3) at relatively small n thanks to the asymptotically exponential decay of $K_1(ny)$. Here we take the summation up to $n = 2$. We also use the asymptotic expansion of the modified Bessel functions. To guarantee accuracy, we expand $K_1(y)$ up to y^{-3} and $K_1(2y)$ up to y^{-1}. Eventually we obtain

$$\widetilde{S}_{\pm}^{(\infty)}(y) = \pm\sqrt{\frac{\pi}{2y}}e^{-y}\left(1 + \frac{3}{8y} - \frac{15}{128y^2} + \frac{105}{1024y^3}\right) + \sqrt{\frac{\pi}{16y}}e^{-2y}\left(1 + \frac{3}{16y}\right). \tag{D.8}$$

Finally, we approximate the shape function given in Eq. (D.3) as

$$S_{\pm}(y) \approx \begin{cases} \widetilde{S}_{\pm}^{(0)}(y), & \text{for } y < 2, \\ \widetilde{S}_{\pm}^{(\infty)}(y), & \text{for } y \ge 2. \end{cases} \tag{D.9}$$

The partitioned fitting curve for the shape function constructed here has an accuracy $E = 1.73 \times 10^{-3}$ for S_- and $E = 2.06 \times 10^{-3}$ for S_+, where $E \equiv \|1 - \widetilde{S}_{\pm}(y)/S_{\pm}(y)\|_\infty$. Note that, as a result of the naive matching of the two functions, $dV_T^{1-\text{loop}}/dT$ is discontinuous at $y = 2$ by construction. However, this is not problematic, since the amplitude of the discontinuity in dV_T/dT at $y = 2$ is on the order of 0.1%.

References

[1] B. P. Schmidt, Rev. Mod. Phys. **84**, 1151 (2012).

[2] A. G. Riess *et al.* [Supernova Search Team Collaboration], Astron. J. **116**, 1009 (1998) [astro-ph/9805201]; S. Perlmutter *et al.* [Supernova Cosmology Project Collaboration], Astrophys. J. **517**, 565 (1999) [astro-ph/9812133].

[3] A. A. Starobinsky, Phys. Lett. B **91**, 99 (1980).

[4] K. Sato, Mon. Not. Roy. Astron. Soc. **195**, 467 (1981); A. H. Guth, Phys. Rev. D **23**, 347 (1981).

[5] A. D. Linde, Phys. Lett. B **108**, 389 (1982); A. Albrecht and P. J. Steinhardt, Phys. Rev. Lett. **48**, 1220 (1982).

[6] D. H. Lyth and E. D. Stewart, Phys. Rev. D **53**, 1784 (1996) [hep-ph/9510204].

[7] K. Yamamoto, Phys. Lett. B **168**, 341 (1986).

[8] M. Y. Khlopov and A. D. Linde, Phys. Lett. B **138**, 265 (1984); J. R. Ellis, J. E. Kim and D. V. Nanopoulos, Phys. Lett. B **145**, 181 (1984).

[9] G. D. Coughlan, W. Fischler, E. W. Kolb, S. Raby and G. G. Ross, Phys. Lett. B **131**, 59 (1983); T. Banks, D. B. Kaplan and A. E. Nelson, Phys. Rev. D **49**, 779 (1994) [hep-ph/9308292].

[10] B. de Carlos, J. A. Casas, F. Quevedo and E. Roulet, Phys. Lett. B **318**, 447 (1993) [hep-ph/9308325].

[11] T. Asaka, J. Hashiba, M. Kawasaki and T. Yanagida, Phys. Rev. D **58**, 083509 (1998) [hep-ph/9711501]; T. Asaka and M. Kawasaki, Phys. Rev. D **60** (1999) 123509 [hep-ph/9905467]; K. Choi, W. I. Park and C. S. Shin, JCAP **1303**, 011 (2013) [arXiv:1211.3755 [hep-ph]].

[12] R. Easther, J. T. Giblin, Jr., E. A. Lim, W. -I. Park and E. D. Stewart, JCAP **0805**, 013 (2008) [arXiv:0801.4197 [astro-ph]].

[13] A. Kosowsky, M. S. Turner and R. Watkins, Phys. Rev. Lett. **69**, 2026 (1992); A. Kosowsky and M. S. Turner, Phys. Rev. D **47**, 4372 (1993) [astro-ph/9211004].

[14] M. Kamionkowski, A. Kosowsky and M. S. Turner, Phys. Rev. D **49**, 2837 (1994) [astro-ph/9310044].

[15] S. Kawamura, M. Ando, N. Seto, S. Sato, T. Nakamura, K. Tsubono, N. Kanda and T. Tanaka *et al.*, Class. Quant. Grav. **28**, 094011 (2011).

[16] S. Phinney *et al.*, NASA Mission Concept Study.

[17] T. Hiramatsu, Y. Miyamoto and J. Yokoyama, in preparation.

[18] M. Morikawa, Phys. Rev. D **33**, 3607 (1986); M. Gleiser and R. O. Ramos, Phys. Rev. D **50**, 2441 (1994) [hep-ph/9311278].

[19] M. Yamaguchi and J. Yokoyama, Phys. Rev. D **56**, 4544 (1997) [hep-ph/9707502].

[20] J. Yokoyama, Phys. Rev. D **70**, 103511 (2004) [hep-ph/0406072].

[21] C. Greiner and B. Muller, Phys. Rev. D **55**, 1026 (1997) [hep-th/9605048].

[22] D. Baumann, arXiv:0907.5424 [hep-th].

[23] M. Sasaki, Prog. Theor. Phys. **76**, 1036 (1986); V. F. Mukhanov, Sov. Phys. JETP **67**, 1297 (1988) [Zh. Eksp. Teor. Fiz. **94N7**, 1 (1988)].

[24] J. Martin, C. Ringeval and V. Vennin, Phys. Dark Univ. (2014) [arXiv:1303.3787 [astro-ph.CO]].

[25] A. D. Linde, Phys. Rev. D **49**, 748 (1994) [astro-ph/9307002].

[26] A. D. Linde, Phys. Lett. B **129**, 177 (1983).

[27] E. W. Kolb, M. S. Turner, *The Early Universe*, 1990, Addison-Wesley, Frontiers in Physics, 69.

[28] S. Dodelson, *Modern Cosmology*, 2003, Academic Press, ISBN: 9780122191411.

[29] A. Chodos, R. L. Jaffe, K. Johnson, C. B. Thorn and V. F. Weisskopf, Phys. Rev. D **9**, 3471 (1974).

[30] G. Aad *et al.* [ATLAS Collaboration], Phys. Lett. B **716**, 1 (2012) [arXiv:1207.7214 [hep-ex]]; S. Chatrchyan *et al.* [CMS Collaboration], Phys. Lett. B **716**, 30 (2012) [arXiv:1207.7235 [hep-ex]].

[31] S. P. Martin, Adv. Ser. Direct. High Energy Phys. **21**, 1 (2010) [hep-ph/9709356].

[32] A. Vilenkin and E. P. S. Shellard, *Cosmic Strings and Other Topological Defects*, Cambridge University Press, Cambridge, England, 2000

[33] M. Le Bellac, *Thermal Field Theory*, Cambridge University Press, Cambridge, England, 1996.

[34] L. Dolan and R. Jackiw, Phys. Rev. D **9**, 3320 (1974).

[35] N. P. Landsman and C. G. van Weert, Phys. Rept. **145**, 141 (1987).

[36] V. P. Nair, *Quantum Field Theory: A Modern Perspective*, Springer Science & Business Media, 2005.

[37] E. Calzetta and B. L. Hu, Phys. Rev. D **61**, 025012 (2000) [hep-ph/9903291].

[38] E. Calzetta and B. L. Hu, *Nonequilibrium Quantum Field Theory*, Cambridge University Press, Cambridge, England, 2008.

[39] A. Berera, I. G. Moss and R. O. Ramos, Phys. Rev. D **76**, 083520 (2007) [arXiv:0706.2793 [hep-ph]].

[40] Y. Miyamoto, H. Motohashi, T. Suyama and J. Yokoyama, Phys. Rev. D **89**, 085037 (2014) [arXiv:1308.4794 [hep-ph]].

[41] D. Boyanovsky, H. J. de Vega, R. Holman, S. P. Kumar and R. D. Pisarski, Phys. Rev. D **58**, 125009 (1998) [hep-ph/9802370].

[42] M. Drewes and J. U. Kang, Nucl. Phys. B **875**, 315 (2013) [arXiv:1305.0267 [hep-ph]].

[43] A. D. Linde, Contemp. Concepts Phys. **5**, 1 (1990) [hep-th/0503203].

[44] A. H. Guth and E. J. Weinberg, Phys. Rev. D **23**, 876 (1981).

[45] N. Seto, S. Kawamura and T. Nakamura, Phys. Rev. Lett. **87**, 221103 (2001) [astro-ph/0108011].

[46] E. D. Stewart, M. Kawasaki and T. Yanagida, Phys. Rev. D **54**, 6032 (1996) [hep-ph/9603324]; D. -h. Jeong, K. Kadota, W. -I. Park and E. D. Stewart, JHEP **0411**, 046 (2004) [hep-ph/0406136]; M. Kawasaki and K. Nakayama, Phys. Rev. D **74**, 123508 (2006) [hep-ph/0608335]; S. Kim, W. I. Park and E. D. Stewart, JHEP **0901**, 015 (2009) [arXiv:0807.3607 [hep-ph]]; K. Choi, K. S. Jeong, W. I. Park and C. S. Shin, JCAP **0911**, 018 (2009) [arXiv:0908.2154 [hep-ph]];

[47] M. Kawasaki, T. Takahashi and S. Yokoyama, JCAP **0912**, 012 (2009) [arXiv:0910.3053 [hep-th]].

[48] H. P. Nilles, Phys. Rept. **110**, 1 (1984).

[49] G. F. Giudice and R. Rattazzi, Phys. Rept. **322**, 419 (1999) [hep-ph/9801271].

[50] M. Kawasaki, K. Kohri, T. Moroi and A. Yotsuyanagi, Phys. Rev. D **78**, 065011 (2008) [arXiv:0804.3745 [hep-ph]]; K. Kohri, T. Moroi and A. Yotsuyanagi, Phys. Rev. D **73**, 123511 (2006) [hep-ph/0507245].

[51] M. Kawasaki, K. Kohri and T. Moroi, Phys. Rev. D **71**, 083502 (2005) [astro-ph/0408426].

[52] T. Moroi, H. Murayama and M. Yamaguchi, Phys. Lett. B **303**, 289 (1993).

[53] M. Kawasaki and T. Yanagida, Phys. Lett. B **399**, 45 (1997) [hep-ph/9701346].

[54] M. Yamaguchi and J. Yokoyama, Nucl. Phys. B **523**, 363 (1998) [hep-ph/9805333].

[55] T. Shiromizu, M. Morikawa and J. Yokoyama, Prog. Theor. Phys. **94**, 805 (1995) [astro-ph/9509018].

[56] R. Fukuda and T. Kugo, Phys. Rev. D **13**, 3469 (1976).